VYSOKÉ UČENÍ TECHNICKÉ V BRNĚ
BRNO UNIVERSITY OF TECHNOLOGY

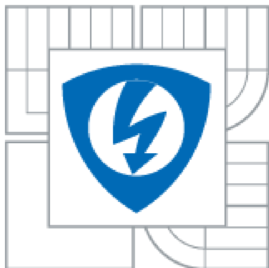

FAKULTA ELEKTROTECHNIKY A KOMUNIKAČNÍCH TECHNOLOGIÍ
ÚSTAV FYZIKY

FACULTY OF ELECTRICAL ENGINEERING AND COMMUNICATION
DEPARMENT OF PHYSICS

NON-DESTRUCTIVE LOCAL DIAGNOSTICS OF OPTOELECTRONIC DEVICES

NEDESTRUKTIVNÍ LOKÁLNÍ DIAGNOSTIKA OPTOELEKTRONICKÝCH SOUČÁSTEK

DOKTORSKÁ PRÁCE
DOCTORAL THESIS

AUTOR PRÁCE DINARA SULTANOVNA DALLAEVA, MSc.
AUTHOR

VEDOUCÍ PRÁCE Prof. RNDR. PAVEL TOMÁNEK, CSc.
SUPERVISOR

BRNO 2015

Abstract

To obtain novel materials for emerging optoelectronic devices, deeper insight into their structure is required. To achieve this, the development and application of new diagnostic methods is necessary.

To contribute to these goals, this dissertation thesis is concerned with local diagnostics, including non-destructive mechanical, electrical and optical techniques for examining the surface of optoelectronic devices and materials. These techniques allows us to understand and improve the overall efficiency and reliability of optoelectronic device structures, which are generally degraded by defects, absorption, internal reflection and other losses.

The main effort of the dissertation work is focused on the study of degradation phenomena, which are most often caused by both global and local heating, resulting in increased diffusion of ions and vacancies in the materials of interest.

From a variety of optoelectronic devices, we have chosen two representative devices: a) solar cells - a large p-n junction device, and b) thin films - substrates for micro optoelectronic devices. In both cases we provide their detailed surface characterization. For the solar cells, scanning probe microscopy was chosen as the principal tool for non-destructive characterization of surface properties. This method is described, and both positive and negative aspects of the methods used are explained on the basis of literature review and our own experiments. An opinion on the use of probe microscopy applications to study solar cells is given.

For the thin films, two interesting, from the stability point of view, materials were chosen as candidates for heterostructure preparation: sapphire and silicon carbide. The obtained data and image analysis showed a correlation between surface parameters and growth conditions for the heterostructures studied for optoelectronic applications.

The thesis substantiates using these prospective materials to improve optoelectronic device performance, stability and reliability.

Keywords

Local characterization, optoelectronics, material, silicon solar cells, aluminum nitride, silicon carbide, heterostructure, thin film, scanning probe microscopy, atomic force microscopy, scanning electron microscopy, image processing, statistical analysis, fractal analysis

Abstrakt

Chceme-li využít nové materiály pro nová optoelektronická zařízení, potřebujeme hlouběji nahlédnout do jejich struktury. K tomu, abychom toho dosáhli, je však nutný vývoj a aplikace přesnějších diagnostických metod. Předložená disertační práce, jako můj příspěvek k částečnému dosažení tohoto cíle, se zabývá metodami lokální diagnostiky povrchu optoelektronických zařízení a jejich materiálů, většinou za využití nedestruktivních mechanických, elektrických a optických technik. Tyto techniky umožňují jednak pochopit podstatu a jednak zlepšit celkovou účinnost a spolehlivost optoelektronických struktur, které jsou obecně degradovány přítomností malých defektů, na nichž dochází k absorpci světla, vnitřnímu odrazu a dalším ztrátovým mechanismům. Hlavní úsilí disertační práce je zaměřeno na studium degradačních jevů, které jsou nejčastěji způsobeny celkovým i lokálním ohřevem, což vede ke zvýšené difúze iontů a vakancí v daných materiálech. Z množství optoelektronických zařízení, jsem zvolila dva reprezentaty:

a) křemíkové solární články – součástky s velkým pn přechodem a

b) tenké vrstvy – substráty pro mikro optoelektronická zařízení.

V obou případech jsem provedla jejich detailní povrchovou charakterizaci. U solárních článků jsem použila sondovou mikroskopii jako hlavní nástroj pro nedestruktivní charakterizaci povrchových vlastností. Tyto metody jsou v práci popsány, a jejich pozitivní i negativní aspekty jsou vysvětleny na základě rešerše literatury a našich vlastních experimentů. Je také uvedeno stanovisko k použití sondy mikroskopických aplikací pro studium solárních článků. V případě tenkých vrstev jsem zvolila dva, z hlediska stability, zajímavé materiály, které jsou vhodnými kandidáty pro přípravu heterostruktury: safír a karbid křemíku. Ze získaných dat a analýzy obrazu jsem našla korelaci mezi povrchovými parametry a podmínkami růstu heterostruktur studovaných pro optoelektronické aplikace. Práce zdůvodňuje používání těchto perspektivních materiálů pro zlepšení účinnosti, stability a spolehlivosti optoelektronických zařízení.

Klíčová slova

Lokální charakterizace, optoelektronika, materiál, křemíkový solární článek, safír, karbid křeníku, heterostruktura, tenká vrstva, skenovací sondová mikroskopie, AFM mikroskop, SEM, zpracování obrazu, statistická analýza, fraktálová analýza

Dallaeva, D. S. Non-destructive local diagnostics of optoelectronic devices, Brno: Vysoké učení technické v Brně, Fakulta elektrotechniky a komunikačních technologií, 2015, 108 s. Thesis supervisor prof. RNDr. Pavel Tománek, CSc.

Affirmation

I declare that my thesis "Non-destructive local diagnostics of optoelectronic devices", was elaborated by myself under professional leadership by my supervisor, and on the basis of the recommended technical literature, which is completely cited in the References.

Brno, August 4, 2015 ……………………………………………

Dinara Sultanovna DALLAEVA

Acknowledgments

I would like to express great thanks to my supervisor Prof. RNDr. Pavel Tománek, CSc. for his patient guidance on my study, for his precious advice, and for all his devoted time, that made this research feasible.

My deep gratitude also goes to Prof. Ing. Lubomír Grmela, CSc., head of the Physics Department, Faculty of Electrical Engineering and Communication, Brno University of Technology, for his constant support, as well as to our working team in the Physics Department for its encouragement in my work, especially to Ing. Pavel Škarvada, Ph.D. and Ing. Robert Macků, Ph.D.

The research is not the work of one person. I need to express my gratitude to Prof. Stefan Talu (Technical University of Cluj-Napoca, Romania) and his team for their help in mathematical processing of our experimental results, and Dr. Ramazanov and M.A. Gitikchiev (Dagestan State University, Machachkala, Dagestan Republic, Russian Federation) for their help with samples preparation and compositional analysis.

I also gratefully acknowledge my previous employers for their support in sources of materials and devices which allowed me to finish my Ph.D. study: Dagestan State University and Dagestan State Technical University for sample preparation and probe microscopy, Moscow Physical-Technical Institute for electron microscopy. The study in Russia was supported by Federal task programs and president studentship.

I also want to emphasize the role of my current employer, Brno University of Technology for the possibility to use the atomic force microscopy, scanning near-field optical microscopy, scanning tunneling microscopy.

Last but not least, I would also like to thank Prof. Steve Smith from South Dakota School of Mines and Technology, Rapid City (USA) for his willingness to read the text and correct my English in this thesis.

I thank my parents and my friends for their emotional support.

Research described in this thesis was financially supported by the European Centre of Excellence CEITEC CZ.1.05/1.1.00/02.0068, by project Sensor, Information and Communication Systems SIX CZ.1.05/2.1.00/03.0072, the Czech-American cooperation grant MSMT - Kontakt LH11060, Visegrad Fund Scholarship (Contract No.51401290) as well as by grant FEKT-S-14-2240. These supports are gratefully acknowledged.

Brno, August 4, 2015 Dinara Sultanovna DALLAEVA

CONTENT

1 INTRODUCTION - 15 -
1.1 Subject of study - 15 -
1.2 Formulation of the problem - 16 -
1.3 State of the art - 17 -
1.4 Objectives of dissertation - 20 -
1.5 Organization of thesis - 22 -
2 MORPHOLOGY CHARACTERIZATION TECHNIQUES - 23 -
2.1 SEM and AFM surface characterization - 23 -
2.2 Scanning electron microscopy (SEM) - 24 -
2.3 Scanning probe microscopy (SPM) - 25 -
2.3.1 SPM types - 25 -
2.3.1.1 Scanning near field optical microscopy (SNOM) - 25 -
2.3.1.2 STM - 27 -
2.3.1.3 Spectroscopy - 29 -
2.3.1.4 Lithography - 29 -
2.3.1.5 AFM - 30 -
2.3.1.5.1 AFM modes assignment - 30 -
2.3.1.5.2 Lennard-Jones curve - 30 -
2.3.2 Probes - 31 -
2.3.3 Types of AFM sensors - 32 -
2.3.4 Artifacts - 33 -
2.3.4.1 Artifacts caused by probe - 33 -
2.3.4.2 Artifacts caused by scanner - 35 -
2.3.4.3 Artifacts caused by surrounding - 35 -
2.3.5 Free software possibilities - 35 -
2.4 Using of SEM and SPM in study of solar cells - 36 -
3 SOLAR CELLS TOPOGRAPHY CHARACTERIZATION - 38 -
3.1 Types of solar cells - 38 -
3.2 Role of solar cells surface characterization - 39 -
3.3 Solar cells surface texture - 41 -
3.4 Hydrophobicity and self-cleaning of surface - 43 -
3.5 Topography characterization - 44 -

3.5.1 SEM and AFM of polycrystalline solar cells ... - 45 -
3.5.2 AFM of GaAs solar cells ... - 46 -
3.5.3 Processing of the topographic images ... - 48 -
3.6 Contacts to solar cell ... - 50 -
4 LOCAL TOPOGRAPHY OF OPTOELECTRONIC SUBSTRATES PREPARED BY DRY PLASMA ETCHING PROCESS ... - 52 -
4.1 Dry etching ... - 52 -
4.2 Materials choice ... - 53 -
4.3 Experimental results ... - 54 -
4.4 Etching rate ... - 55 -
4.5 Atomic force microscopy ... - 56 -
4.6 Influence of processing electrical parameters ... - 61 -
4.7 Dry etching in optoelectronics ... - 71 -
5 PREPARATION OF THIN FILMS BY MAGNETRON SPUTTERING ... - 72 -
5.1 Substitution of the material and method choice ... - 72 -
5.1.1 Aluminum nitride ... - 72 -
5.1.2 Magnetron sputtering ... - 72 -
5.1.3 Magnetron sputtering in optoelectronics applications ... - 73 -
5.2 Deposition of aluminum nitride films ... - 74 -
5.2.1 Description of set-up ... - 74 -
5.2.2 Substrate choice and processing ... - 75 -
5.3 Influence of process parameters on film morphology ... - 75 -
5.3.1 AFM of the surface ... **- 75 -**
5.3.2 SEM of the structure ... - 78 -
6 AFM IMAGING AND CHARACTERIZATION OF TOPOGRAPHY ... - 79 -
6.1 Study of aluminum nitride topography ... - 79 -
6.1.1 Role of surface analysis ... - 79 -
6.1.2 Materials and methods ... - 80 -
6.1.3 Atomic force microscopy ... - 81 -
6.1.4 Fractal analysis of surface roughness ... - 83 -
6.1.5 Statistical analysis of morphological features ... - 85 -
6.1.6 Discussion ... - 87 -
6.2 Characterization of surface failure of solar cells by AFM data processing ... - 88 -
REFERENCES ... - 94 -

Appendix 1. List of publication .... - 105 -
in impact journals .... - 105 -
Appendix 2. List of publication .... - 106 -
cited in Scopus .... - 106 -
Professional CV .... - 108 -

List of symbols and abbreviations

AFM – atomic foce microscopy

AlN – aluminum nitride

Al_2O_3 – aluminum oxide

CIGS – (copper indium gallium selenide)

C-UV – ultraviolet C

D_f – fractal dimension

E_g – band gap

GaN – gallium nitride

IR – infrared

KPFM – Kelvin probe force microscopy

LED – light-emitting diode

Lx – correlation length in the x axis

Ly – correlation length in the y axis

SEM – scanning electron microscopy

SiC – silicon carbide

SFM – scanning force microscopy

SNOM – scanning near-field optical microscopy

SPM – scanning probe microscopy

STM – scanning tuneling microscop

STS – scanning tuneling spectroscopy

Vmc – core material volume

Vmp – peak material volume

Vvc – core void volume

Vvv – dales void volume

List of figures

Figure 1.1. Interconnection of fields involved in the thesis.

Figure 1.2. Scheme of tandem (multilayer) solar cell.

Figure 2.1. a) AFM image of SiC wafer topography and b) SNOM image in reflection of the same area. Scanning area of (35 x 35)μm^2.

Figure 2.2. STM image of SiC monocrystalline wafer.

Figure 2.3. Separation of polytype and the sequence of the atomic layers of moncristalline 2H-SiC.

Figure 2.4. AFM vector lithography on the piece of compact disc (scan area is 6x6 μm^2).

Figure 2.5. Lennard-Jones potential curve.

Figure 2.6. a) supposed profile, b) tip shapes, c) possible difference in profile imaging.

Figure 2.7. a) Imaging of the broken SNOM probe, b) artifact of edge duplication.
(scan area is 120x120 μm^2)

Figure 3.1. Some semiconductor materials and bandgaps which find their optoelectronic application in different light wave range.

Figure 3.2. a) Hydrophobic surface (angle > 90°), b) hydrophilic surface (angle < 90°).

Figure 3.3. a) Demonstration of hydrophobic surfaces in nature (left: butterfly wing, right: peacock feather), b) Polycrystalline silicon solar cell and GaAs solar cells with a drop of water on the cell surface.

Figure 3.4. SEM of polycrystalline solar cell.

Figure 3.5. AFM of polycrystalline solar cell: a) 2D image, b) 3D image, c) 3D image of smaller area.

Figure 3.6. AFM of GaAs solar cell: a) 2D image, b) 3D image, c) 3D image of smaller area.

Figure 3.7. Semi-contact error mode image of GaAs solar cell

Figure 3.8. a) Polycrystalline and b) monocrystalline solar cell image thresholding, demonstrating geometrical features of the topography.

Figure 3.9. Watershed segmentation of the surface topography of a) polycrystalline and b) monocrystalline solar cells.

Figure 3.10. Metallic contacts to a) polycrystalline solar cell and b) to GaAs solar cell.

Figure 4.1. Dry plasma etching of the surface.

Figure 4.2. Scheme of physical dry-etching device.

Figure 4.3 Demonstration of the angle dependent cleaning. The slope of the substrate influences the trajectory and amount of etched material from the surface.

Figure 4.4. a) Scheme of wafer position to argon flow, b) angular dependence of the sputtering rate of Al_2O_3 and SiC.

Figure 4.5 Surface topography and horizontal profile of Al_2O_3 a) before and b) after dry etching.

Figure 4.6. Surface topography and horizontal profile of SiC a) before and b) after dry etching.

Figure 4.7 a. SiC wafer, etched on 20° slope at 3 kV (morphology, heights histogram, correlation curve).

Figure 4.7 a. SiC wafer, etched on 20° slope at 3 kV (morphology, heights histogram, correlation curve). Scan area 50x50 μm.

Figure 4.7 b. SiC wafer, etched on 20° slope at 3kV (morphology, heights histogram, correlation curve). Scan area 5x5μm.

Figure 4.7 c. SiC wafer, etched on 20° slope at 3kV (morphology, heights histogram, correlation curve). Scan area 1x1μm.

Figure 4.7 d. SiC wafer, etched on 20° slope at 4kV (morphology, heights histogram, correlation curve). Scan area 50x50μm.

Figure 4.7 e. SiC wafer, etched on 20° slope at 4kV (morphology, heights histogram, correlation curve). Scan area 5x5μm.

Figure 4.7 f. SiC wafer, etched on 20° slope at 4kV (morphology, heights histogram, correlation curve). Scan area 1x1 μm.

Figure 4.7 g. SiC wafer, etched on 20° slope at 5kV (morphology, heights histogram, correlation curve). Scan area 50x50μm.

Figure 4.7 h. SiC wafer, etched on 20° slope at 5kV (morphology, heights histogram, correlation curve). Scan area 5x5μm.

Figure 4.7 i. SiC wafer, etched on 20° slope at 5kV (morphology, heights histogram, correlation curve). Scan area 1x1 μm.

Figure 5.1. Scheme of magnetron sputtering proces (El – particles of sputtering material, RG – reactive gas which bring chemical component to the deposited layer, Ar – argon, which often used as inert gas for target sputtering, e – electrons).

Figure 5.2. Height histogram for the AlN samples morphology obtained at a) 1000K, b) 1300K and c) 1500K.

Figure 5.3. Morphology of AlN samples obtained at a) 1000K, b) 1300K and c) 1500K.

Figure 5.4. SEM image of the aluminum nitride layer on sapphire substrate in cross-section.

Figure 6.1. AFM images (contact mode) of AlN epilayers on the sapphire substrate obtained at a) 1000K, b) 1300K and c) 1500K.Scanning area of (5 x 5)μm^2. The vertical range of the displayed data (in nanometres [nm]) and the color bar are shown on the right side of the AFM images.

Figure 6.2. The depth histogram for theAlN epilayers on sapphire substrates obtained at: a) 1000K, b) 1300K and c) 1500K. The Abbott-Firestone curve (red).

Fig. 6.3. Enclosed volume for AlN epilayers on sapphire substrates deposited at:
a) 1000K, b) 1300K and c) 1500K. The fractal dimension is obtained from the slope(s) of the graphs.

Figure 6.4. Face of AFM 3D images (left side) and graphical study of volume parameters (right side): *Vmp*, *Vvc*, *Vmc* & *Vvv* parameters based upon the Abbott curve calculated on the surface. Two bearing ratio thresholds are defined (using the vertical bars that are drawn with dotted lines). By default, these thresholds are set at bearing ratios of 10 % and 80 %. The first threshold, *p1* (default: 10 %), is used to define the cut level *c1* (and *p2* defines *c2*, respectively). AlN epilayer on the sapphire substrate obtained at: a) 1000K, b) 1300K and c) 1500K.

Figure 6.5. The height-height correlation function. AlN epilayer on the sapphire substrate obtained at: a) 1000K, (Correlation lengths: Lx = 319nm, Ly = 356nm); b) 1300K, (Correlation lengths: Lx = 317nm, Ly = 212nm); c) 1500K, (Correlation lengths: Lx = 224nm, Ly = 81.5nm).

Figure 6.6. SEM of monocrystalline silicon solar cell.

Figure 6.7. a) AFM image of the solar cell area without surface defects, b) histogram of heights distribution

Figure 6.8. a) AFM image of the solar cell area without surface defects, b) histogram of heights distribution

List of tables

Table 2.1. SPM probes classification

Table 6.1. The fractal dimensions D_f, for scanning square areas of (5×5)μm^2 of AlN epilayers on sapphire substratesdepositedat: a) 1000K, b) 1300K and c) 1500K

1 INTRODUCTION

1.1 Subject of study

The subject of the thesis is nondestructive surface characterization of optoelectronic devices, both widespread commercial devices (solar cells) and just heterostructures (at the material preparation and properties investigation stage). The thesis differs from the previous studies in optoelectronics. The subject of the study was chosen in the following way:

- First, the samples, provided by producers of solar cells were studied by SPM and SEM. Solar cells were chosen as readily available specimens for measurements since their efficiency strongly depends on the quality of the surface, and industry demands continuous improvement. This study brings additional information about state-of-the-art photovoltaic devices.
- Then, heterostructure surfaces, prepared as prospective solar cell materials, were analyzed. The prepared structures were characterized at each step of fabrication: from substrate choice and processing to structure preparation. Stable materials with promising properties and proven potential are of great interest for modern optoelectronics.

The aim is to study problems of material surface condition by a nondestructive approach; therefore attention in this work is also given to an explanation of the choice of method for surface characterization. The metrology plays a role and is considered in terms of the description of the surface.

The most important results could are obtained at the intersection of the fields of science and development (Fig.1.1). SPM and SEM are used for qualitative and quantitative description of the optoelectronic structures. Using modern characterization approaches, the results may influence both the design of new structures and enhance performance of existing optoelectronic devices.

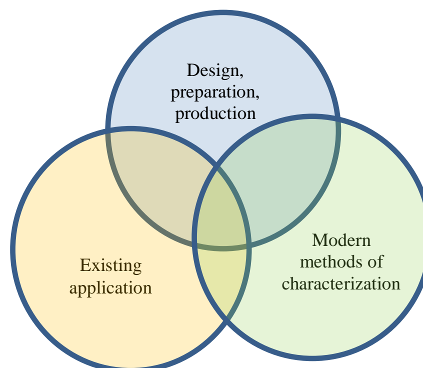

Figure 1.1. Interconnection of fields involved in the thesis.

The theoretical and experimental importance of the work is reflected in the interest of scientists working on problems of a similar nature: the reference list of this thesis reflects only small part of an enormous amount of studies in this field.

1.2 Formulation of the problem

Today, there is a considerable increase in global energy demands. Use of solar energy decreases consumption of nuclear, coal, gas and oil resources. Worldwide solar energy capacity in 2015 is approximately 17.5 GW [1], and the market is anticipated to grow in the forseable future. This energy can supply different electrical devices or be converted to other types of energy, heating, for example, or stored for later use in bataries.

Gathering solar electric energy is a difficult task and strongly depends on the quality of the solar cells employed. Solar cells are produced with a number of different technologies: monocrystalline and polycrystalline silicon based technologies; thin films solar cells, based on second generation materials such as cadmium telluride, copper indium gallium diselenide, and amorphous silicon; multiple junction solar cells based on epitaxial III-V compounds; dye-sensitized solar cells; organic solar cells. Progress in solar cell technology brings society closer to using clean power.

Chandra et al. [2] explains the three key characteristics for wide penetration of solar energy in everyday life: a) increasing of efficiency of energy conversion, b) improved reliability and longer life expectancy, and c) reducing cost. The reduction of materials cost and elimination of fabrication process complications are trends for modern technologies to provide high production capacity [3]. For example, the authors of [4] highlight some of the many advantages of tandem solar cells such as reduced thermalization and below-bandgap absorption losses.

Tandem cells, impurity-band and intermediate-band devices, hot-electron extraction, and carrier multiplication, are a few of the so-called “third generation” technologies proposed to improve solar cell efficiency [3]. Tandem solar cells represent combinations of several layers in one multi-junction stack [3]. They absorb a broader spectrum using several heterojunctions and/or light interaction mechanisms. These cells contain different materials with varying bandgaps. The wider the variation in bandgaps, the wider the spectral range of the cell. Tandem solar cells also reduce some of the materials cost while increasing efficiency [4].

The complicated structure of tandem solar cells requires scientists to understand the properties of the different materials which comprise the various subcells. It is necessary to protect the solar cell from ambient conditions and their influence on degradation. For this reason the upper layer should have both larger bandgap and superior stability. In this work we investigate materials which are suitable for the upper layers of a tandem cell. According to literature review, and as determined by our studies, the surface morphology of the layers influences the lattice matching of heterojunctions, impurity

concentrations, stresses, and dislocation densities, consequently strongly affecting the efficiency of the sub cells.

In [4] the authors address the current state of tandem solar cell fabrication, such as the preparation (epitaxial grown), choice of substrate (expensive Ge or III–V substrates), and design structure (large bandgap structures vertically stacked on top of small bandgap structures).

Due to their expense, tandem cells are used for space applications, but as noted in [3] Si cell efficiency is low and also Si is susceptible to radiation damage. Presently, GaAs based materials are well suited to tandem solar cell technologies.

Concentrated solar power plants and solar selective coatings stable in air at high temperatures demand stable materials with low defect structure, and preferably compatible with current electronics fabrication techniques [5].

The characteristics of solar cells depends on the influence of radiation. Some types of radiation have a damaging effect on the cells. These effects in turn depend on the elevation of the solar panel installation (from ground fields up to space orbits). Space UV band radiation generally compromises the properties of solar cells. The high energy ultraviolet part of the solar spectrum decreases the duration of field operation for photovoltaic modules [6]. Transparency of the encapsulating glasses of solar panels generally decreases under UV radiation, causing a degredation in performance. One approach is the applications of UV reflected coatings and filters to prevent degradation. Another approach is preparation and investigation of new prospective materials for photovoltaics with superior performance in this spectral range.

Space radiation also influences the temperature of solar panels, thus a temperature stable material should be chosen. For this purpose, the wide bandgap materials provide possibilities for design and application of photovoltaic elements. One candidate is aluminum nitride (AlN). AlN provides a new technological opportunity for solar cell design, especially for tandems solar cells.

1.3 State of the art

Most modern low-cost solar cells have only one p-n junction. Only the photons with higher or equal energy to the bandgap of the absorber can generate current. The use of multilayer elements can improve the spectral bandwidth of absorption. A combination of different materials with a variation in bandgap obviously will provide lower losses, since such elements work with a wider portion of the solar spectrum (Fig.1.2).

High energy photons are to be absorbed at the upper layers, so it is necessary to situate the subcells made from wide bandgap material on the top and other layers with lower bandgap towards the bottom of the cell. Obviously, the top material should be stable to extreme conditions and transparent to other part of the spectrum.

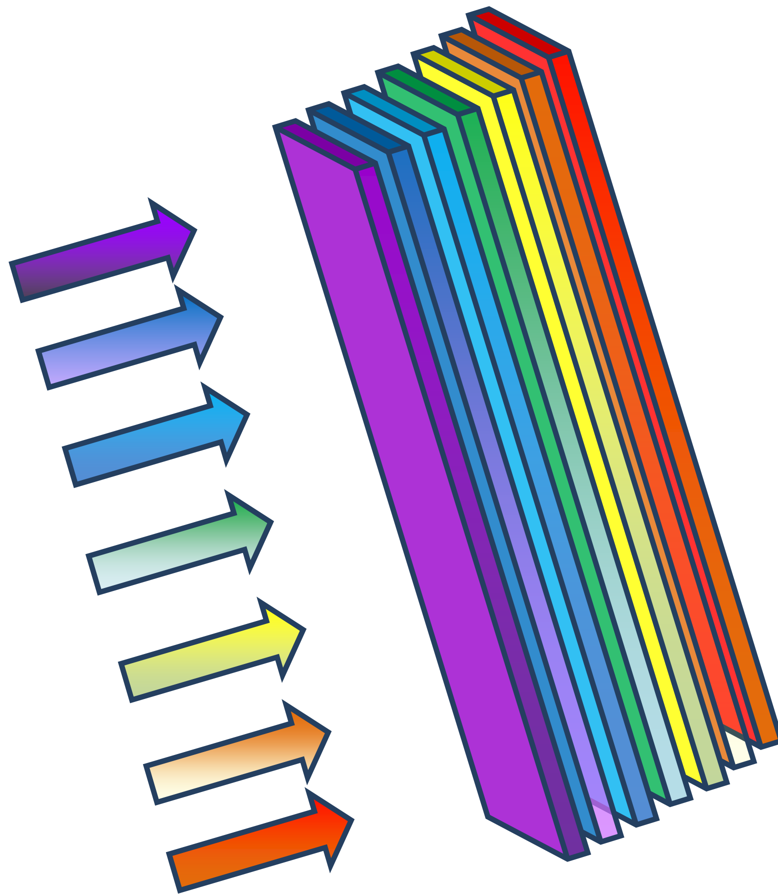

Figure 1.2. Scheme of tandem (multilayer) solar cell.

Design of high efficiency solar cells is important both for earth (autonomic electric stations, alternative energy sources) and space (ships, satellites) applications. Solar cells provide a considerable fraction of the energy for space vehicles. Solar cells for space applications demand a specific design due to the harsh conditions of space exploration.

The authors of [3] summarize that nanotechnology can improve solar cell quality by providing improvements in crystalline semiconductor III–V materials, polymer materials, and carbon-based nanostructures. Efficient energy conversion depends on the thermodynamic properties of photovoltaic materials and their device structures.

Silicon is currently the most abundantly used material for solar cell production. However, developing solar energy technologies requires new kinds of structured layers. A lot of factors should be considered in order to obtain high efficiency solar cells, such as the composition of the layers and the optical behavior of light at each layers' interface. Using the proper buffer materials is important. The high resistance multi-layer AlN/AlGaN/GaN is often used for Si-based devices, since a thin AlN protective layer provides low contact resistance between silicon and subsequent films [7].

Wurtzite structure semiconductor materials are promising for a wide range of optical devices (light-emitting devices, solar cells, microsensors, photocatalysts), due to their variety in crystal size, orientation and morphology [8]. Their stability at extreme conditions has attracted global attention to aluminum nitrate for the implementation of high-efficiency nitride photovoltaic devices. AlN is applicable not only to silicon, but also to copper-indium-gallium-selenide solar cells as a barrier to improve conversion efficiency [9].

The focus of reference [10] is solar selective absorbing coatings on the basis of titanium and aluminum nitride multilayer structures obtained by magnetron sputtering. According to [11] the quasi-solid-state dye-sensitized solar cell with 0.1wt% of AlN in gel polymer electrolyte exhibited high power-conversion efficiency. Reference [12] describes thin AlN buffer layers prepared on the n-type Si (111) wafers. It caused p-doping of the Si wafer by Al in-diffusion. On top of the AlN buffer is situated an n-type GaN layer. Thus, a pn-junction occurs with low lattice mismatch. The authors of reference [13] discuss thin layers of hydrogenated aluminum nitride as a combined anti-reflective coating and passivation layer in n-type cells. For photovoltaics, it could be an alternative to silicon oxide, silicon nitride and aluminum oxide.

Compounds based on AlGaN are potentially useful as optical, solar-blind sensors, and UV emitters [14]. Aluminum nitride also can be used as a solar coating not only in thin film form, but also as a ceramic material, as was described and successfully modeled in reference [15]. Nano-AlN composite was reported in [16] as an efficient thermal storage material, which can provide thermal energy for utilization when a light source is absent.

AlN is also a very interesting material due to its attractive electrical and physical properties [17,18]. AlN has high hardness, high electrical resistivity, excellent thermal conductivity [19], stability at high temperatures and resistance to corrosive media. It could be applied in III-nitride epitaxy as a substrate for fabrication of optoelectronic, high-power photonic devices [20] and is currently in competition with sapphire-based technologies [21]. Wide bandgap semiconductors provide advantages in photovoltaic design. As we reported in [22, 23] the bandgap of solid solutions with silicon carbide could be controlled and the required optical properties could be obtained.

The optical bandgap range provides an opportunity for preparation of structures for ultraviolet applications. The results can be applied to the design of optoelectronic devices with prescribed light emitting properties for devices used under extreme conditions.

AlN is interesting as an anti-reflection layer due to the combination of its' thermal and optical properties [24]. Its' solar selective absorption could find a place in solar cells preparation. Aluminum nitride is a good substrate of electrical and optoelectronic devices, due to high thermal conductivity. Aging experiments show that AlN and Al_2O_3 based materials have high thermal stability and are promising in the solar power industry [25]. All these properties make AlN a good candidate for surface passivation

and antireflective coatings of solar cells, both silicon [26] and A_3B_5. Use of AlN as a passivating layer was also reported in [26].

Films of AlN deposited on Copper-Indium-Gallium-Selenide solar selective foils are suitable as an insulation barrier, and improve crystalline quality of contacts and conversion efficiency [9]. AlN is a suitable material for optical coatings or surface passivation even better than Si_3N_4 [27]. The author of [28] brought to our attention that further improvement of the fabrication process of AlN films with a high quality is necessary. Aluminum nitride/oxide was also suggested for applications as a top layer for tandem solar absorbers. Solar absorbance of 0.96 was reached for experimentally prepared solar selective absorber coated surfaces on the basis of an aluminum–aluminum nitride composite [29]. The progress in AlN technologies shows that it is not limited by C-UV (ultraviolet C) since Yoshitaka Taniyasu et al. [30] reported a fabrication of AlN homojunction LED with an emission wavelength of 210nm. AlN can be transparent down to 200nm [31]. Experiments in this field will allow improved flexibility in novel solar cells design.

All mentioned studies were accompanied directly or indirectly by the purpose of finding a solution to alternative energy problems, and make aluminum nitride an interesting material for energy conversion and storage. The goals of making higher efficiency solar cells and reducing the cost of solar energy could be advanced by use of the prospective materials studied and giving attention to their morphology.

1.4 Objectives of dissertation

The study is focused on the local micro- and nano-meter scale optical and electronic characterization of optoelectronic materials and structures, including wide-bandgap semiconductor films for optoelectronics. All contributions to this emerging field are original due to the cutting edge nature of the technology.

The development of thin films for optoelectronic devices presents challenges of both fundamental and empiric character. For instance, the problem of contacts with systems of several materials, e.g. point imperfections, and grain boundaries. All these affect diffusion of charges, segregation, recombination, and current transfer.

These problems should be investigated in combination with the parameters of complete devices, including the effects of other materials and their local characteristics. During the optoelectronics element formation, it is necessary to study the quality of each layer after every step of preparation in order to fully understand the structure, chemical composition, optical and electrical properties, and their potential influence on the completed device.

The field of modern microelectronic devices can benefit greatly by the development of new material classes, particularly the design of materials which are stable when exposed to high-temperatures and radiation. The electrophysical properties of wide-bandgap

semiconducting materials such as AlN, GaN, SiC, diamond, and the solid solutions $(SiC)_{1-x}(AlN)_x$, make them useful in fabrication of devices for power and microwave electronics. These materials are the subject of advanced research for their applications to devices for the short-wavelength spectral region (ultraviolet light photoconverters and photodetectors, high-temperature laser diodes). AlN is characterized by a wide band-gap (E_g = 6.28eV), high values of critical (electrical) breakdown field, and high stability to temperature influences and radiation. However, obtaining perfect AlN epilayers is difficult because of the absence of epitaxial substrates (of the same material). As a consequence, epitaxial deposition is carried out using foreign substrates of other materials such as sapphire (Al_2O_3) and silicon carbide (SiC).

This choice of substrate is motivated by the fact that the technology for substrate formation of Al_2O_3 and SiC is well developed. Also, these materials satisfy the requirements of electro-physical, mechanical, and thermal properties of materials suitable for extreme conditions devices. Monocrystalline sapphire is one of the hardest oxides, with high hardness at high temperatures, good thermo-physical properties and optical transparency. It is chemically resistant to most acids up to 1300K, and to hydrofluoric acid (HF) below 600K. These properties make sapphire a good material choice when it is necessary to have an optically transparent material in the visible light to near-infrared region.

The quality of prepared structures studied here is evaluated by scanning probe microscopy and scanning electron microscopy.

Optical properties of both Al_2O_3 and AlN are well studied. Based on the literature survey mentioned previously, its exceptional properties could find applications in solar cells. But it is still a challenge to prepare AlN films with the required quality and properties. Texture of the material surface is one indicator of film quality, and will influence efficiency and reliability of the heterostructures. For this reason, the work reported here is oriented toward the description of surface morphology using modern surface characterization systems. The goal of the work is not only to reveal the basic processes of thin films morphology and control, but also to provide perspectives on new materials implementation and their possible application in optoelectronics.

The choice and preparation of the substrate for individual subcells, as well as the deposition and processing techniques used, are important steps that need to be optimized in solar cell production.

The objectives of this study include investigation of:
1. texture and morphology of solar cell surface layers,
2. new methods for morphological characterization,
3. explanations for the choice of materials used in heterostructure preparation,
4. the influence of preparation condition on thin film morphology
5. a statistical description of morphology characterization.

1.5 Organization of thesis

A short introduction and overview was given above about the current progress in the field of solar cells designs and application of prospective materials for optoelectronics. Chapters 2 and 3 concern existing problems, possibilities and perspectives of defects detection by emerging technologies. Chapter 2 describes two types of microscopy suitable for solar cells morphology characterization and their comparison: Atomic force microscopy and scanning electron microscopy provide information about surface texturization at the micro- and nano-scale and are of interest for nondestructive optoelectronic device characterization. Chapter 3 contains nondestructive morphology characterization data of silicon and gallium arsenide solar cells, including mathematical processing of the results using freely available, shared software.

Chapters 4-6 represent the core of this thesis and describe the experiments of heterostructure preparation and analysis. Chapter 4 demonstrates the advantages of plasma etching substrates for cleaning and further deposition of layers. The optimal conditions are described and characterized by a number of AFM measurements. Chapter 5 discusses film preparation, choice of the depostion method and parameters, including the substrate near-surface area processing to obtain textured layers. Chapter 6 includes statistical and fractal analysis of the data, carried out in collaboration with Prof. Talu and his team. This information was also published in our common publication and these articles are in the attachments. Finally, the main results are summarized in a discussion which includes further suggestions and perspectives on this field of study and conclusions.

2 MORPHOLOGY CHARACTERIZATION TECHNIQUES

This chapter describes two advanced metrological tools for surface study, characterization and modification. Considerations of the interaction between the tool and the sample allow avoiding the influence of artifacts on the results of scanning a solar cell surface. The usefulness of the methods as applied to solar cells is shown. An overview of free software for processing data exported from the instrument software is given and the advantages of these resources are demonstrated.

2.1 SEM and AFM surface characterization

Advanced characterization of optoelectronic devices demands several microscopy techniques based on different physical principles with nano- and micro-meter resolution in order to locate nanosize features of the device structure. SEM and AFM are promising methods to study solar cell topography that can be used in during fabrication to afford fine surface control. These measuring techniques are widespread in the scientific and industrial world, and have an important role in the the field of optoelectronics. AFM and SEM illustrate surface texturization at micro- and nano-scale, and thus are powerful instruments of nanotechnology.

SEM and AFM are complementary methods, each giving access to different information about topography. The images obtained contain information about the distribution of light in the near-surface area. Such studies can contribute towards the improvement in efficiency of solar cells, as the surface condition influences the optical properties of the cells. Surface condition also affects the reliability of the device. It is thus necessary to minimize the formation of defects in every fabrication step. Texturing of a solar cell surface is a way to improve light trapping and thereby gain an enhancement in efficiency [32]. The properties of materials in the micro- and nano-scale can be dominated by the geometry of the surface, and, in such cases, will therefore be a function of the dimensions [32].

It is possible to extract qualitative and quantitative information about solar cells (electrical properties of grain boundaries, nano-scale optical properties and morphology) from AFM and SEM data [33]. Based on the scale of modern semiconductor technologies, to the nanometer level, there is a demand for SEM and AFM analysis. Surfaces and surface phenomena are also of great interest for fundamental physics, since the atomic structure of surface atoms is different than for those in the volume of a bulk material. One main factor which distinguishes SEM and SPM is the necessity to maintain high vacuum in an SEM, while an SPM can be operated at ambient conditions

[33]. Combinations of different types of microscopy considerably improves the scientific quality of solar cell investigation results [34].

Both AFM and SEM characterization methods can give important information and demonstrate the critical role of surface roughness and feature size distribution. In spite of the fact that both methods give findings about surface topography, there is a contrast in this information rooted in the different principles of each method, each of which could be more applicable to specific types of surface measurements [33]. There are plenty of possibilities to find additional information connected to these principles [35], for instance, the interaction of an electron beam with the surface provides the possiblity to detect secondary electrons, backscattered electrons, X-rays, Auger electrons, cathodoluminescence, electron energy-loss, transmitted electrons, and diffracted electrons [33]. In turn, interaction of an SPM probe with a surface can give information based on the measurement of atomic force, current, magnetism, light emission, etc. Combinations of different methods were applied to surface characterization more than 20 years ago [35], and successfully used since then, providing the benefits of more reliable interpretation regarding morphology by exposing the correlation of the data obtained by different techniques.

2.2 Scanning electron microscopy (SEM)

Scanning Electron Microscopy (SEM) measurements are in the range of micro- and nano-metrology. SEM has some advantages over AFM when the height and depth of of morphological features exceeds the limited range of an AFM. There are a number of devices which need to be characterized at both milli-, micro- and nano-scale; while their components are designed in milli and micro-scale, nanoscaled morphology influences strongly their characteristics and lifetime (e.g. optoelectronic, microelectromechanical, microoptoelectromechanical devices) [32]. In some cases [36] AFM seems to be more reliable for fine profile characterization.

Beam parameters define the final resolution and depth of electron interaction with surfaces [33]. In comparison to SPM, SEM has quite a large depth of focus. SEM has become a widely used tool for imaging and manipulating nanostructures. SEM applications are expanded from nanoscience laboratories to many fields of industry where micro- and nano-scale control is essential. A focused ion beam, which is quite often combined with SEM, is also of great interest in the semiconductor and materials science fields [37]. There are many factors that must be taken into account for obtaining good images with an SEM: proper sample preparation, elimination of noise and undesired effects (spherical aberration, chromatic aberration, diffraction, astigmatism [33]), etc.

2.3 Scanning probe microscopy (SPM)

Scanning probe microscopy (SPM) has better resolution then traditional instruments, such as a profilometer or optical microscope [38], and can be adapted to bare and untreated surfaces without complicated sample preparations. The results reported in reference [39] demonstrate SPM as a powerful tool in III–V semiconductor device structure metrology. SPM is one of the best modern methods for studying morphology and local properties with high resolution. The method has progressed from a strange and unusual scientific tool to widespread way to study surfaces in many applications. Progress in SPM has enabled new methods in nanotechnology for structure characterization. Since AFM gives both the possibility to watch atomic structure of the surface and global information about whole surface, precise information about surface details could be extracted with high resolution. Another advantage is the sample will not be damaged by exposure to a high energy beam, as could be happen in scanning electron or ion methods. There many classes and modifications of SPM, as many scanning modes and methods have been invented. Nevertheless, there is still a large unstudied potential for the use of SPM for investigation of defects. Most importantly, AFM measurements allow evaluation of surface roughness parameters with a high degree of precision.

2.3.1 SPM types

There are a large number of techniques which rely on the interactions between a sample surface and a proximal probe. This interaction defines the type of probe microcopy. As a consequene, SPM methods give further insight into a number of morphological properties. Alongside topography, SPM can characterize optical, electrical and mechanical surface properties, and may find correlations between them. These many possibilities to use SPM to characterize devices defines the range of possibilities for surface characterization. There are a number of reports that concern application of SPM methods to study a wide range of materials, from soft biological samples (cells, proteins, DNA, etc.) and polymers [40] to hard diamond containing materials. Modifications of specific SPM hardware can be realized provided common demands, such as the minimization of mechanical vibration and other sources of noise are maintained.

2.3.1.1 Scanning near field optical microscopy (SNOM)

SNOM has been studied by a large number of scientists for measuring optical properties on a subwavelength scale due to the non-destructive nature of the method and the capability of simultaneous topographic imaging with a nanometer scale (but nevertheless, usually lower than the resolution of SFM) [40]. Even 20 years ago Buratto

in [41] wrote “The future for NSOM as a characterization tool in materials science looks bright.” SNOM resolution is not limited by diffraction, and is defined by the aperture of the scanning probe (50-100 nm) [42], which is situated a few nanometers from the sample surface [43].

Near-field optical microscopy uses a sub-wavelength sized aperture which can illuminate the surface. Very sensitive photomultipliers collect the reflected or transmitted light [44]. It allows studying of subwavelength structures and defects in near-surface area of films and heterojunctions. This method rapidly spread to applications in optoelectronics and photovoltaic characterization. There are attempts of scientist to use low temperature SNOM (at temperature of liquid nitrogen and liquid helium) [45].

As noted in [44] it is possible to find additional information about the sample such as polarization, spectroscopic, magnetic properties, transparency, optical thickness, topography, lateral structure, etc. One example is the widely used (in optoelectronics) SiC monocrystal wafer: the defect prolongation is better shown in a SNOM image, whereas the scale of the defect is smaller in the AFM image, and it is observed only in the surface (Fig. 2.1).

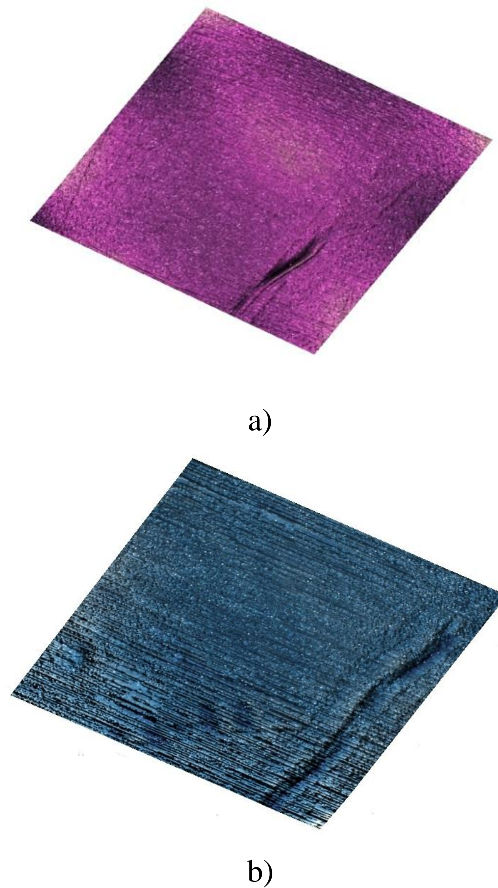

a)

b)

Figure 2.1. a) AFM image of SiC wafer topography and
a) SNOM image in reflection of the same area.
Scanning area of (35 x 35)µm^2.

2.3.1.2 STM

Scanning tunneling microscopy (STM) uses the tunneling of electrons between a conductive sample and a probe at small distances (10nm). Measurements on the basis of tunneling and horizontal scanning were proposed by Binnig et al [46]. STM has better resolution compared to other SPM methods and therefore conducting materials often show higher resolution data from SPM techniques [47]. The scanning allows imaging with high resolution in horizontal direction (lower than 1.0nm) and in vertical direction (lower than 0.1nm) which is enough for single atom detection. The limitation of this method is in materials choice. The scanning surface should be sufficiently smooth and be conductive for making possible tunneling effect between the surface and the probe. It is applicable to metals, their solutions and semiconductors [48, 49].

Using of scanning tunneling microscopy (STM) and spectroscopy (STS) for surface investigation excludes data averaging since it has high resolution (0.1Å) and allows measuring of physicochemical characteristic of single adsorbed particles, defects and nanostructures. At the same time it is difficult to obtain reproducible results in either topography or spectrography. This is connected with thermal drift and soiling of the probe and changing of charge state of defects. For this reason, drastic improvements in STM and STS methods are needed for practical applications [50].

The main set-up used in this work for scanning probe microscopy is the Ntegra Prima, a femtocurrent scanning device (part number ST020NTF) with a thermal stage with variable temperature range up to 450K, adequate for investigation of surface structures of SiC [50]. Typically used parameters for scanning were: scanning frequency 0.2-0.5Hz; cutoff frequency of low-pass filter for signal height ADC is 100Hz-300Hz. At room temperature, STM-images of the surface of wide bandgap semiconductors are not clear and there are a lot of measurement artifacts .Figure 2.2 shows the STM image of heated SiC wafer surface. The sufrace area is full of defects caused by broken chemical bonds, nevetheless there is a similarity to data of [52] which chematically describes atomic sequences (Fig.2.3).

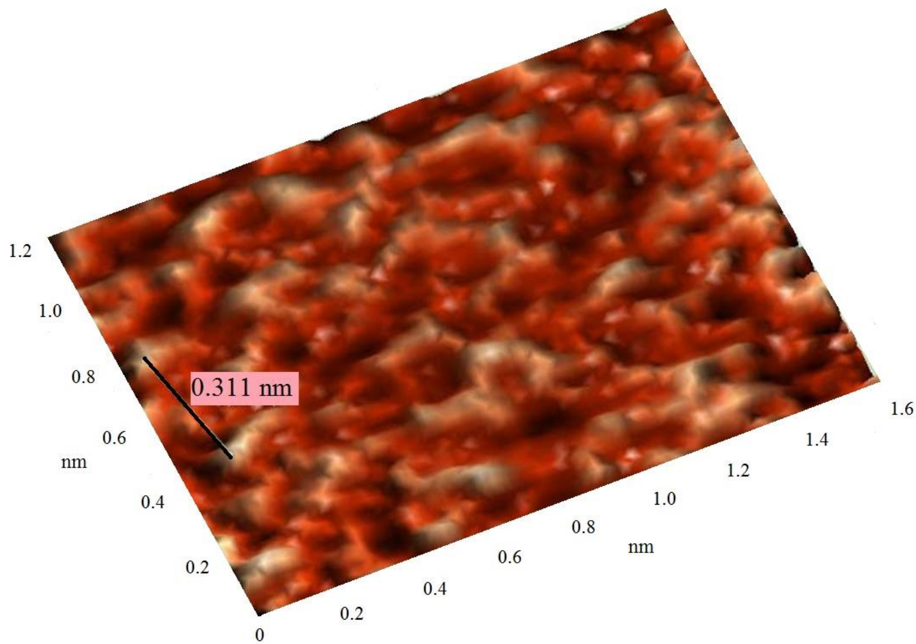

Figure 2.2. STM image of SiC monocrystalline wafer [51].

For comparison we can take a look to [52] where the author describes the position of atoms for 2H polytype of SiC (Fig. 2.3): the dots in the corners of hexogon represent atoms. The same is observed in figure 2.2, where the peaks of tunnel current noted position of the atoms on the surface.

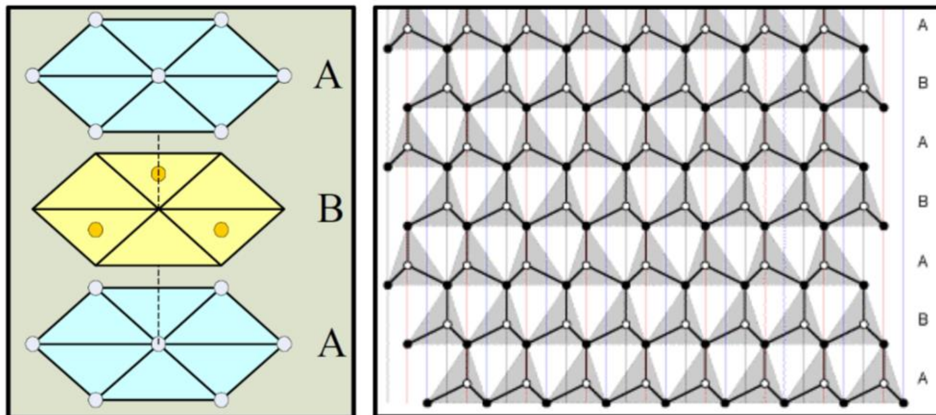

Figure 2.3. Separation of polytype and the sequence of the atomic layers of moncristalline 2H-SiC [52].

2.3.1.3 Spectroscopy

Scanning tunneling spectroscopy (STS) is the most well-known SPM tip based spectroscopy method, it allows to probe the local electronic density of states, which depends on the surface reconstruction, composition and doping in single crystal materials (and is more complex in polycrystaline materials) at one point of the sample. This is an informative method for the study of contacts or areas of localized states, which allows to obtain on-the-spot characteristics. In this case the tip influences a certain point of the specimen and acts as a sensor to register the response. There are also variations on SPM tip based spectroscopy: force spectroscopy which allows to study mechanical properties (Young's modulus, adhesion, hardness), and electrical spectroscopy for definition of work function of surface, bond states etc. [48].

2.3.1.4 Lithography

Nanolithography is an important process in the design of nanostructures for electronics (for example organic thin-film transistors [53]). SPM lithographic techniques are capable of making nanometric scale features [54]. Lithography can be carried out by using force or electric interaction between the sample surface and the probe. When the tip is in a contact with the surface, structures are created by elastic and plastic deformations of the substrate [55] (Fig. 2.4). For electric lithography, modifications are achieved by changes in the material conductivity and humidity during AFM anodization, which strongly affect the lithography [56] and thus should be controlled.

Figure 2.4. AFM vector lithography on the piece of compact disc (scan area is 6x6 μm^2)

Since the pressure is dependent on tip area, a sharp tip can easily force its way into the surface of a soft material.

2.3.1.5 AFM

2.3.1.5.1 AFM modes assignment

The modes of AFM could be distinguished by their dependence on distance between the probe and surface. The mode should be chosen considering sample properties (hardness, stability to local influence of probe) and the probe (parameters given in product specification). The chosen mode also defines further measurement possibilities such as local electrical, magnetic, mechanical (indentation, phase distribution) surface characterization.

- *Contact mode*

If the probe has direct contact with the sample, actually touching the surface then the contact mode is chosen. Obviously this mode is not suitable for soft or easily damaged samples. All contact techniques for detection of local elastic properties use tip-sample contact stiffness [57].

- *Tapping mode*

Intermittent (semicontact or tapping) mode uses probe oscillations and detect shift of oscillation parameters (amplitude, phase, frequency) to detect morphology features. Intermolecular interaction forces between the tip and sample [58] are responsible for imaging.

- *Non-contact mode*

Non-contact mode is also a dynamic mode and applicable when high attractive forces are present [32]. Non-contact atomic force microscopy overcomes limitations of lateral resolution of force microscopy [59]. The “probe-sample“ distance depends on time in this mode and the distance between the tip and the surface is around 50–150Å [60].

2.3.1.5.2 Lennard-Jones curve

Since the distance between probe and the specimen is extremely small (atomic distance) the interaction in this system could be described by a Lennard-Jones potential curve [61]. This potential combines the attractive van der Waals (long range) and repulsive atomic (short range) forces [62] and is shown in Fig. 2.5.

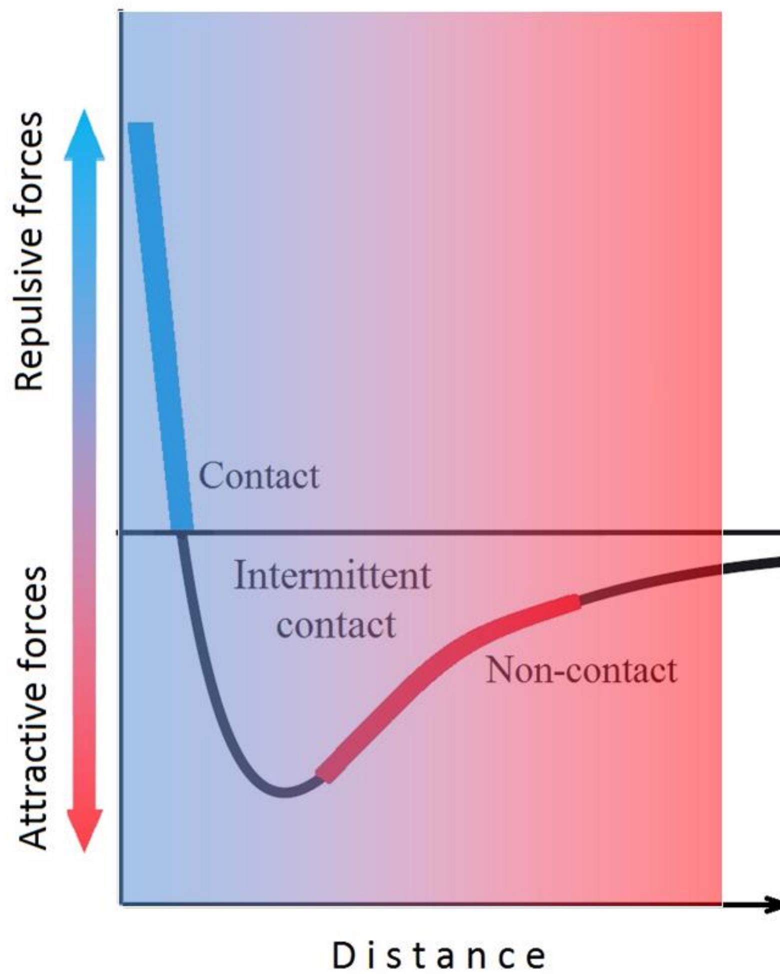

Figure 2.5. Lennard-Jones potential curve [32].

2.3.2 Probes

20 years ago it was noted that the highly individual and even changing characteristics of AFM tips interfere with the quality of the surface image [63]. In spite of a lot of studies in this field there is still a problem of the proper AFM tip choice. Some classification of AFM probes is given in the table 2.1 (according to literature review for today), since there is a continuous progress in tip design it cannot be considered as comprehensive.

Table 2.1. SPM probes classification

Type of probe	**Preparation**	**Properties**	**Application**
W wire probe	electrochemical etching processes	low cost, high stiffness and elastic modulus	surface topography, electrical measurements
Pt wire probe	cutting, electrochemical etching (polishing)	does not easily oxidize	surface topography, electrical measurements
Cantilevers with silicon tip	micromachining could be modified by FIB	resonant frequency uniform geometry, low cost	surface topography, mechanical measurements
Cantilevers on nanostructures (Whiskers)	vapor–liquid–solid mechanism	high aspect ratio	surface topography
Cantilevers with conductive probes	deposition and patterning	conductivity of the tip	surface topography, electrical measurements
Cantilevers with magnetic probes	deposition	magnetizability of the tip	surface topography, measurements of magnetic characteristics

2.3.3 Types of AFM sensors

There are several technologies to detect mechanical reaction of "tip-sample" system. The deflection of a cantilever or changing of its resonance frequency could be realized by piezo techniques, optical methods, etc. [48]. The sensors realized on piezo technique represent tiny piezoceramic tube with conductive electrode inside. The probe in this case could be easily prepared by electrochemical etching. This allows fast preparation and sharpening of tips with quite cheap materals such as tungsten wire and hydroxide. The optical detection methods realized by a laser-probe / photodiode system. In this case the light reflected by the back side of the cantilever is important. The movement of the laser beam which is reflected from the probe is registered by a photodiode.

2.3.4 Artifacts

It is necessary to take into consideration the artifacts of SPM measurements which are caused by interaction of the device components and the sample. The study of artifacts helps to carry out more reliable measurements. Some factors add parasitic information to measured data and degrade achievable resolution [32]. These factors present difficulties in imaging on the nanoscale and join up signal with parasitic artifact data produced by different sources [64]. Below several common scanned probe artifacts are discussed.

2.3.4.1 Artifacts caused by probe

Tip condition, its shape and size affects the AFM image. AFM tips can result in distorted images of actual surface geometry [65]. An AFM image is forming serially line by line and it limits the speed of microscopy in comparison for example to optical techniques [66]. The shape of the probe also influence the scanning image, especially at the edges of features (Fig. 2.6, 2.7). Figures 2.6 a 2.7 demonstrate possible false imaging cased by obtuse and splited tip (respectively)

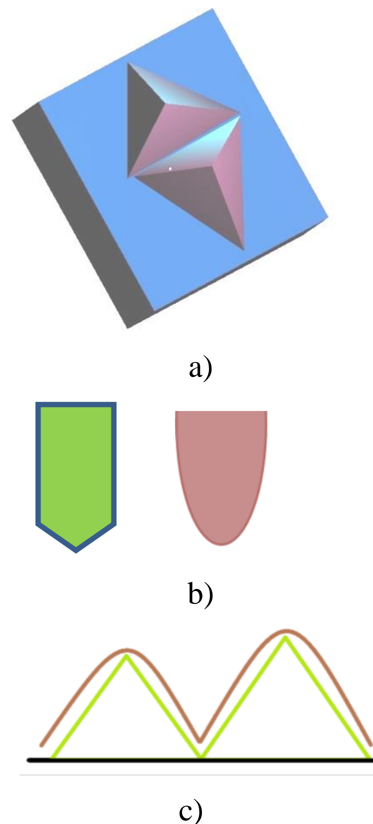

Figure 2.6. a) supposed profile, b) tip shapes, c) possible difference in profile imaging [67].

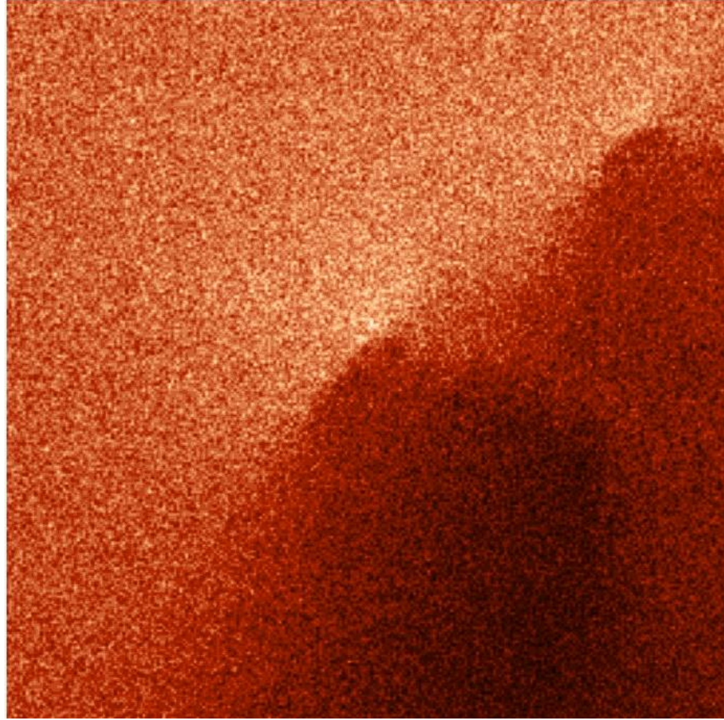

a)

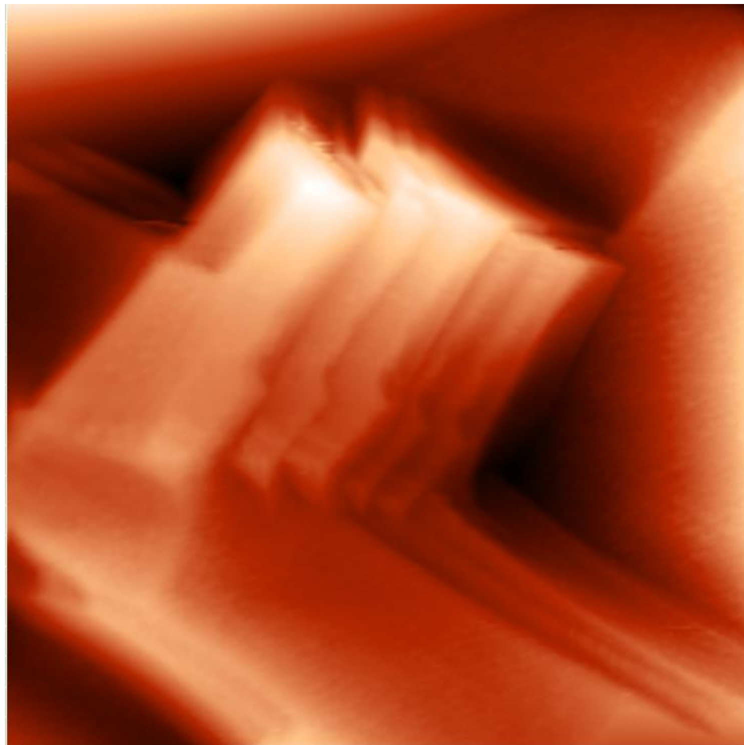

b)

Figure 2.7. a) Imaging of the broken SNOM probe, b) artifact of edge duplication. (scan area is 120x120 μm^2)

2.3.4.2 Artifacts caused by scanner

The scanner is the part of an SPM which is responsible for the smallest steps and displacement in the scanning process. Drive voltage and the resulting displacement of the piezoelectric tube scanner have a non-ideal relation which includes non-linearities, hysteresis, creep, cross-coupling between axes [68], aging and drift [69] The inferior characteristics of piezoelectric tube scanner limits the quality of AFM measurements [38]. There are some possibilities to limit scanner caused artifacts. These methods are based on materials choice, construction variation [38, 70], or further correction and filtering [71]. In reference [38] a separate the z scanner from the xy scanner was used to prevent coupling between xy and z directions, and eliminate background curvature artifacts. An ultra-high-precision positioning stage is one of the keys to the next-generation of nanotechnology [72].

2.3.4.3 Artifacts caused by surrounding

To achieve atomic resolution, vibration isolation is essential [73]. The antivibration system should be realized for better scanning results. It is easy to note that acoustic noise brings its component to the signal, especially if it is sensible at the nanoscale or femtocurrent measurements. The SPM and device under test should be protected from electrical and electrostatic influence and some shelter could be applied. The temperature gradient in ambient also will cause undesired motion of the tiny measuring system probe-sample. The attention to the temperature stability should be taken into consideration when the sample is heating during the measurements. Thermal drift influences STM for heated samples. An example is STM of SiC monocrystal atomic resolution images. Heating allows application of STM to semiconductors since it increases their conductivity [51]. The influence of noise could be decreased by scanning smaller areas of the surface [32].

2.3.5 Free software possibilities

Most tools of AFM and SEM measurements are accompanied by user-friendly software which provides carrying out measurements and further processing of results. But sometimes the most appropriate algorithm for image processing and threshold is absent. Such algorithms must be determined for better interpretation of the results [74]. The efforts of a number of scientific groups are combined in free software programs such as Gwyddion [74], Image J [75] etc. The processing is interesting for both image perception improvement and for recognition and calculation of surface structural charactiristics (roughness, length of borders between phases, etc).

2.4 Using of SEM and SPM in study of solar cells

Performance improvements of solar cell technology supports microscopy progress. AFM and SEM techniques are non-destructive considering solar cells surface properties. Lateral resolution of AFM and SEM are the same, but AFM has better depth resolution [76] and AFM image Z axis data correspond to actual surface feature high and depth. So AFM can be used to zoom in and investigate the features that were found by SEM. SEM and SPM methods for characterization of solar cells recently attracted great attention. It has been shown that there are usefull insights between cell morphology and solar cells properties.

The quantitative analysis of the surface morphology defines the differences between the samples. Morphology of solar cells could be well studied by scanning electron microscope. Mendis et el. noted that electron microscopy is vital for characterizing the microstructure/morphology of solar cells and dedicate the review to this field [77]. SEM images provides information that cannot be found by optical devices and it has sufficient depth of field. Cross sectional views made by SEM can show the nature of shunts in solar cells p-n junctions. SEM is very usefull for characterization of the solar cells surface microstructure [78]. The non-destructive nature of SEM makes it interesting for scanning electron acoustic microscopy for study of morphological defects of polycrystalline solar cells [78].

Surface elements should be large enough for the processing and measuring. In case of SEM it is gray scale range, in case of AFM these are borders, texture, features good enough to be scanning by probe. AFM use image coloration for better perception. Electrical scanning probe microscopy uses conductive probes and describes the electrical function of materials [79] and it could serve to measure the photoinduced current in solar cells. Electric measurements using conductive probes provides observation of solar cells contact area [79].

Conductive atomic force microscopy (C-AFM) characterization GaAs/Ge solar cells has revealed influence of structural defects known as antiphase domains to homogeneity in the conductivity of the layer [79]. Bulk hetero-junction solar cell could be investigated by these method to study photogenerated charge separation along with other optical-electric characteristics [80]. Sensitive to ambient photovoltaic materials samples such as polymer solar cell could be studied in an inert atmosphere [81].

Use of KPFM (Kelvin Probe Force Microscopy) for solar cells allows studying of individual grain boundaries which play a role in defect states, as seen with spatially resolved measurements [82] and microelectrical characterizations in junctions [83], to observe changes of surface potential, which originated from the photovoltaic effect, and voltage distribution along the cross-section of an operating solar cell [84]. Illuminated Kelvin Probe Force Microscopy also reveals interlayer electric fields in bulk heterojunction solar cells [85].

Use of AFM for study of morphology and surface quality is an important field of physics of surfaces, as there are growing demands for micro- and nano-structure diagnostics, since surface roughness in micro and nanoscale influences physical (from mechanical up to electrical) and chemical properties. AFM allows investigation of the interface length between the domains of donor and acceptor in polymer solar cells by the phase image [86].

There is a relation between the statistical surface parameters and properties of the optoelectronic materials surface [87], since performance stability is related to structure and morphology. Detailed wafer characterization results are a useful and important contribution in photovoltaic materials growth and structures preparation [87].

3 SOLAR CELLS TOPOGRAPHY CHARACTERIZATION

This chapter is devoted to the description of solar cell topography and choice of the method for surface study. It is important because the surface condition can predefine the behavior of both a heterojunction and the efficiency of a device. A detailed description of solar cell morphology is given in this chapter. The impact of surface structure to solar cells performance, including the description of hydrophobic and self-cleaning surfaceswhose transparency and reflective properties are essential to the design of solar panels.

3.1 Types of solar cells

A solar cell could be classified on the basis of different characteristics: by size, by the method of preparation, by the basic material, by price, etc. The choice of material depends on the area of application. For example, polymer solar cells are mechanically flexible, light and cheap [87], but have inferier properties for space applications due to meteoric erosion, thermal impulse, and radiation hardness [88]. For space applications, a multi-junction architecture are typically used. Tandem solar cells prepared by pulsed magnetron sputtering and RF magnetron sputtering were reported in [89].

The combination of different band gap materials (according to current literature) allows using a larger fraction of the solar spectrum (Fig. 3.1). It is well known that portions of the solar spectrum are absorbed by the upper layers of the atmosphere, such as short wave UV radiation. However, consideration of wide band gap semiconductors will help to use even this part of the sun‘s energy for devices which work above the ozone layer.

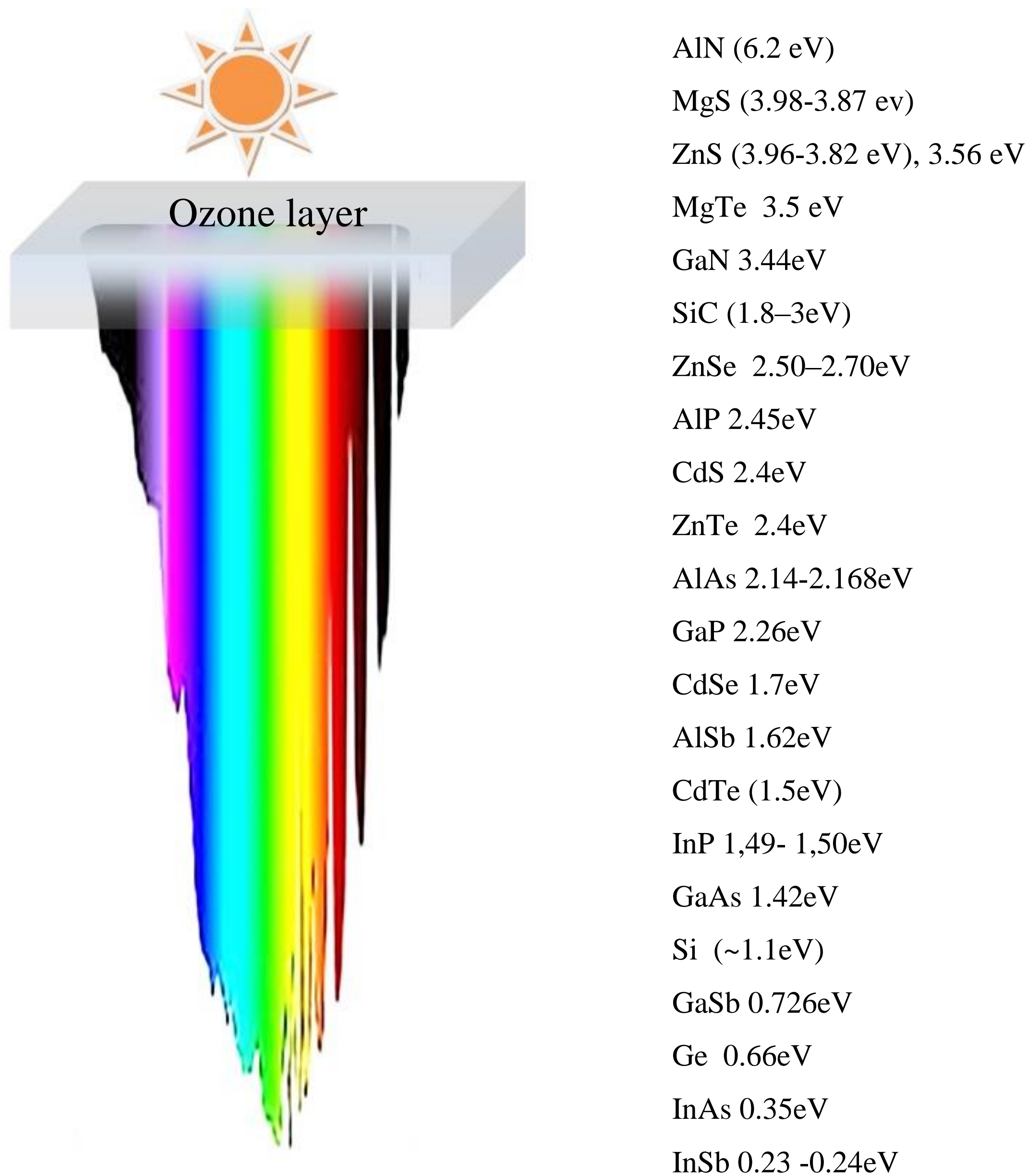

Figure 3.1. Some semiconductor materials and bandgaps which find their optoelectronic application in different light wave range.

3.2 Role of solar cells surface characterization

For optoelectronic device fabrication it is necessary to study every layer during heterostructure preparation. Study [90] emphasizes that surfaces and interfaces are a key problem in the solar cell manufacturing process. Efforts to increase surface absorption and the fraction of absorbed light within the active layers, improving light scattering at the interfaces, and reducing losses should also include the study of surface texture [90, 91, 92].

Surface texturing (roughness) is often used to minimize reflection losses, and is important for solar cells. Improving the performance of solar cells without significantly increasing their cos tis an important goal: texturing reduces reflectance of silicon solar cells from 35% to 11% with minimal added cost [93]. Micro- and nano-scale surface morphology plays an essential role in the properties of electronic materials. The smaller dimension is considered to have a larger influence on the surface condition.

The wide adoption of texturing solar cell layers motivated a lot of studies in this field, both theoretical and experimental. Light losses are huge when the optical system consists of elements with high refractive indexes. The photocurrent is strongly dependent on texturation, as was theoretically and experimentally shown by Dmitruk et al [94].

There are a number of factors that influence solar cell performance: interfaces between different layers, grain boundaries, and point defects due to production processes belong to these factors. Topography influences also contact formation, which was found and statistically described in [95] for silicon solar cells. Light trapping ability, as noted in [96], can be improved by the increased effective path length of scattered light resulting from textured films.

Textured substrates can be used in order to increase the light path within the absorber layer [97]. Surface texture has a critical influence on optical and electrical properties [97, 98]. There are a number of methods to create appropriate texturing, such as: application of nanostructures, vapor–liquid–solid growth of structures, dry etching, lithography, chemical wet etching [98], and variation of parameters in electrochemical film deposition [99]. Yang et al. [97] reported a deposition of solar cells on a modulated surface textured glass substrate and explained that the structure with smoother peaks showed higher performance, due to a lower density of defects. Argon plasma-etching treatment can smooth rough surface morphology, which is sometimes necessary for high-performance solar cells [100]

The dependence of thin film solar cell performance on surface preparation and processing was studied in reference [101]. Even the substrate roughness has a large influence on the properties of the solar cell junction from which they are prepared [102].

Multicrystalline silicon solar cells are cheaper and have good conversion efficiency [98]. But Zeman et al. noted in reference [103] that “while the use of randomly textured morphologies is at present the standard approach to achieve efficient scattering inside a solar cell, scattering of light from periodic textures such as diffraction gratings is an alternative way to manipulate light inside the solar cell.” The effect of different periodic substrate textures on electrical properties of a *a*-Si:H/*μc*-Si:H solar cells was analyzed by simulation in [104]. The light distribution, reflection and dependence on shape of the solar cell surface can be described by geometrical optics [105].

Improvement of solar cell performance can also be achieved by using select materials as intermediate reflectors and choice of layers thickness [106]. Morphology also influences

the electrical characteristics of photovoltaic structures in the spectral range from UV to IR [107] both at the surface and in the interplay of the layers [108]. Increasing the absorption and decreasing reflection is possible by using pyramidal structured surfaces. Acids or alkalines are usually used for to form pyramids on Si solar cell surfaces [109].

Modeling of solar cells provides optimization of the strucuture, identification of the optimal operating point, losses, influences of temperature, angles of light radiation and shading [110] (since in case of shading, solar cells can act as loads without power generation [111]). Optical 2-D and 3-D modeling of *a*-Si:H/*μc*-Si:H solar cells considered in reference [112] shows the textures that can improve optical properties and increase the short-circuit current density of the bottom cell by 97.6 %. Random nano-textured interfaces are essential for light scattering modeling of thin films solar cells [112] Many programs for solar cell modeling were developed in universities and research institutes, they are mostly free for download and the core of these programs are Poisson‘s equation and the continuity equations for electrons and holes [113]. Such a model is used in reference [114], which predicts the dependency of short circuit current on bulk heterostructure solar cell device parameters.

3.3 Solar cells surface texture

Surface texturing (roughness) is often used to minimize reflection, and is important for solar cells. The performance of solar cells demands improvements: only the texturing reduces reflectance of silicon solar cells from 35% to 11% [93]. The sizes and shapes of surface morphology play an essential role in behavior and properties of materials in micro and nanoscale. The smaller dimension is considered the larger is influence of the surface condition.

Demands of texturing layers caused a lot of studies in this field both theoretical and experimental. Light losses are huge when the optical system consists of elements with high reflective indexes. The photocurrent depends on texturation, as it was theoretically and experimentally proved by Dmitruk et al [94].

There are a number of textural factors that influence solar cells performance: interface of different layers, grain bounderies, point defects of production belong to these factors. Topography influences also the contact formation which was found and statistically described in [95] for silicon solar cells. Light trapping ability as noted in [96] could be improved by the prolonged effective path length of the scattered light and textured films could be applied for this purpose.

Textured substrate could be used in order to increase the light path within the absorber layer [97]. Surface texture has a critical influence to optical and electrical performance [97, 98]. There are a number of methods to create appropriate texturing such as: application of nanostructures, vapor–liquid–solid growth of structures, dry etching, lithography, chemical wet etching [98], variation of parameters in electrochemical films

deposition [99]. Yang et al. [97] reported a deposition of solar cells on a modulated surface textures glass substrate and explained that the structure with smoother peaks shows the higher performance due to lower amount of defects. Argon plasma-etching treatment makes smoother rough surface morphology what sometimes is necessary for high-performance solar cells [100]

The dependence of thin film solar cell performance on surface preparation and processing was studies in [101]. Even the substrate roughness for the solar cell junction preparation has a large influence on the properties [102].

Multicrystalline silicon solar cells are cheaper and have good conversion efficiency [98]. But Zeman et al. noted in [103] that "while the use of randomly textured morphologies is at present the standard approach to achieve efficient scattering inside a solar cell, scattering of light from periodic textures such as diffraction gratings is an alternative way to manipulate light inside the solar cell."

Effect of different periodic substrate textures on electrical properties of a *a*-Si:H/*μc*-Si:H solar cell was analyzed by simulation in [104]. The light distribution, reflection and dependence on shape of the solar cell surface could be described by geometrical optics [105].

Improvement of performance can also be achieved by using some materials as intermediate reflectors and choice of layers thickness [106].

Morphology influences the electrical characteristics of the photovoltaic structures in spectral range from UV up to IR [107] both for surface and the interplay of the layers [108].

Increasing of absorption and decreasing of reflection is possible by using of pyramidal structures. Acids or alkalines are usually used for pyramids formation on the Si solar cells surface [109].

Modeling of solar cell provides optimization of the scheme, definition of the optimal working point, losses, influences of temperature, angles of light radiation and shading [110] (since in case of shading solar cell can work as loads without power generation [111]). Optical 2-D and 3-D modeling of *a*-Si:H/*μc*-Si:H solar cells considered in [112] shows the textures that can surpass optical properties and increase the short-circuit current density of the bottom cell to 97.6 %. Random nano-textured interfaces are really essential at light scattering modeling of thin films solar cells [112]

A lot of programs for solar cells modeling were developed in universities and research institutes, they are mostly free for download and the core at these programs are Poisson equation and continuity equations of electrons and holes [113]. Such the model in [114] exhibits the dependency of short circuit current on bulk heterostructure solar cell preparation parameters.

3.4 Hydrophobicity and self-cleaning of surface

A study of textured morphologies is also motivated by the need to improve the self-cleaning and hydrophobic properties of solar cell surfaces, to reduce the influence of weather agents, while simultaneously absorbing the maximum range of of the solar spectrum [115, 116]. Hydrophobic and hydrophilic surfaces can be characterized by the angle between the site of a water drop and the surface, the so-called contact angle (Fig. 3.2). Hydrophobic and antireflective disordered sub-wavelength silicon structures with surfaces prepared by dry plasma etching are one very promising technology for Si-based solar cells [117].

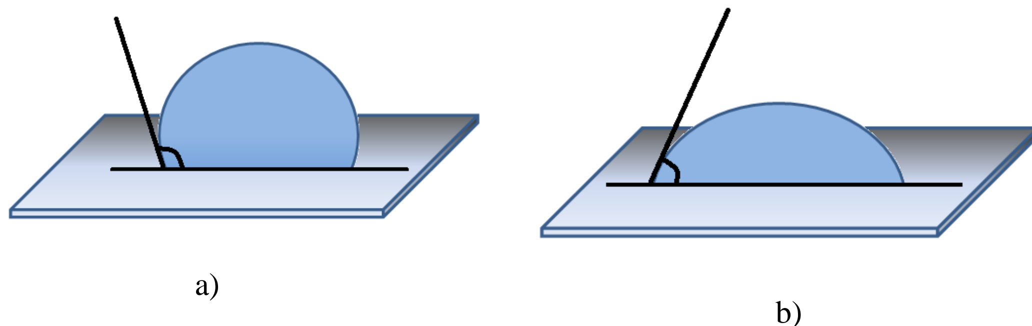

Figure 3.2. a) Hydrophobic surface (angle $> 90°$), b) hydrophilic surface (angle $< 90°$).

Environmental erosion can change optical properties of the surface of a solar cell, therefore cleaning is essential [118]. Some structures found in nature demonstrate such outstanding integrated optical and mechanical properties of surface they have inspired solar cell designs. An example of such a structure, which exhibits near perfect light absorptivity, was used as template for solar cells by Wang Zhang et al [119] and Di Zhang et al [120]. Further possibilities for optical structures based on bio-inspired topographies are reviewed in references [121, 122]. A variety of surface structures [32] demonstrate hydrophobicity (Fig. 3.3) and hence self-cleaning of the surface; these structures are applicable in different fields due to interconnected dependence of surface condition, optical quality and mechanical stability. These structures could be described by statistical instruments [123] and could be random, regular or quasi-regular.

a)

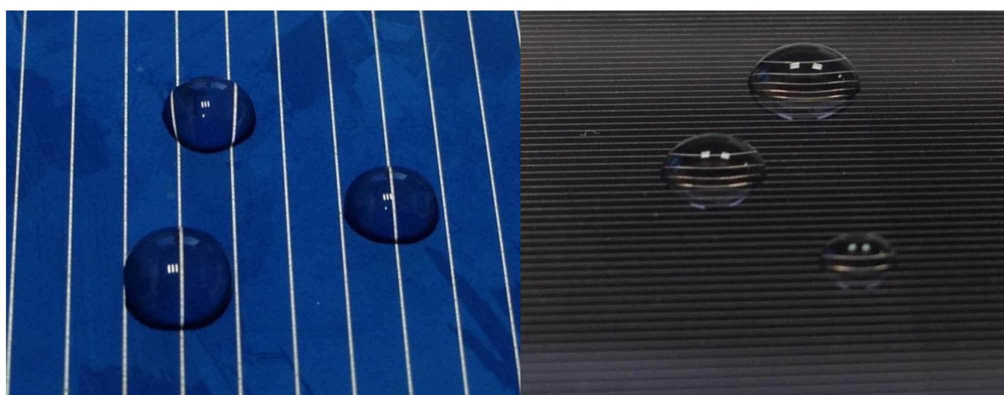

b)

Figure 3.3. a) Demonstration of hydrophobic surfaces in nature (left: butterfly wing, right: peacock feather), b) Polycrystalline silicon solar cell and GaAs solar cells with a drop of water on the cell surface.

In summary, geometrical factors of solar cell surface morphology play a role in the contact angle between the surface and liquid [124]. The efforts of scientists and engineers to find a suitable template for optoelectronic devices which take inspiration from nature once again show the importance of morphology and surface condition in structures preparation for optoelectronics application.

3.5 Topography characterization

In the following experiments we have used two types of microscopy (SEM and AFM) for evaluation and measurement of substrates, thin films and solar cell surfaces micro-geometry. SEM allowed to study large areas of the solar cells with considerable surface roughness (more than 10µm) and AFM was carried out on relatively smooth areas, but is truly 3D measurement. Currently, probe methods are more applicable for studying solid materials surfaces. SPM is a 3D surface morphology technique that provides quantitative information about surfaces, and characterizes roughness of the surface, and

sizes of morphological features, such as grains. Numerical evaluation of the morphology allows statistical estimates of surface roughness.

3.5.1 SEM and AFM of polycrystalline solar cells

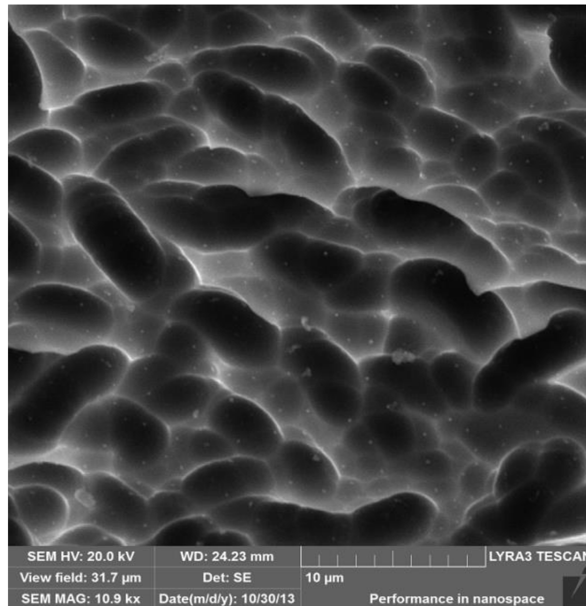

Figure 3.4. SEM of polycrystalline solar cell.

Multicrystalline solar cell performance depends on the types of grain boundaries present, as some of them reduce the cells efficiency. Deflections in surface morphology could be caused by mechanical stress between solar cell layers. This stress affects electron mobility and diffusion length, band structure, and surface passivation. Both SEM (Fig. 3.4) and AFM (Fig. 3.5) types of microscopy are suitable for characterization of polycrystalline solar cells, the elements of texture are well distinguished even without any special preparation of the sample.

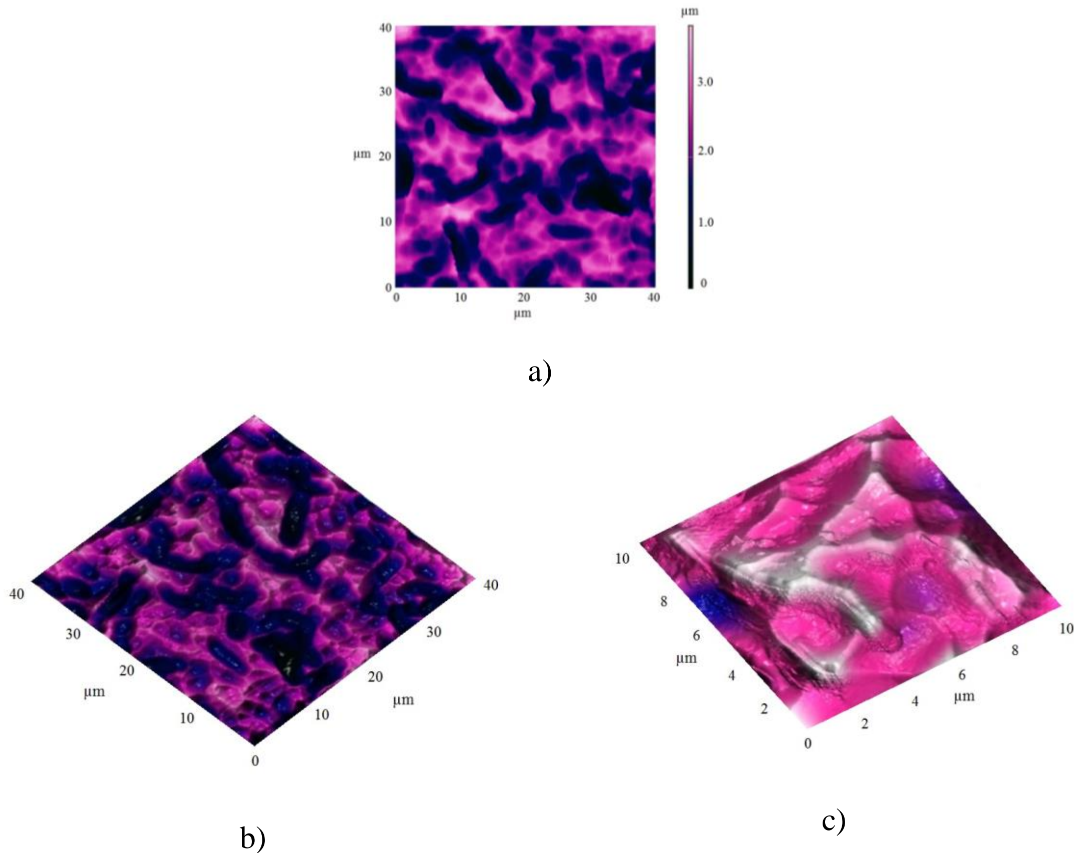

Figure 3.5. AFM of polycrystalline solar cell: a) 2D image, b) 3D image, c) 3D image of smaller area.

Figures 3.5 a-c show topography of polycristalline solar cell. The scale at figure 3.5a shows real values of the highs and depths of the surface features. These features are presented with different magnification in figures 3.5 b and 3.5 c. They are differently oriented silicon graines, which also contain impruties and defects.

3.5.2 AFM of GaAs solar cells

The sample of GaAs cells exhibited smoother topography. For this reason the AFM, which has higher magnification, was suitable for scanning the surface (Fig. 3.6). Furthermore, in this case it was quite useful to apply semi-contact error mode for better perception of the surface features (Fig. 3.7). The measured AFM data generates an array (image) of the investigated topographic data and allows fast access to valuable data.

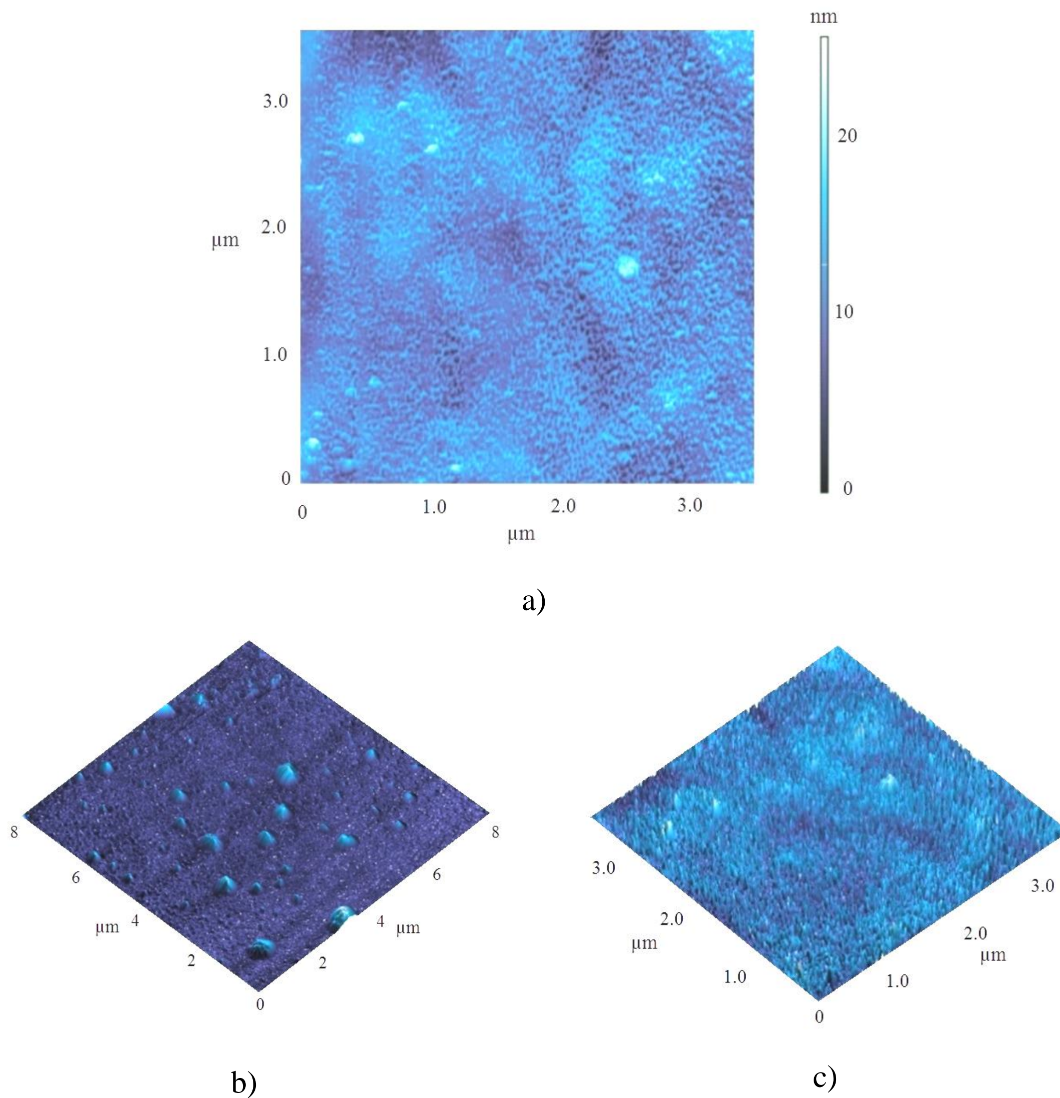

Figure 3.6. AFM of GaAs solar cell: a) 2D image, b) 3D image, c) 3D image of smaller area

Figures 3.6 a-c show topography of commersionaly available solar cell on the basis of GaAs. The high of surface featrures is about 25-30 nm (Fig. 3.6 a). Figures 3.6 b, c present topography of different scan areas (8x8) µm and (3.5x3.5) µm correspondingly. Decreasing of scan area allows obtaining of higher resolution and makes visible smaller features of the surface.

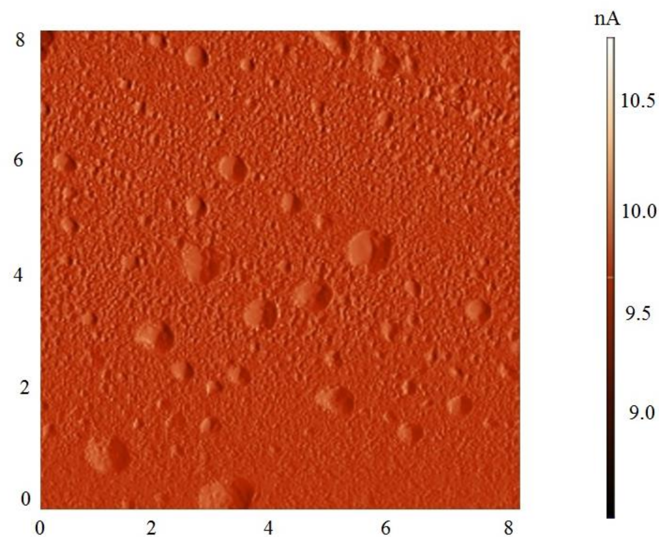

Figure 3.7. Semi-contact error mode image of GaAs solar cell.

3.5.3 Processing of the topographic images

Statistical processing of AFM images provides statistical information about topography. An analysis was carried out using our AFM data for AlN films in cooperation with Talu´s group. In reference [91] the authors studied the aspect ratio effect on the reflectance and noted that higher aspect ratios provide advantages. Optimized periodic textures can surpass optical properties of random textures [90]. Fractal analysis allows to quantify morphological variance, and identify the links between the fractal dimension and the physical processes. Edges of grains influences recombination, current, and diffusion, and should be studied in combination with local characteristics. Slopes, holes, heights, valleys, scratches, and contact areas influence the light wave behavior at the near surface area. Such structures traps light waves and change the direction of their propagation. AFM and SEM images can be thresholded to get information for evaluation of discrete areas with certain levels within a given range. An example which was carried out for both a polycrystalline and monocrystalline solar cell is shown in figure 3.8. ImageJ software [75] was used for evaluating geometrical elements (areas, sizes, lengths) [42] of the topography.

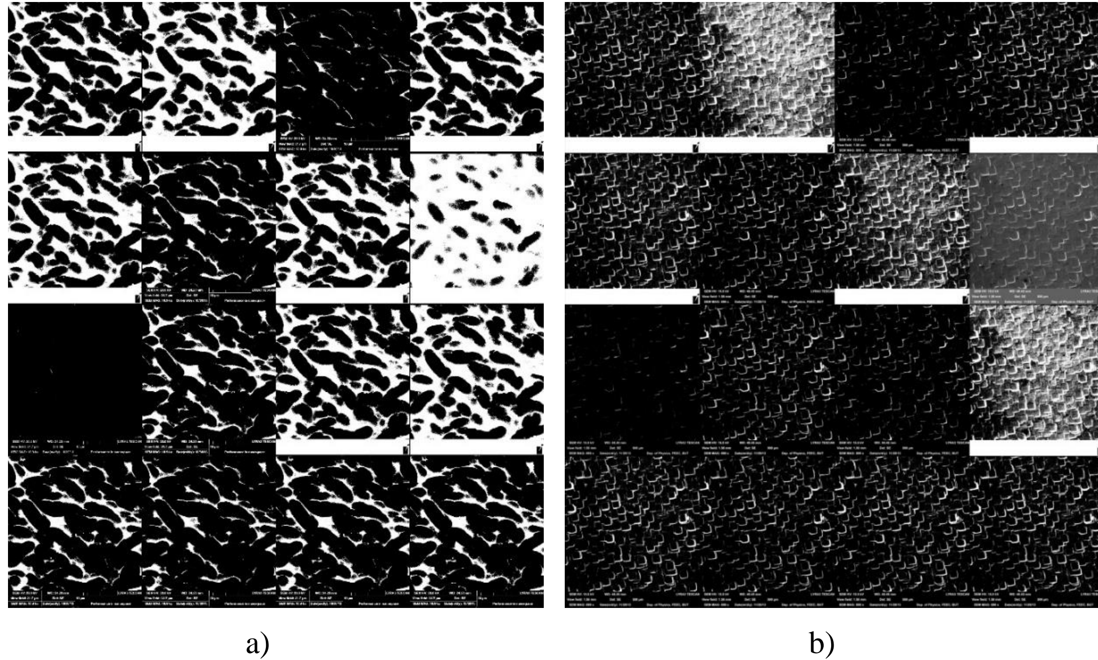

a) b)

Figure 3.8. a) Polycrystalline and b) monocrystalline solar cell image thresholding, demonstrating geometrical features of the topography.

In the case of solar cells, statistical parameters such the volume fracture parameter give a measure of materiál properties. By these well known microscopy methods it is possible to obtain both qualitative and quantitative measures of a surface. Qualitative data include the distribution of the values at the surface and quantitative their precise values. Texture is a measure of surface roughness. Watershed segmentation is helpful when it is necessary to divide and to count the texture features. This is a really interesting method when surface elements are barely recognized, for example in the case where image quality is lacking.

This method receives its‘ name because of lines which divide topography elements. They look like the channels where water trickles down from the peaks of features. But this method is not suitable for overlayed features or to extremely rough morphology. A comparison of wave characteristics of light with moving water waves allows a good description of surface topography. As in the case of water waves, interference, reflection and transmission depend on the feature sizes of the sample.

The morphology of grains (roundness and sphericity) is important in textural characterization. Watershed segmentation (Fig. 3.9) was applied here to grain boundary detection in the texture of the solar cells. This helps to carry out statistical analysis and optical texture determination. A large fraction of trapped light and charges lay inside separated phases and defects in morphology.

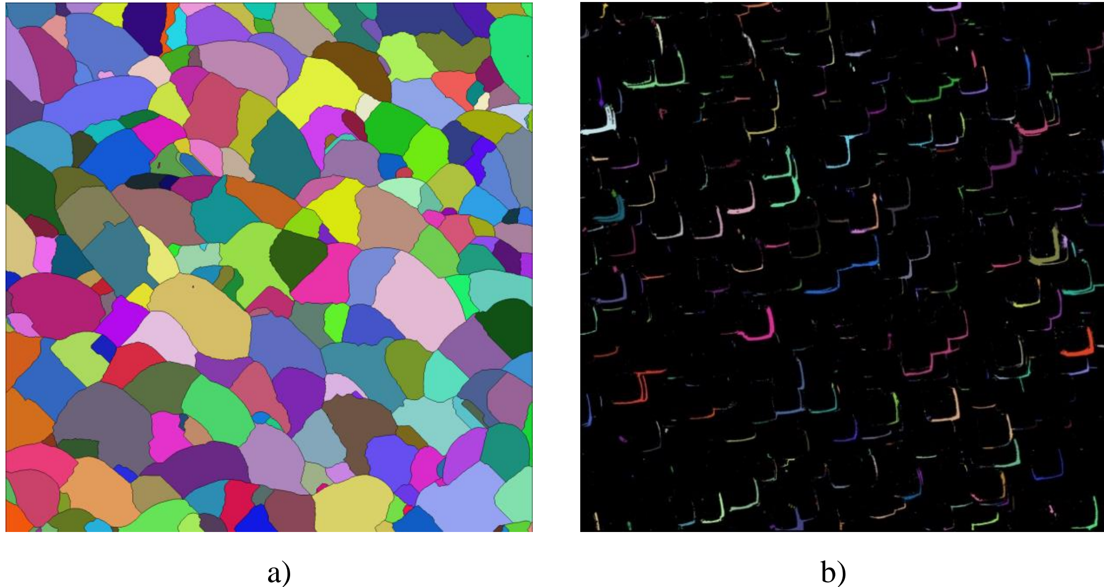

a) b)

Figure 3.9. Watershed segmentation of the surface topography of a) polycrystalline and b) monocrystalline solar cells.

These figures show organization of silicon graines in the material The shape of grain borders are similar in monorcristalline solar cell (Fig. 3.9 b) and are quite various in polycrystalline sollar cell (Fig. 3.9 a).

These processing methods are conducive to the realization of better morphology. The choice of method should be adapted to the specifics of the sample. The right choice of devices, methods and modes for a given field of science is important for measurement results.

3.6 Contacts to solar cell

Shadow effect due to metal contacts reduces solar cell performance [125] and limits semiconductor absorption [126]. The efficiency of energy conversion strongly depends on the total and local fractions [127]. Metal contact design is still one avenue for improving the cell efficiency. Optimization (choice of geometry) of both front and back solar cell contact design can help to achieve beneficial electrical properties, maximize current collection, and minimize the series resistance [128].

In this part of solar cell fabrication, SEM analysis plays a very important role which is shown by a number of studies, such as: investigations at the metal-semiconductor interface in screen printed metal contacts, characterization of solar cell metallization processes, surface morphology before and after processing of contacts [129,130]. Because of the limitations of AFM mentioned above, SEM is more suitable for contact studies. SEM imaging provides good quality information about layer structure and contact quality.

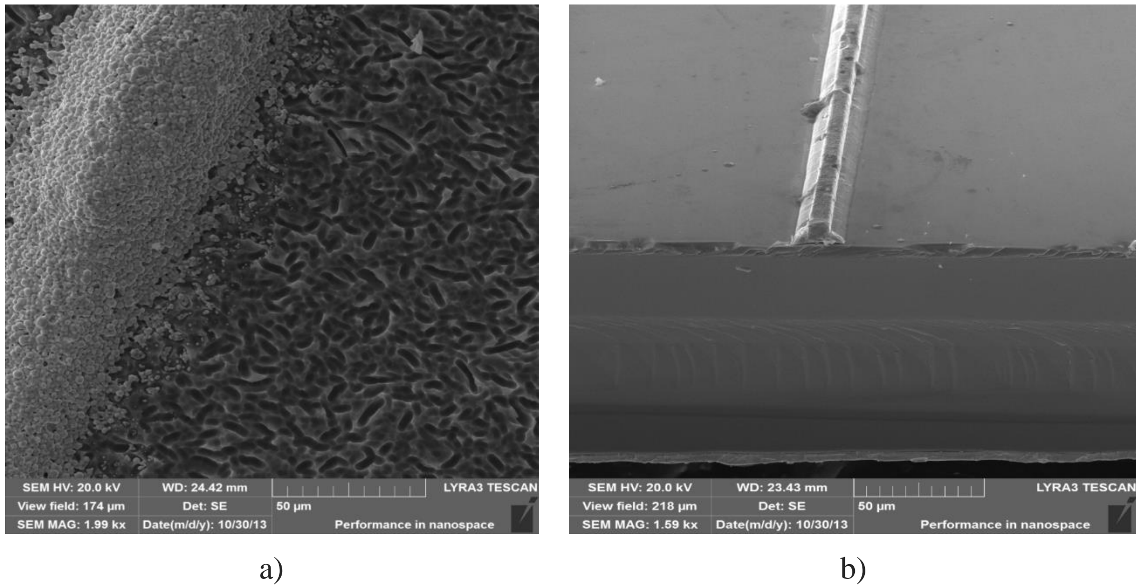

Figure 3.10. Metallic contacts to a) polycrystalline solar cell and b) to GaAs solar cell.

Figures 3.10. give information about size and shape of the metallic contacts. Figure 3.10a shows the contact from the surface of the polycrystalline solar cells. Figure 3.10b shows the contact to GaAs solar cells and from face side. Both images show homogenious of the contact along the surface and presence of defect area.

4 LOCAL TOPOGRAPHY OF OPTOELECTRONIC SUBSTRATES PREPARED BY DRY PLASMA ETCHING PROCESS

In this chapter the etch rate of silicon carbide and aluminum oxide were studied as a function of the angle of etching material and flow of plasma. Al_2O_3 and SiC are important materials in the design of optical and electronic devices and the topography of the wafers has a large influence on the device quality. Argon was used for the dry etching of Al_2O_3 and SiC wafers. The wafer slope for highest obtained etch is obtained. Atomic force microscopy was used for good morphology control of etched wafers. Statistical and correlation analysis was applied to estimate the surface condition. Interferometry allowed to control etching rate. This chapter is based on the paper published in reference [B1].

4.1 Dry etching

Generally used chemical wet etching is an isotropic etching and selective grain-boundary etching, but it seems to be inappropriate for preparation of thin film structures. Here a dry etching is a more desirable method. Dry etching means the removal of material from a rough surface by bombardment of ions resulting in a reproducible, uniform smooth surface (Fig.4.1). Simple sputtering is non-selective elimination of surface atoms due to plasma-induced non-reactive gas ions which vertically impinge on the surface of the substrate without any method to control the etch print. The anisotropy is a typical quantity of importance for dry etching.

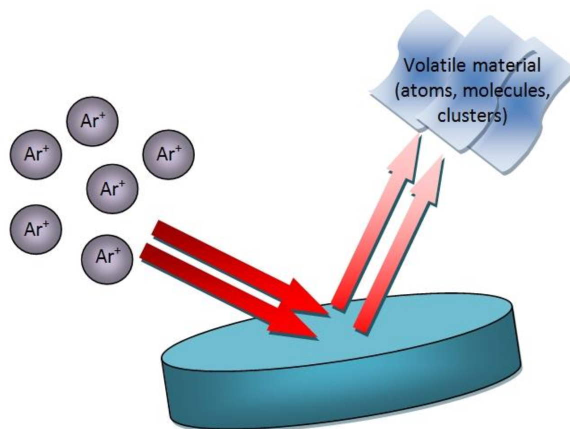

Figure 4.1. Dry plasma etching of the surface.

A choice of etching processing depends on the nature of the material and the required characteristics of the treated surface. Chemical etching provides removal of material from all directions, while physical etching allows precise size control of the processing area. As opposed to chemical etching the physical treatment does not leave the products of the reaction at the surface. There are a number of physical etching techniques useful in semiconductor technologies. Dry etching was considered as a wet etching replacement as far back as the last century [131].

The well etched surface should be characterized by an appropriate profile: reduction of polishing defects, impurities and defects. Nevertheless it is necessary to reckon with some surface changing under the influence of ionized atoms of noble gas. Plasma etching is applicable in the case of materials where overcoming a strong bond energy between the component atoms is necessary. Plasma treatment could also be considered as a method for surface modification in semiconductor technology. Such a study was reported by A. Schneider as random surface texturing for photovoltaic applications [132].

Shape, structure and size of topographic features are a significant consideration for optoelectronic semiconductor structure design. Some roughness of wafer morphologies could be observed because of damage produced by the ion bombardments with excessive energy, but it provides both more flexibility because of anisotropy of the process and better reproducibility of the results.

4.2 Materials choice

The quality of substrate is very important for optical heterostructure preparation. It should be smooth and clean. It has to be sufficiently electrically, thermally and mechanically stable. Composition and morphology should be suitable for the application. Defective substrates lead to heterostructure properties variation. For optoelectronic devices it may lead to local heating and further damage.

Substrates of wide band gap materials find their application in optoelectronic devices. As noted in [133] optical applications demand the mean surface roughness from $\lambda/10$ down to $\lambda/20$ of the wavelength used. Physical and chemical properties of silicon carbide and sapphire provide are suitable for a range of electronic and optoelectronic devices such as light emitting diodes, lasers and transistors. They are optically transparent in visible light and have attractive thermal properties. SiC and Al_2O_3 have a number of physical, chemical and mechanical properties that make them attractive for optical applications in extreme environments [134-136].

One of the motivations for our material choice was the study of Dong-Won Kang et al. [137], where Al_2O_3 was described as an antireflection layer to decrease reflection loss in silicon thin film solar cells. Aluminum oxide is used as a solar absorber material in combination with metal, these coatings are represented by multilayer stacks [138]. Silicon carbide (SiC) is an indirect, wide band gap semiconductor, and sapphire an

insulator presently a prospective material for semiconductor heterostructures used in high power, high frequency, and high temperature optoelectronic applications.

Sapphire is aluminium oxide (Al_2O_3) in the purest form with no porosity or grain boundaries, making it theoretically dense. The combination of favourable chemical, electrical, mechanical, optical, surface, thermal, and durability properties make sapphire a preferred material for high performance system and component designs. These materials have a perfect combination of properties which make them conform as good and well-founded replacements to standard materials for optoelectronics. For these reasons the substrate materials processing are of interest and this studies results are useful for improving heterostructures preparation.

High-quality substrate preparation is an important procedure which is necessary for subsequently manufactured heterostructures. The task of dry etching of these materials is relevant because of the limited possibilities of their chemical etches. Hence, surface morphology and etching rate of the dry etched substrates are important parameters.

4.3 Experimental results

Plasma etching is possible either by physical sputtering or by etching of chemical reagents. In order to have purely physical etching argon plasma was used (Fig.4.2). A standard vacuum deposition system was used. The experiment was carried out at argon atmosphere at pressure $3\div4\cdot10^{-2}$ Pa for 10 min. The substrates were initially prepared by ultrasonic cleaning. The substrates of SiC and Al_2O_3 were processed by discharge rate 150 mA in the ion source and voltage varying from 3 kV up to 6 kV. Since these materials have a relatively high resistance, a radio frequency field was applied. The substrates were initially prepared by ultrasonic cleaning.

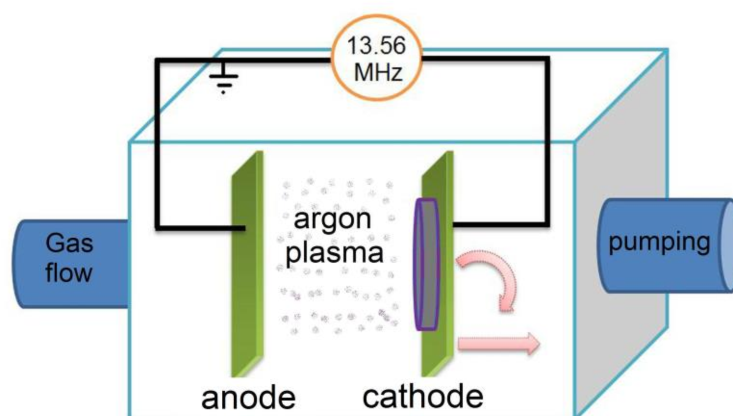

Figure 4.2. Scheme of physical dry-etching device.

The tilt angle between etched substrate and defocused beam of argon ions is a very important parameter of investigation because it also makes differences in the process results (Fig. 4.3). The inspiration for this experiment was taken from the study from [139] where authors noted that tilting optimize the radial uniformity.

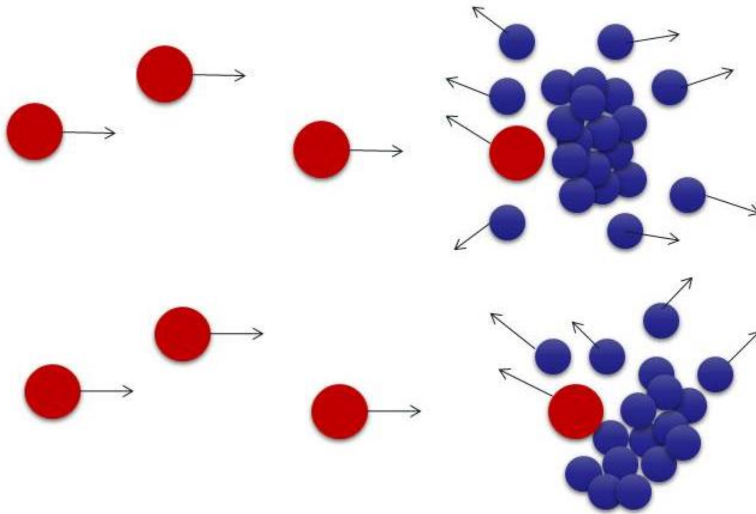

Figure 4.3 Demonstration of the angle dependent cleaning. The slope of the substrate influences the trajectory and amount of etched material from the surface.

4.4 Etching rate

Light interference is a useful and important tool for surface characterization. The Linnik interferometer is easy to operate and allows measuring of topography imperfections (width and depth of holes, scratches, etc.) with accuracy comparable to the wavelength. In order to use this method a part of the sample was isolated from plasma by shield. As a result of interferometric measurement, it was found that the maximum of etching rate is at the 40° tilt (Fig. 4.4). For the measurement we used this quantity.

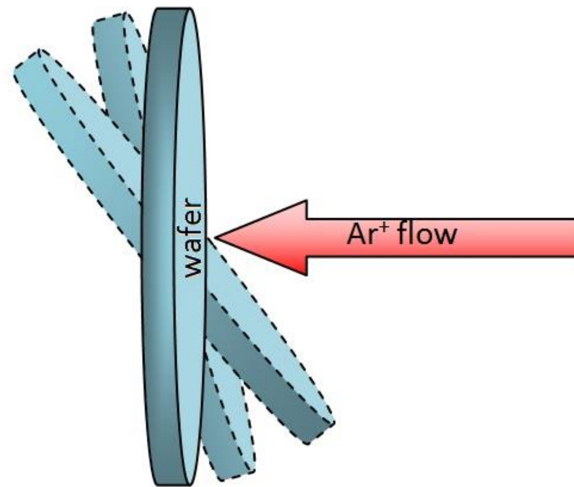

a)

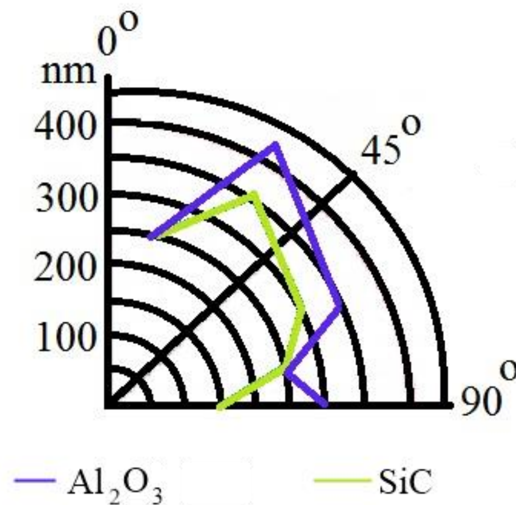

Figure 4.4. a) Scheme of wafer position to argon flow,
b) angular dependence of the sputtering rate of Al_2O_3 and SiC.

4.5 Atomic force microscopy

Atomic force microscopy (AFM) is a direct method for measurement of the surface topography and the data can be used to calculate the surfaces statistical characteristics. It helps that AFM is a nondestructive testing of the surface, indicating even tiny changes in topography. The scanner used was a 120 µm x 120 µm NTEGRA Prima microscope (NT-MDT). The tapping mode was used for scanning. The NSG01 DLC cantilevers, with typically 6 nm curvature radii were used. Figures 4.5 and 4.6 show the behavior of the topography before and after ion etching. The images show the decreasing of the

surface roughness of the studied substrates. The comparison of Figures 4.5 and 4.6 also shows the reduction in the number of major irregularities of mechanical treatment.

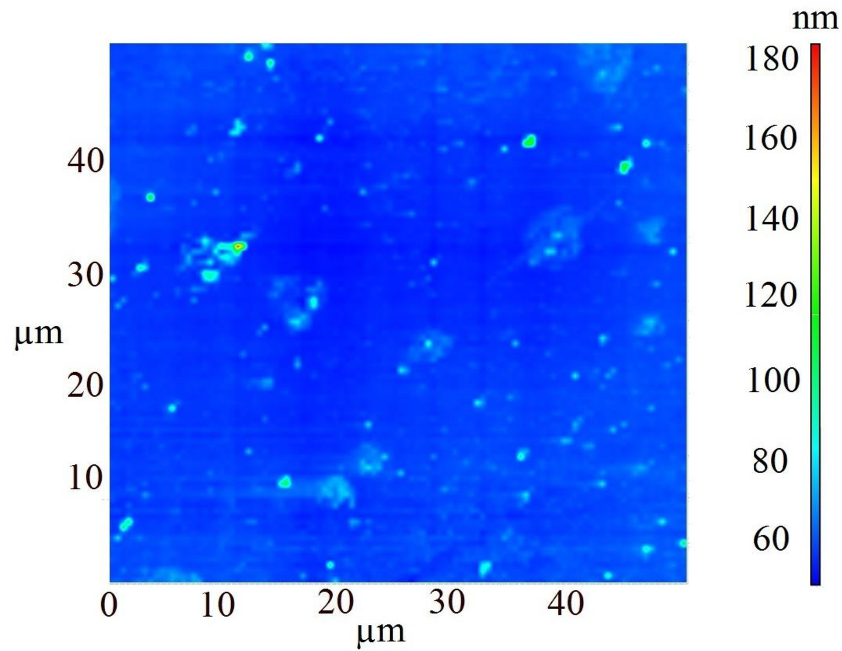

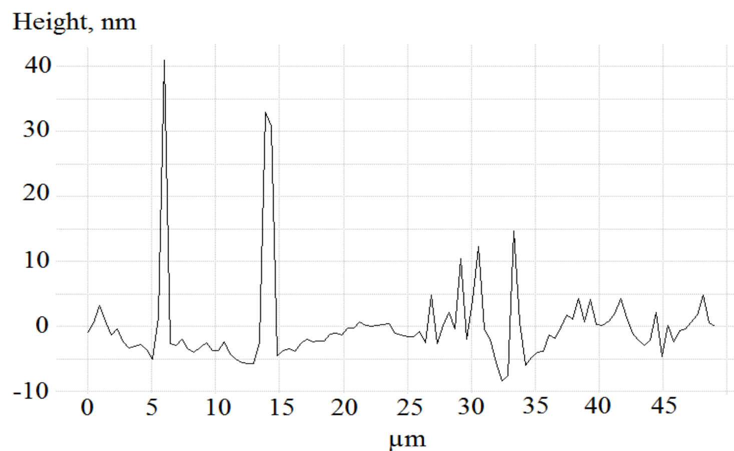

Surface topography and horizontal profile of Al_2O_3 with following characteristics:
Scan area 50x50µm,
Max – 251 nm,
Root Mean Square – 8nm.
a)

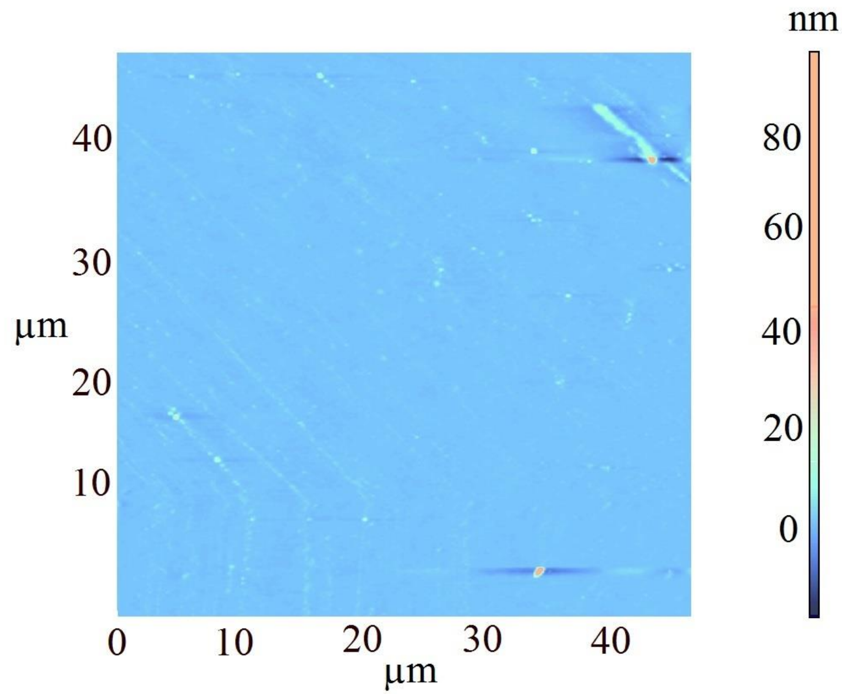

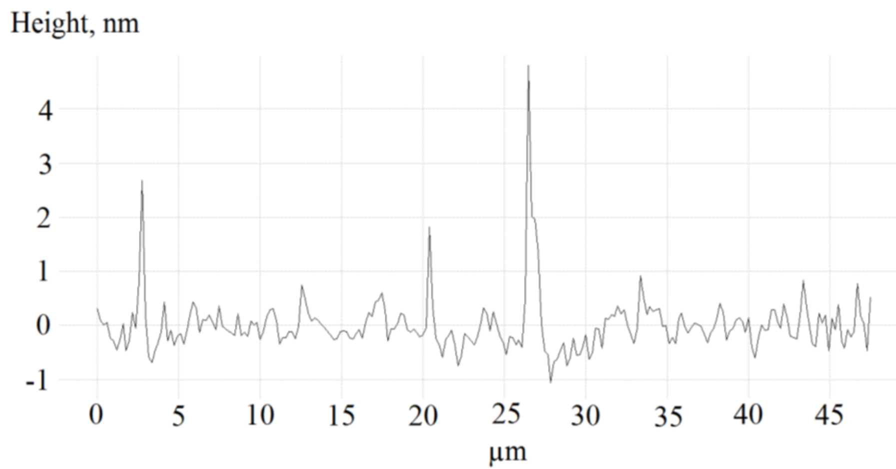

Surface topography and horizontal profile of Al_2O_3 with following characteristics:
Scan area 50x50μm,
Max - 16nm,
Root mean square - 1nm.
b)

Figure 4.5 Surface topography and horizontal profile of Al_2O_3 a) before, and b) after dry etching.

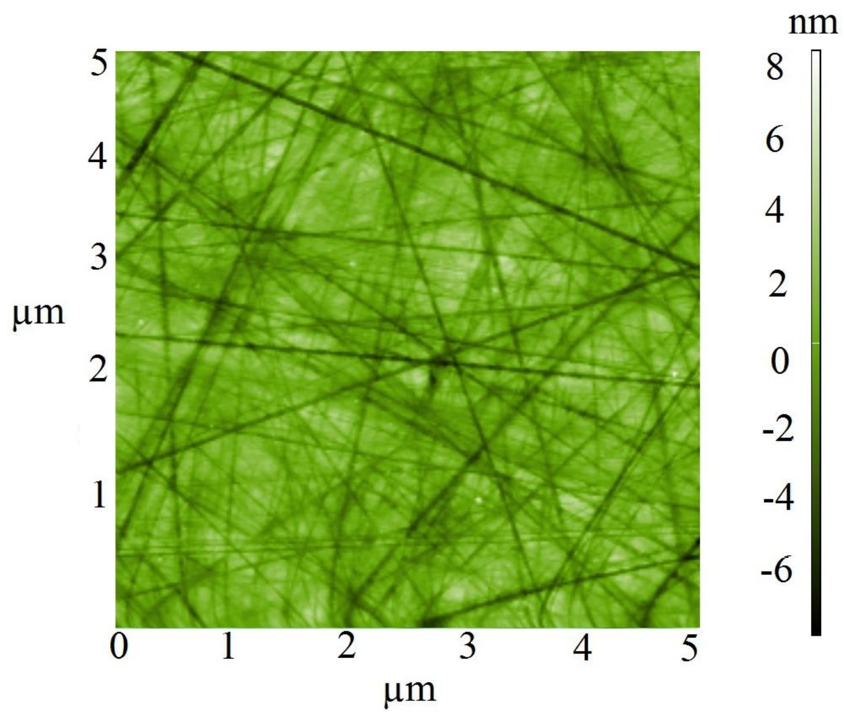

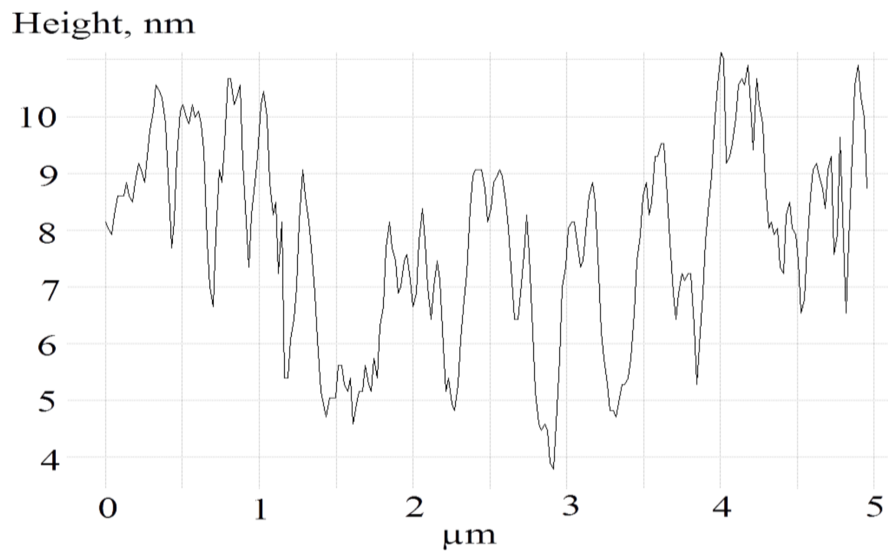

Surface topography and horizontal profile of silicon carbide
with following characteristics:
Scan area 5x5µm,
Max – 15.9516nm,
Root Mean Square – 1.57007nm.
a)

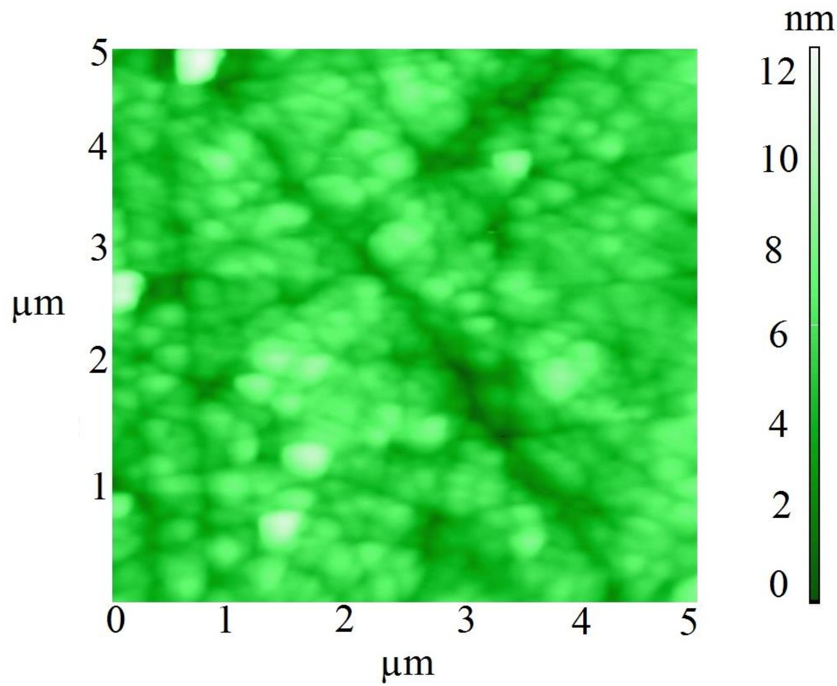

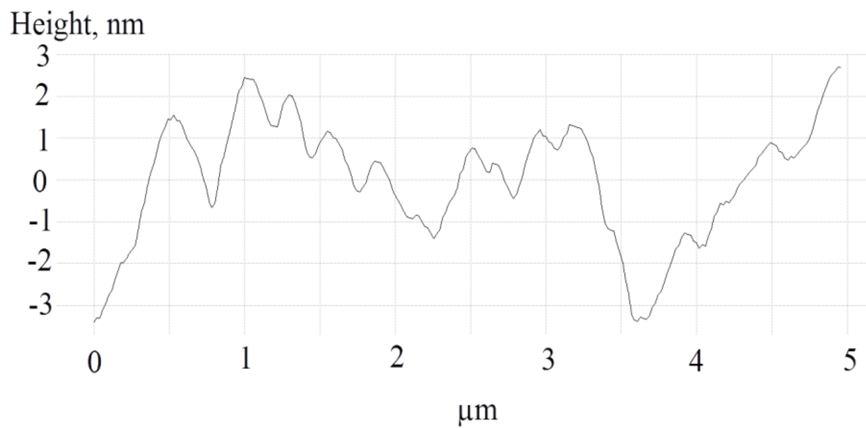

Surface topography and horizontal profile of silicon carbide
with following characteristics:
Scan area 5x5μm,
Max - 13nm,
Root Mean Square - 1nm.
b)

Figure 4.6. Surface topography and horizontal profile of SiC
a) before and b) after dry etching.

Captions of figures 4.5 and 4.6 contain experimental parametes: Scan area, Max, Peak-to peak and Root mean square. They define the square of the image, maximum high at the scanned area, the quadratic mean correspondingly.

4.6 Influence of processing electrical parameters

SiC wafer etched with 20° slope were used for demonstration of morphology behavior during the etching (Fig. 4.7). Surface roughness defines one charachteristic of the substrates. The AFM data of a surface is a complex representation for morphology characterization. Height-height correlation functions provides considerable information about topography (such as estimation of correlation areas, sizes of grains and holes, and the character of their distribution) in a compact form. The results show the correlation length increasing with increasing potential above 3 kV. This is caused by an increasing characteristic distance, after which the correlation is lost between the topographic features.

The results here perform comparison of the etch rates Al_2O_3 and SiC. These materials have a wide range of optoelectronic applications. Cleaning of the substrate and consequent preparation of the heterostructure could be combined in one process cycle using this technology. Variation of the etching parameters allows to find the conditions of substrate processing which will satisfy performance requirements.

The different AFM images show the decreasing of the surface roughness of the studied substrates. Processed substrates were studied by interferometry to define the etch depth, and by atomic force microscopy to study the topography and statistical analysis of surface roughness. The interferometry reveals the dependence of etch rate on the angle between the substrates and defocused beam of argon ions. It is also shown in select small scale images that the surface damage occurs after the substrate treatment. But the more common large area surface topography indicates a decreasing roughness. In the case of stable materials, physical etching is a good alternative to chemical etching: it provides uniformity, reproducibility and could be more suitable in comparison to wet etching.

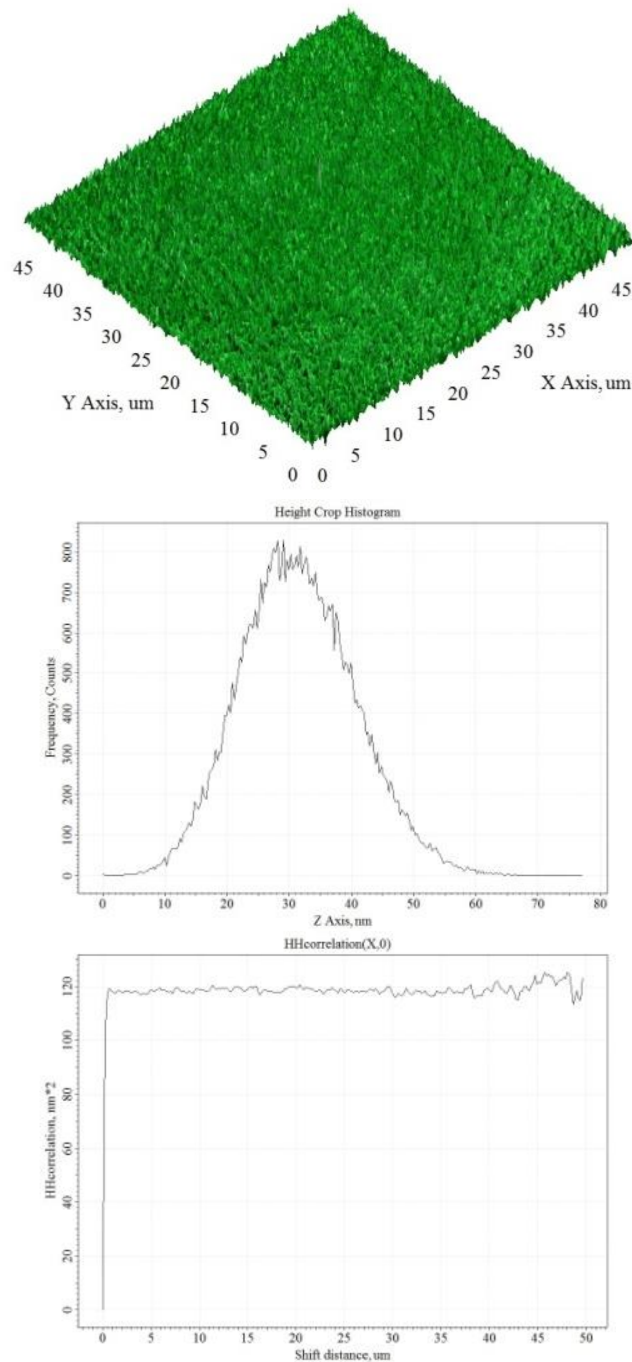

Figure 4.7 a. SiC wafer, etched on 20° slope at 3 kV (morphology, heights histogram, correlation curve).
Scan area 50x50µm.
Root mean square 8nm
Roughness average 6nm

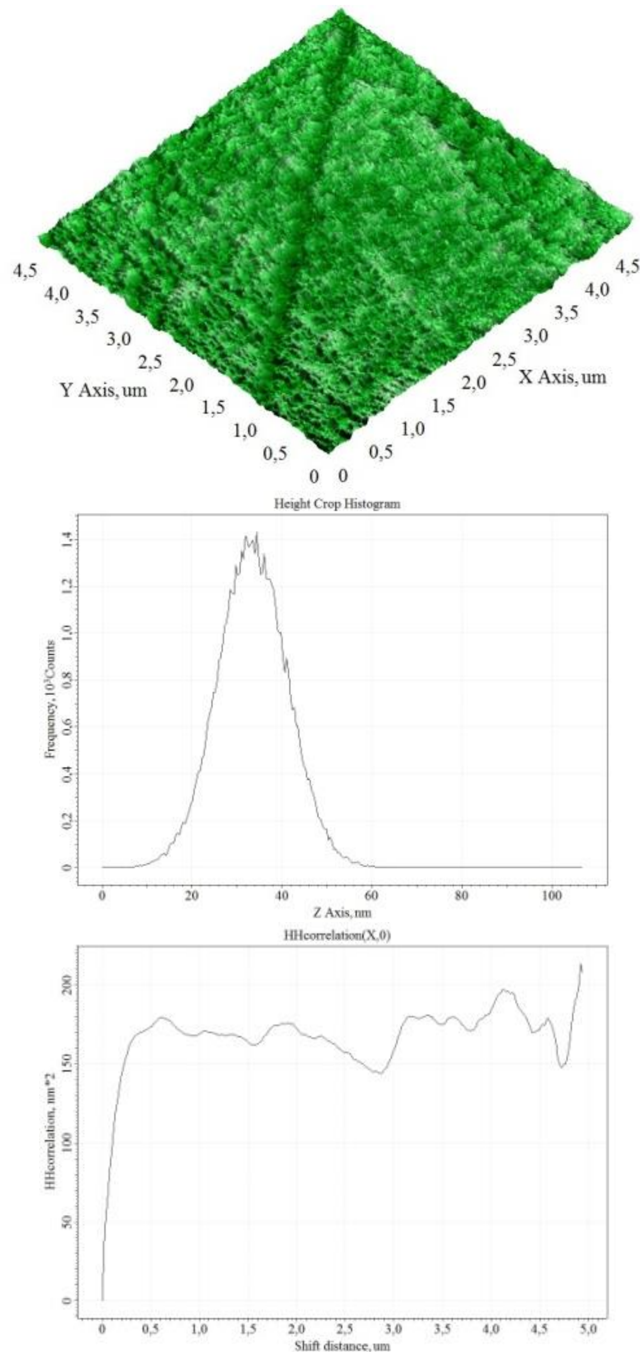

Figure 4.7 b. SiC wafer, etched on 20° slope at 3kV (morphology, heights histogram, correlation curve).
Scan area 5x5µm.
Root mean square 9nm
Roughness average 7nm

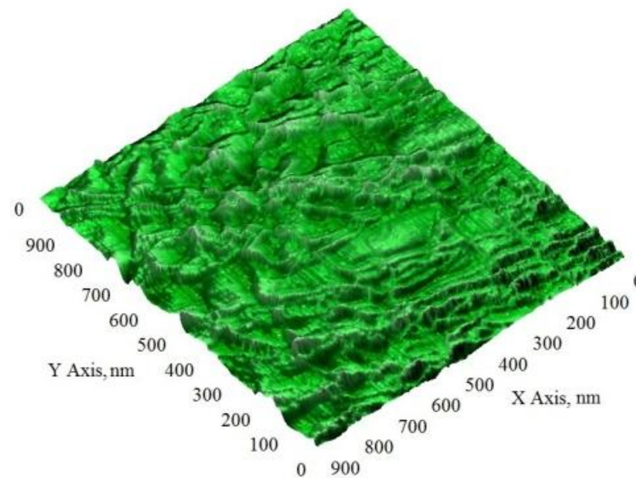

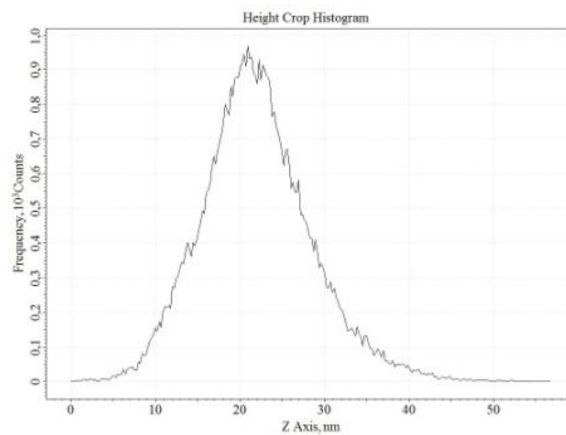

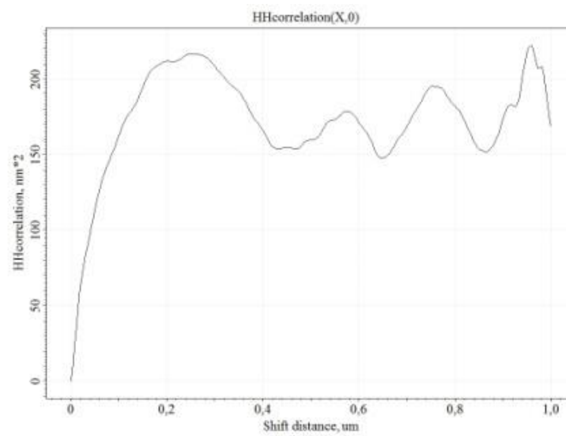

Figure 4.7 c. SiC wafer, etched on 20º slope at 3kV (morphology, heights histogram, correlation curve).
Scan area 1x1µm.
Root mean square 6nm
Roughness average 5nm

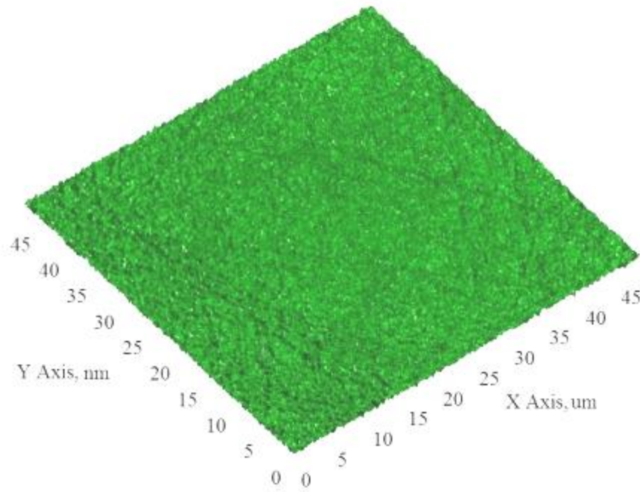

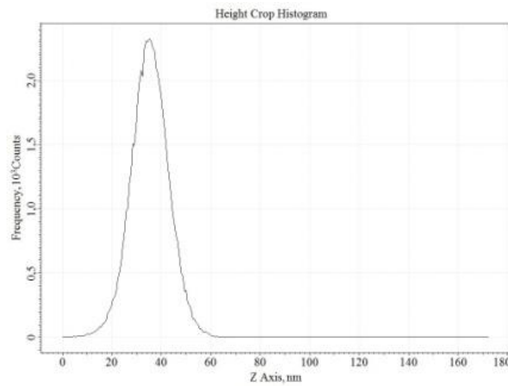

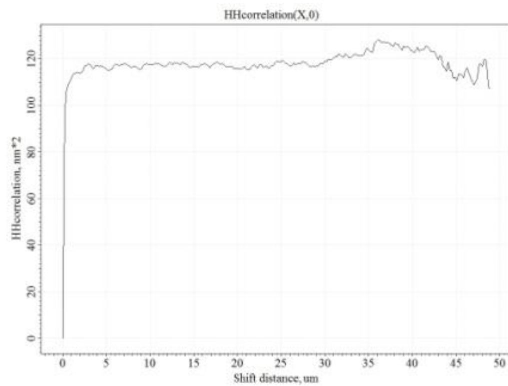

Figure 4.7 d. SiC wafer, etched on 20º slope at 4kV (morphology, heights histogram, correlation curve).
Scan area 50x50µm.
Root mean square, RMS 8 nm
Roughness average 6nm

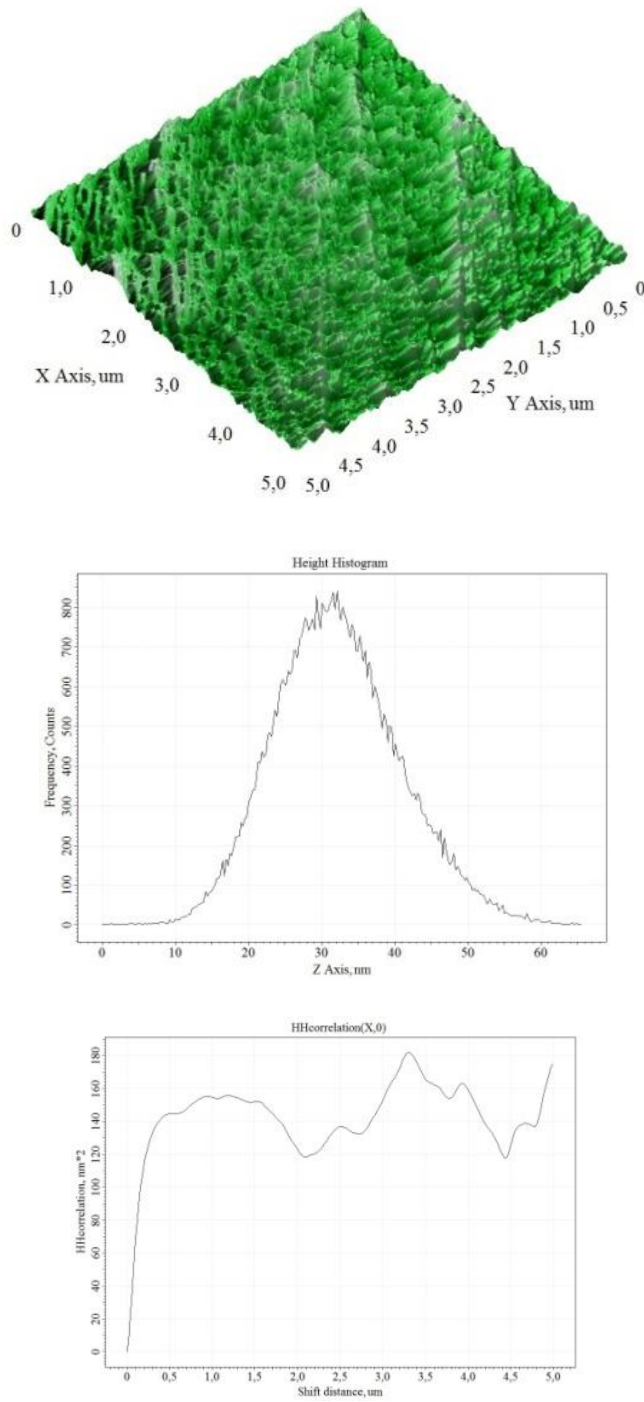

Figure 4.7 e. SiC wafer, etched on 20° slope at 4kV (morphology, heights histogram, correlation curve).
Scan area 5x5µm.
Root mean square, RMS 9nm
Roughness average 7nm

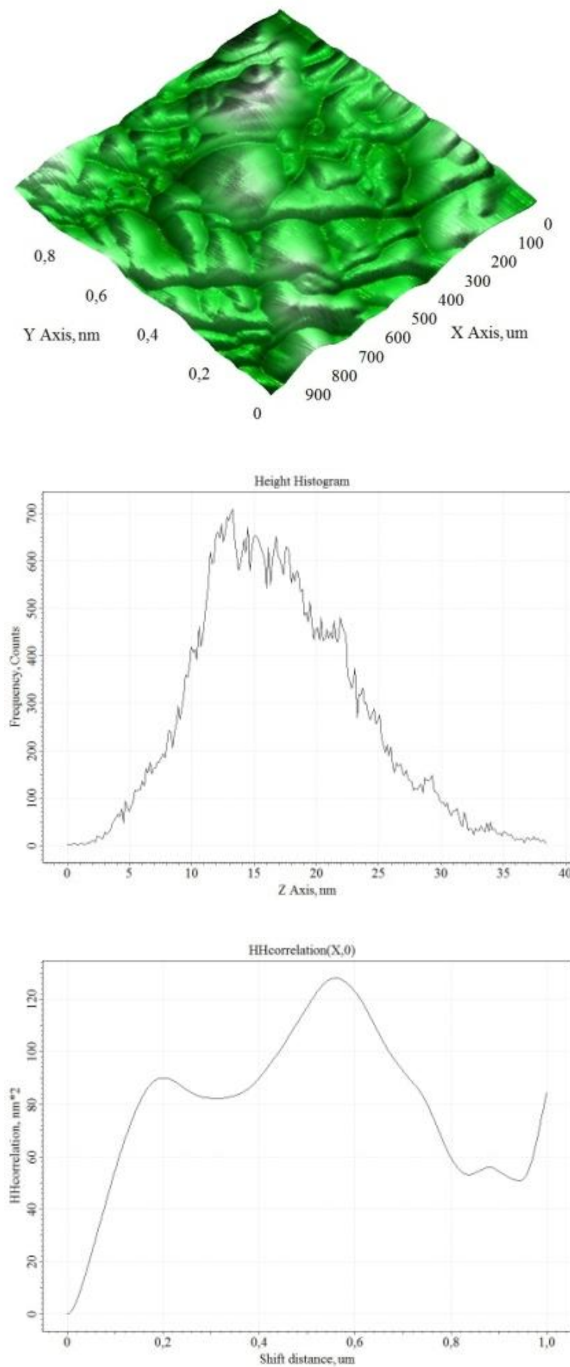

Figure 4.7 f. SiC wafer, etched on 20º slope at 4kV (morphology, heights histogram, correlation curve).
Scan area 1x1 μm.
Root mean square 6nm
Roughness average 5nm

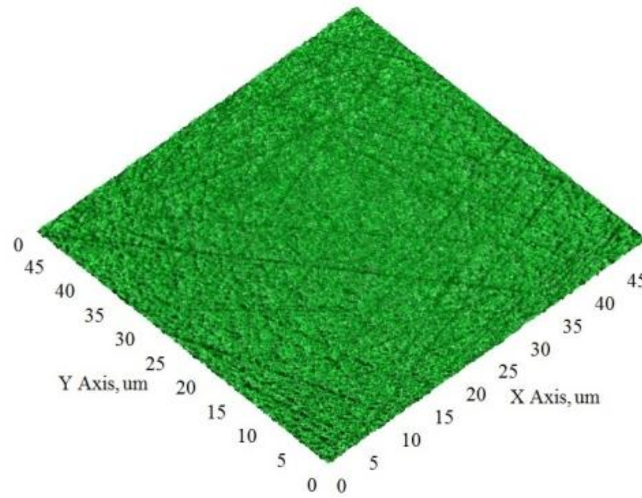

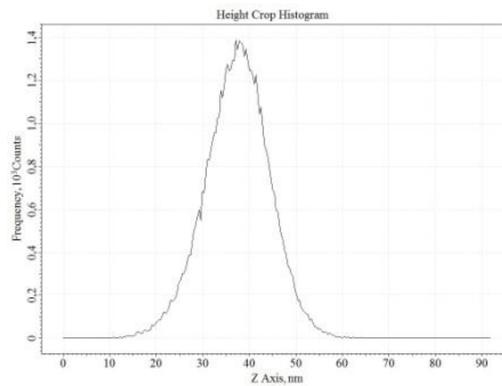

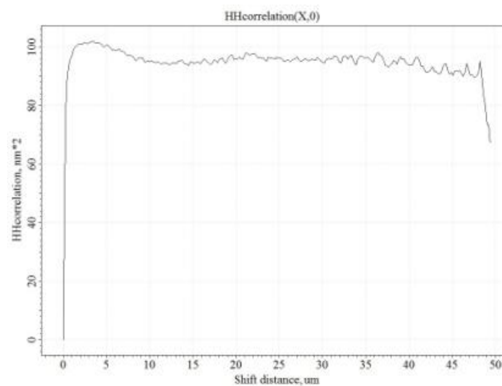

Figure 4.7 g. SiC wafer, etched on 20° slope at 5kV (morphology, heights histogram, correlation curve).
Scan area 50x50µm.
Root mean square 7nm
Roughness average 5nm

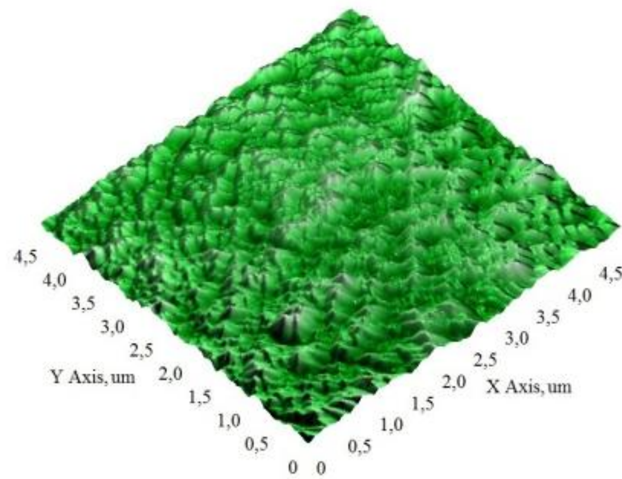

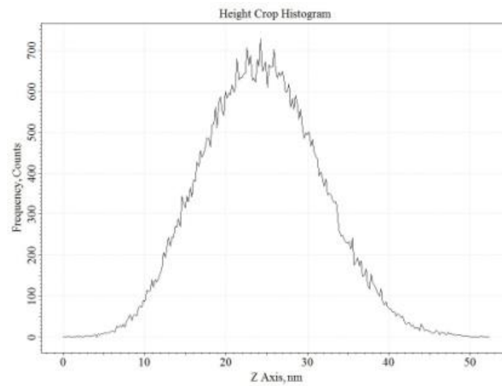

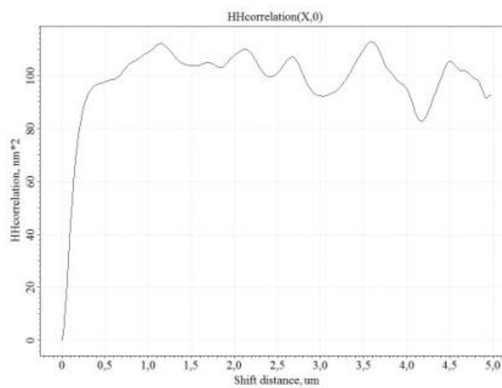

Figure 4.7 h. SiC wafer, etched on 20° slope at 5kV (morphology, heights histogram, correlation curve).
Scan area 5x5µm.
Root mean square 7nm
Roughness average 6nm

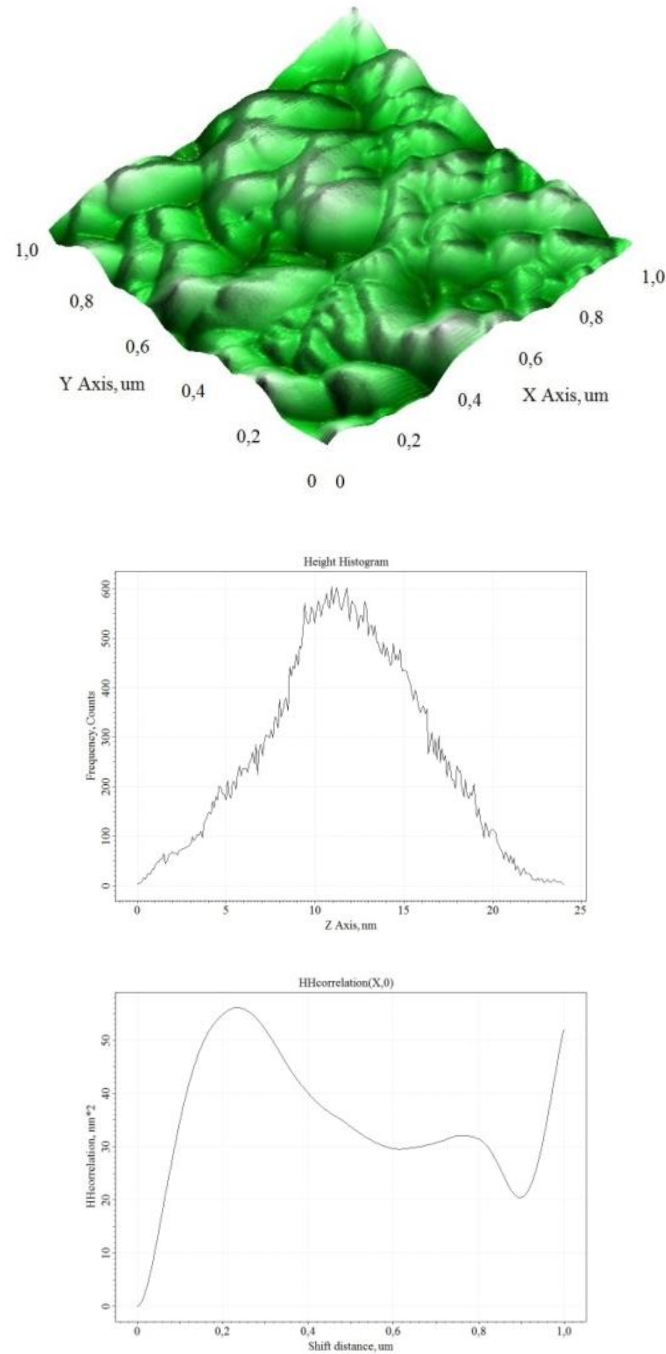

Figure 4.7 i. SiC wafer, etched on 20° slope at 5kV (morphology, heights histogram, correlation curve).
Scan area 1x1 µm.
Root mean square 4.278nm
Roughness average 3.442nm

Figures 4.7 a-i containes information about morphology, heights histogram, correlation lengh. Root mean square and average roughness are wide usefull statistical values.

4.7 Dry etching in optoelectronics

Adoption of new materials and technologies creates environmental challenges in the field of solar cell production. Researchers in materials science as well as industry often use plasma technologies for surface modification. The technologies based on ion etching texturing of Si wafers mentioned in [140] are of great interest for large-area monocrystalline silicon solar cell production. Ion etching is a promising texturing process for solar cell preparation since in comparison with wet etching it has a larger reduction on light reflection. Dry etching process could be used as noted by authors of [10] in combination with e-beam or nano-imprint lithography, they demonstrate in their study Si subwavelength structures with water contact angle of 113.2^{o} and the average reflectance of 2.5%.

Deep reactive ion etching of highly doped Ge-Si alloys which can find a place in solar cells application was carried out in [141]. Even black silicon, which represents a good anti-reflective coating for a commercially viable solar cell, could be prepared through etching [142]. Power conversion efficiency enhancement of III–V solar cells with TiO_2 subwavelength structures were obtained using a dry etching process [143]. It is also known that the crystal structure of the plasma-treated TiO_2 films for dye-sensitized solar cells are much clearer [144]. It was noted in [145] that in case of etching of indium zinc oxide (Transparent conducting oxide for optoelectronic application) the Ar ions determine the etch rate and etch profile. It is shown in reference [146] that "different processing recipes result in different final grating structures".

The importance of angle control in preparation of photocatalytic films is underlined by Michalcik in [147] "The variation of the incident angle enables formation of nanostructured films with oriented columnar structures". AFM measurements are often used for estimation of topography and other parameters (autocorrelation length of the surface) before and after plasma etching [148].

5 PREPARATION OF THIN FILMS BY MAGNETRON SPUTTERING

Aluminum nitride layers prepared on sapphire substrates are examined. The substrate surface was treated by dry plasma etching. The morphology of aluminum nitride thin films was studied by atomic force microscopy. Lateral force atomic force microscopy was used to study the morphology heterogeneity. The dependence of film morphology on the formation conditions has been defined. Some information in this chapter was described in [A1]

5.1 Substitution of the material and method choice

5.1.1 Aluminum nitride

Study and development of prospective materials is relevant from the technological point of view and is very important from an economical point of view. The research in this field is focused on the development of novel materials with superior properties allowing the fabrication of devices with improved performance.

Aluminum nitride (AlN) is a direct wide band gap semiconductor with combined properties of high electrical resistivity and high thermal conductivity. Structure and film texture of AlN has attracted much attention due to its unique properties and the wide range of application of this material. Obviously, nitride semiconductors show properties that can not be found in traditional semiconductors. Materials like silicon and gallium arsenide do not have a large enough band-gap for devices designed for the short-wave spectrum range. Therefore, research of AlN manufacturing processes is a remarkable necessity in the field of optoelectronics. The problem which one meets in AlN thin layers manufacturing is the absence of suitable epitaxial substrates of the identical material. Hence the other materials such as sapphire (Al_2O_3) and silicon carbide (SiC) are used for the growth of AlN.

5.1.2 Magnetron sputtering

There is a number of appropriate methods for thin film growth like sublimation, sputtering, organometallic vapor phase epitaxy, plasma-enhanced, molecular beam epitaxy, etc. Magnetron sputtering is wide-spread method for thin film deposition. Uniform coatings of this type are necessary in many fields of science and engineering, e.g., in microelectronics, and optical industries (thin film sensors, photovoltaic thin films in solar cells, metallic cantilevers and interconnection, etc.). A technological task for research is to find a source material for layer deposition from the target. The deposition begins when the discharge in material occurs (Fig. 5.1). The collision of gas

ions with the target causes extractions of near-surface atoms, molecules and clusters from the source material, and these particles form the thin film on the substrate.

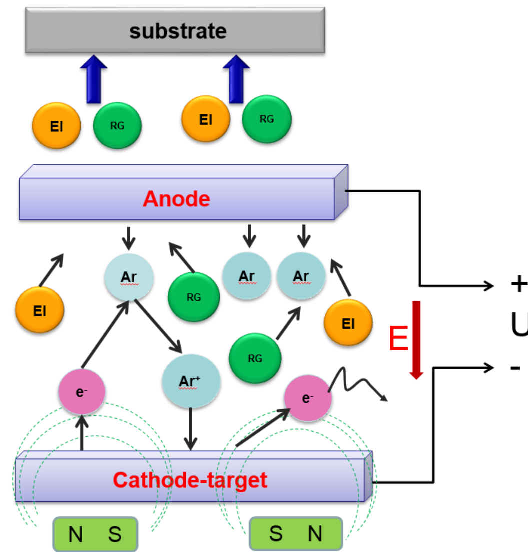

Figure 5.1. Scheme of magnetron sputtering proces (El – particles of sputtering material, RG – reactive gas which bring chemical component to the deposited layer, Ar – argon, which often used as inert gas for target sputtering, e – electrons).

5.1.3 Magnetron sputtering in optoelectronics applications

It is noted in [149] that 80–85% of optical reflectivity is determined by the quality (adhesion, optical and mechanical properties) of the films, and that and rf and DC magnetron sputtering are successfully used for deposition. High power impulse magnetron sputtering could be used for preparation of the anti-reflection SiO_2 coatings for a-Si:H thin film solar cells and LEDs [150]. Multilayer optical coatings could be prepared by reactive magnetron sputtering for spectral filtering of solar radiation. This method of sputtering in reactive gas ambient is promising for the deposition of CIGS absorber films for thin film solar cells [151].

Heterostructures and textured surfaces for solar cells applications could be successfully employed in direct current magnetron reactive sputtering. Dye-sensitized solar cell preparation by DC magnetron sputtering was described in [152] and application of Al_2O_3 by means of magnetron sputtering (since it has stronger dye adsorption and light absorption) was described in [153]. Zinc oxide (ZnO:Al) transparent conductive oxide (TCO) thin films obtained by this method and its optical superior properties, as well as dependence of structural, electrical, and optical properties on the process parameters is mentioned in references [154, 155, 156]. Lin et al [14] reported about pulsed DC magnetron sputtering of molybdenum doped zinc oxide thin films on glass substrates: “after the thin film was deposited, the wet etching process with 0.5 wt.% HCl and 33

wt.% KOH solutions was conducted on the specimens to obtain the ideal light trapping structure for thin film solar cells".

The front side of tandem solar cells should answer the condition of transmittance from UV up to IR range, and such films were prepared via pulsed DC magnetron sputtering on glass substrates [157]. Magnetron *rf* sputtering technique can be used for indium tin oxide (ITO) thin film preparation for a-Si:H/c-Si heterojunction solar cells as front contact or anti-reflection coating [158]. Zhang et al carried out DC magnetron sputtering of tungsten doped zinc oxide (WZO) thin films on glass substrates at various substrate temperatures [159], and the results looks similar to our study since authors noted that "As the substrate temperature increases, the crystallinity of WZO thin films gets deteriorated and the surface becomes even smooth". Temperature-accelerated dynamics [160] influences the scale of the surface topography.

Magnetron sputtering allows preparation of materials with surface topographies which could not be achieved by other methods (because of metastable compound phases [161]) for better light scattering and trapping. Summarizing that written above, we can note that magnetron sputtering in all its modifications is a promising method with good parameter control and reproducibility of results.

5.2 Deposition of aluminum nitride films

5.2.1 Description of set-up

A standard vacuum deposition system was used with two ring-type magnetrons and an ion source. There is a substrate heater, a reactor of rf-activated nitrogen plasma, and gas flow regulators. The main parts of the deposition process are the crystalline substrate, which has to satisfy requirements of deposition of epitaxial growth on it, and a source of the desired product. Fabrication of high-quality thin films is a complicated and multiparametric problem. The main operating parameters are

a) crystal-lattice orientation of the substrate,
b) deposition rate defined by gas supersaturation, and
c) gas-dynamic behavior of the reactor.

The ionizing efficiency can be improved by use of a magnetic field, so ions are generated relatively far from the target and the probability of energy loss is high in ordinary planar diode systems. The magnetic field lines cross the lines of electric field. The mechanism of the device is based on the braking of electrons in the crossed magnetic and electric fields. Thus the trajectory of an electron in a magnetron device changes under simultaneous effect of electric and magnetic fields. Electrons appear out of the cathode as a result of ionization, and consequently they are localized above the surface of the sputtering material. Electrons are trapped by magnetic field which makes them move on cycloidal path, and also by electric field repulsion from cathode to anode. As a result, the probability and number of electron collisions with argon molecules, and

consequently the ionization, sharply increases. Ionization rate varies in the deposition area because of inhomogeneity of electric and magnetic fields in the near-cathode region. A maximum of ionization then occurs in the area where the magnetic lines are perpendicular to electric-field lines, and the minimum is obtained in an area in which the field directions are parallel. So, the localization of plasma at the near-cathode surface allows to get significantly greater ion current density at lower pressure and hence provides a high sputtering rate.

5.2.2 Substrate choice and processing

In spite of all the advantages of this method, there are a lot of features to investigate yet. One of them is the choice of the source with convenient target material, and its formation and preparation. The target is supposed to be without pores and hollows in order to avoid local melting and sprinkling of the material as there is high power at the small area of the target. So, a high-purity aluminum target was used in this study.

Substrate preparation includes dry etching and nitration by nitrogen implantation into the sapphire substrate (0001 orientation), with subsequent high-temperature annealing at 1400-1600K in a nitrogen atmosphere. The average resistance-type heater was used for preheating of the substrate during the structure formation. The main condition of construction and making of the heater is to ensure a non-gradient thermal field on the surface of the substrate, and regulation and maintenance at a given temperature. Water-cooled air-tight feed-through terminals of the heater are in the wall of the vacuum chamber. The temperature should be chosen according to some necessary prerequisites for material properties, constructive features and requirements to the structure of the film, method of deposition, etc. The substrate heater is on a rotator-carrousel and it is possible to use it as a heating radiation or for prior degassing of the vacuum chamber.

5.3 Influence of process parameters on film morphology

One of the most important parameters of the deposition process is the temperature of the deposited films. Surface temperature is connected to adhesion strength, surface structure, and level of residual coating stress. By changing the deposition surface temperature, it is possible to change the structure of films and thus their mechanical and electro-physical properties. Adhesive strength increases with the temperature growth.

5.3.1 AFM of the surface

The morphology of the deposited layers was examined by atomic force microscopy. The statistical distribution of heights is show in figure 5.2.

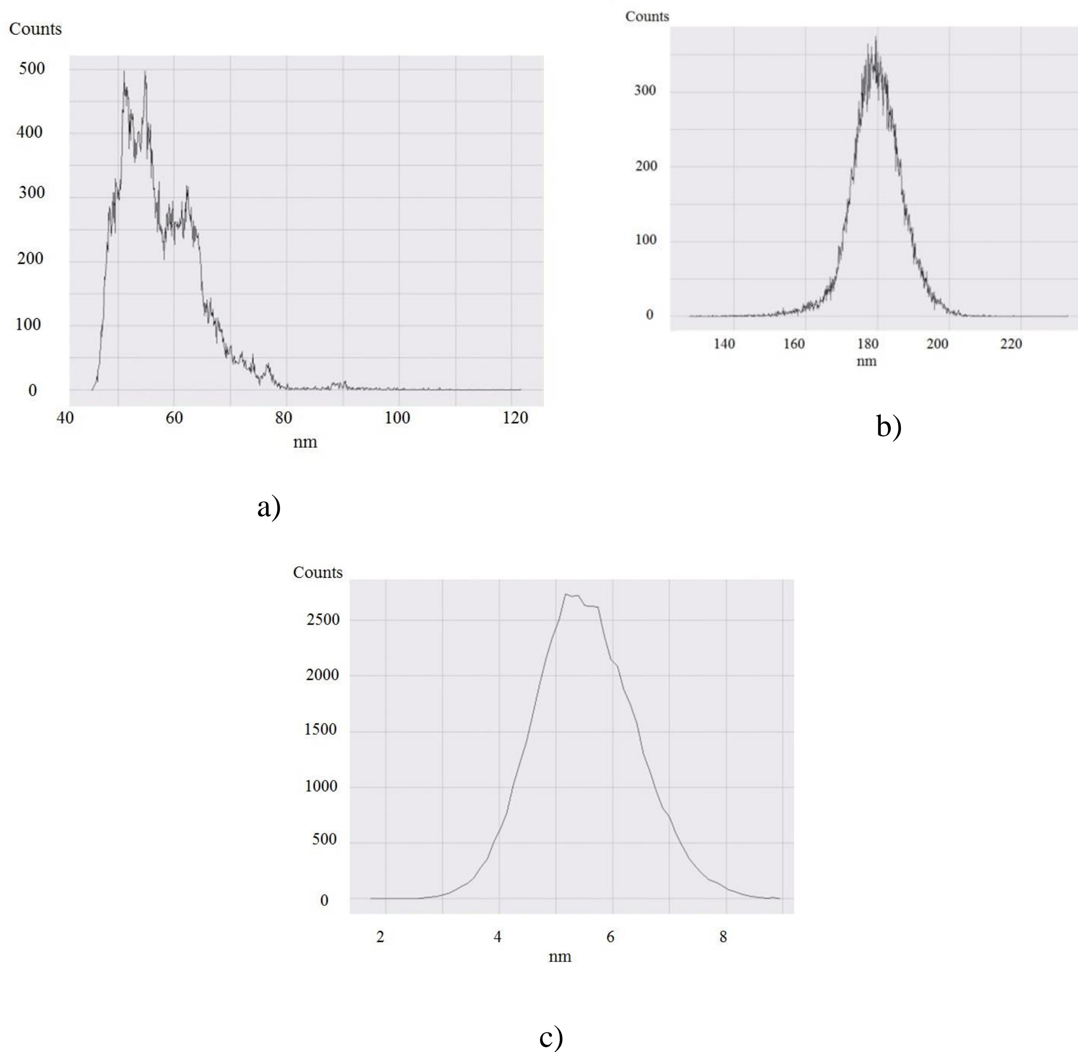

Figure 5.2. Height histogram for the AlN samples morphology obtained at a) 1000K, b) 1300K and c) 1500K.

Lateral force microscopy (LFM) was used to measure the AlN film morphology with nanometers precision (Fig. 5.3). LFM measures frictional forces on a surface. By measuring the "twist" of the cantilever, rather than merely its deflection, one can qualitatively determine areas of higher and lower friction [162]. The temperature should be chosen according to some necessary prerequisites for material properties, constructive features and requirements to the structure of film, method of deposition, etc. LFM allows the imaging of heterogeneities in materials, thin films or monolayers at high spatial resolution. Furthermore, LFM is increasingly used to study the frictional properties of nanostructures and nanoparticles [163]. I used it to obtain more presise images of the films surface, edges and borders of surface features.

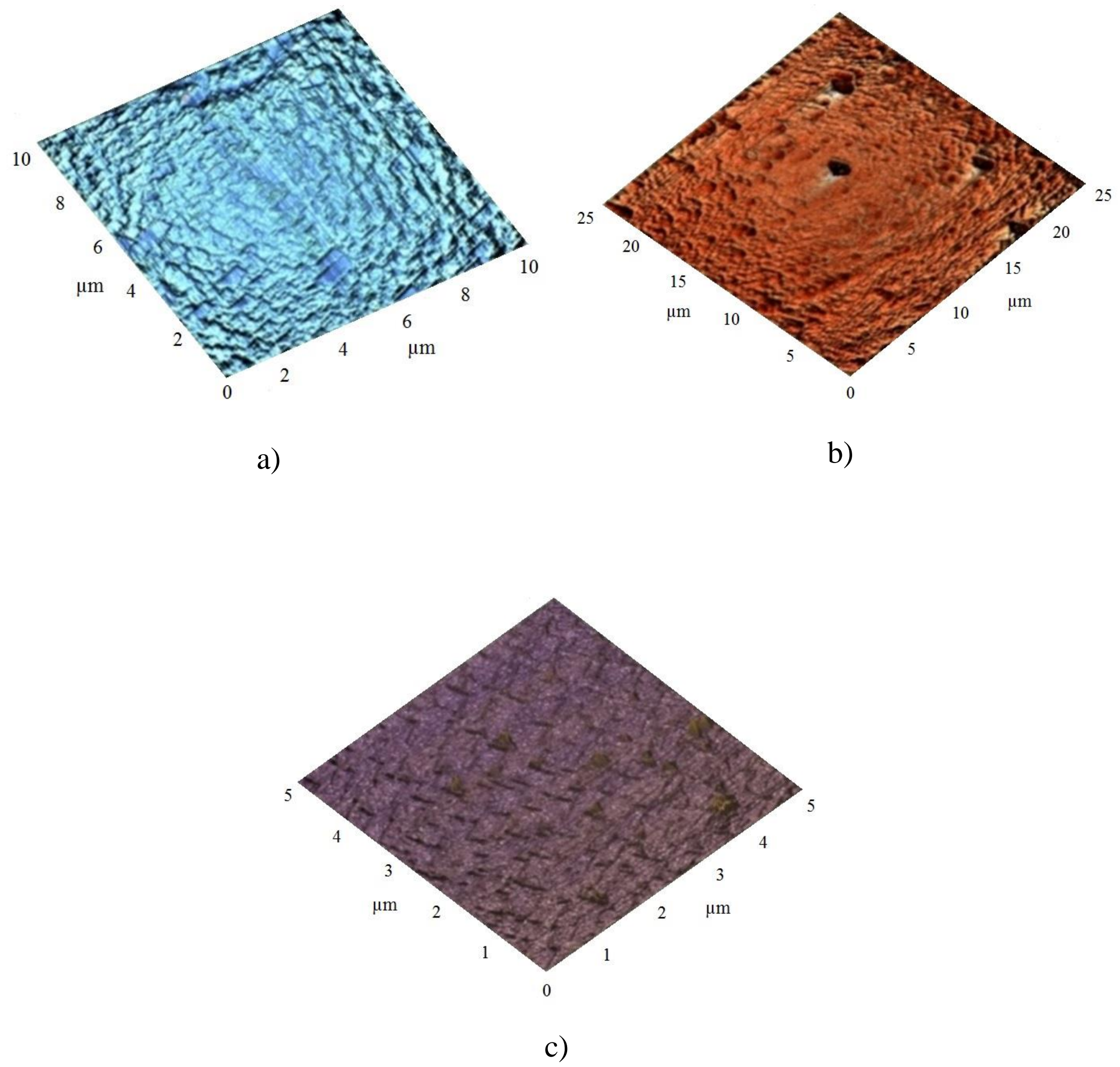

Figure 5.3. Morphology of AlN samples obtained at a) 1000K, b) 1300K and c) 1500K.

5.3.2 SEM of the structure

The heterostructure of (0001)AlN/(0001)Al_2O_3 was produced and its scanning electron microscopy (SEM Quanta 200 from FEI) image is in figure 5.4.

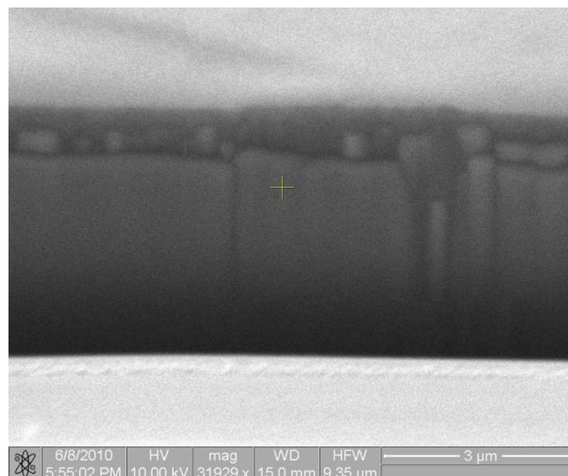

Figure 5.4. SEM image of the aluminum nitride layer on sapphire substrate in cross-section.

This measurement shows the occurrence of AlN film on the Al_2O_3 substrate. It means that the typical AlN growth occured. There are crystalline columnar grains of AlN there in the image of cross-section analysis image. They have flat tops and not sharp shown faceting of the surface.

6 AFM IMAGING AND CHARACTERIZATION OF TOPOGRAPHY

This chapter is based on the paper which was published in Applied Surface Science journal [A2]. It is about AFM imaging and characterization of 3D surface morphology of AlN epilayers on sapphire substrates prepared by magnetron sputtering. Due to the effect of temperature changes on the epilayer's surface during the fabrication, surface morphology is studied by combination of atomic force microscopy (AFM) and fractal analysis methods. Both methods are useful tools that may assist manufacturers in developing and fabricating AlN thin films with optimal surface characteristics. Moreover, they provide different yet complementary information to that offered by traditional surface statistical parameters. This combination is used for the first time for measurement on AlN epilayers on sapphire substrates, and provides the overall 3D morphology of the sample surfaces (AFM imaging), and reveals the existence of self-similar and fractal characteristics in the surface morphology (fractal analysis).

6.1 Study of aluminum nitride topography

6.1.1 Role of surface analysis

Because of the growing interest in thin film engineering in modern manufacturing technology, different imaging and characterization techniques such as atomic force microscopy, scanning tunneling microscopy, transmission electron microscopy, secondary electron microscopy and optical imaging techniques, as well as diffraction techniques (electron, atom, light and X-ray scattering), have been extensively used to investigate the surface roughness of thin films.

The quantitative characterization of surface morphology of thin films is important due their electrical, optical, tribological and chemical properties, which depend on the surface morphology. In the last few decades, Atomic Force Microscopy (AFM) of thin films surface topography has been developed as a useful research tool for exploring the surface morphological features of thin films in the area of surface engineering.

Two main approaches may be distinguished to investigate the 3D surface roughness of thin films: statistical and fractal descriptions. The fractal geometry proposed by Mandelbrot, may be used to describe the surface morphology and complexity of irregular microstructures, whose complex geometry cannot be characterized by traditional Euclidean geometry.

The irregularities of thin films surfaces are not homogeneously distributed, and differences in thin films effective 3D surface roughness values have been observed at different magnifications. The topography of 3D surfaces adds a new level of

understanding to nanotribology processes, such as adhesion, contact formation, friction of adsorbed layers, seen on an atomic level. Conventionally, a 3D rough surface is assumed to be a random process, to exhibit fractal characteristics, which can be characterized by fractal parameters that are independent of the scale of the roughness. The 3D surface topography of thin films possess only statistical self-similarity, which takes place only in a restricted range of spatial scales.

The fractal dimension D_f (the main distinctive attribute of a fractal object) describes how the fractal object occupies the metric space to which it belongs. In the case of 3D surfaces, the fractal dimension indicates how much the fractal surface fills the 3D volume. Generally, the fractal dimension D_f of a surface is a non-integer value within the range $2 \leq D_f \leq 3$, where $D_f = 2$ (for ideally smooth surfaces) and $D_f = 3$ (for rough surfaces that occupy all available volume). An increasing value of D_f indicates a higher level of fractality, a more irregular shape of the surface roughness. In addition, a fractal surface maintains the characteristics of continuity, non differentiability and self-similarity of the structure. Different studies suggest a correlation between the different surface roughness parameters and the fractal dimension D_f .

The fractal analyses does not depend on the experimental and methodological parameters involved in the AFM measurements, such as: measurement system, diversity of samples, image acquisition, type of image, image processing, fractal analysis methods including the algorithm and specific calculation used etc..

6.1.2 Materials and methods

Three different structures of AlN epilayers deposited on sapphire Al_2O_3 substrates under three different substrate temperatures (T = 1000, 1300 and 1500 K) were studied. A standard vacuum deposition system with two ring-type magnetrons and an ion source were used for the experiments. The apparatus is equipped with a substrate heater, which ensures a non-gradient thermal field on the surface of the substrate, a reactor of HF-activated nitrogen plasma, and gas flow regulators.

Crystalline substrates which satisfy requirements for epitaxial deposition, and the sources required for the desired product are the main components of the deposition process. The target should be without pores and hollows in order to avoid local melting and sprinkling of the material as there is high power in the small area of the target. A high-purity aluminum target was used in this study. A substrate preparation includes dry etching and nitration by nitrogen implantation into the sapphire substrate (0001 orientation), with subsequent high-temperature annealing at 1400-1600 K in a nitrogen atmosphere. X-ray fluorescence was used for elemental analysis of the sapphire substrates after nitration (PHI 5500 ESCA, Physical Electronics). As we reported elsewhere [A1], there is a gradually decreasing nitrogen concentration with sputter depth. The presence of the nitridization sapphire layer provides a good condition for

subsequent growth of AlN epilayers in the (0001) plane. Before a deposition of AlN epilayers at different temperatures, Al_2O_3 substrates were treated by dry plasma etching.

The Scanning Probe Microscope system, an NTEGRA Prima (NT-MDT, Russia) with optical viewing system and its own software, Nova were used for measurement and for AFM data visualization of the morphology of the deposited layers. AFM analysis was carried out in contact mode over different surface areas. For tapping mode, a silicon cantilever, Model NSG01 DLC (AFM «Golden» Silicon Probes) with the following nominal specifications: resonant frequency 150 kHz, force constant 5.1N/m, length 125μm, width 30μm and thickness 2μm was used. The tip specifications were: tetrahedral shape, height 14μm, tip curvature radius 6nm, and cone angle at the apex 7°-10°. For AFM contact mode a silicon cantilever, Model FMG01 (AFM «Golden» Silicon Probes) with the following nominal specifications: resonant frequency 60kHz, force constant 3N/m, length 225 μm, width 32 μm and thickness 2.5 μm was used. The tip specifications were: tetrahedral shape, height 14 μm, curvature radius 6 nm, and cone angle at the apex 7°-10°.

Fractal analysis of the stereometric files was conducted based on our original algorithm (in MATLAB software R2012b, MathWorks, Inc.), which consists of fractal scaling (in many approximation steps) of the surface measured with an AFM. In our study, for these surfaces the best method of fractal analysis uses morphological envelopes [164]. An analysis of the stereometric files was conducted based on the original algorithm (in Matlab), which consists in fractal scaling (in many approximation steps) of the surface measured with an AFM. For an AFM file by selecting every 105th, 70th, 42nd, 35th, 30th, 21st, 15th, 14th, 10th, 7th, 6th, 5th, 3rd, 2nd and 1st measuring point, the whole area measured, 15 scalings of the surface were obtained, thus approximating its real appearance. A change of measured density is a form of surface scaling required during fractal analysis. The entire algorithm is described in [165].

6.1.3 Atomic force microscopy

The fractal dimension is the basic concept of the systems description for which symmetric scaling takes place. This means self-similarity of the element under consideration at a variable magnification scale. A magnified view of one part of the surface not too precisely reproduces its whole image but has the same qualitative appearance. No real fracture surface profiles has, therefore, strictly self-similar properties. Thus, a surface description with the application of a single dimension is not possible. A segmental character of a doubly log-log plot shows that the fracture surface is characterized by more than one fractal dimension. Since the fracture surface does not exhibit a form of a purely self-similar fractal, the self-similarity is local only. The surface irregularity distribution changes depending on the analysed region, e.g. concentration of large surface irregularities occurs only in a few places and concentration of small irregularities, in many places.

All sample images were acquired by Scanning Probe Microscope NTEGRA Prima (NT-MDT, Russia) at a scan rate of 1 Hz with a 256×256 pixels image definition over different square areas. All measurementswere performed immediately after layer formation in the same laboratory, at room temperature (296 ± 1K) and 65 ± 1% relative humidity. The measurements were repeated four times for each sample on different reference areas, to validate the reproducibility of these features. The temperature should be chosen according to some necessary prerequisites for material properties.

Representative topographic images (AFM contact mode) of the AlN epilayers on the sapphire substrate obtained at T =1000, 1300 and 1500 K, for scanning a square area of 5 µm x 5 µm, are shown in figure 6.1.

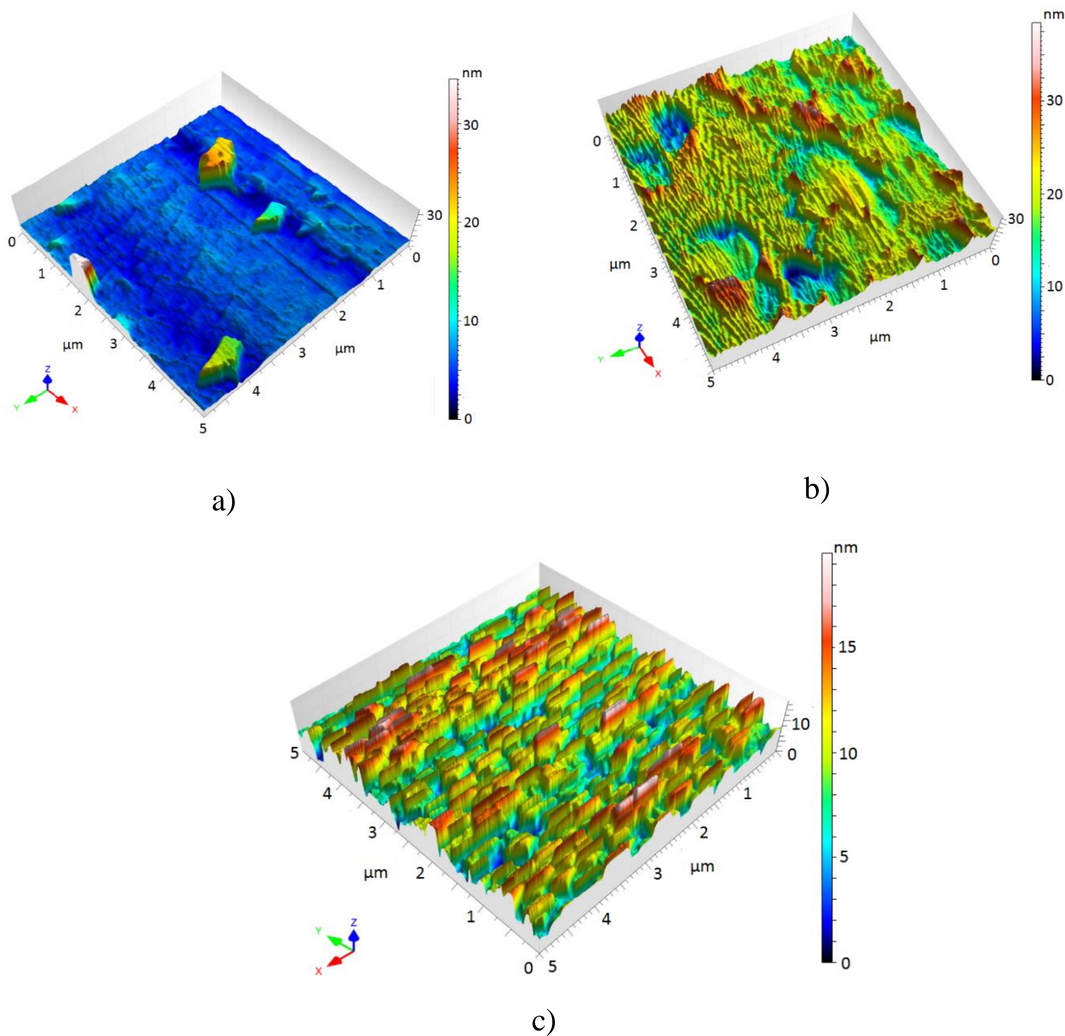

Figure 6.1. AFM images (contact mode) of AlN epilayers on the sapphire substrate obtained at a) 1000K, b) 1300K and c) 1500K.Scanning area of (5 x 5)µm^2. The vertical range of the displayed data (in nanometres [nm]) and the color bar are shown on the right side of the AFM images.

6.1.4 Fractal analysis of surface roughness

The AFM data from measured AlN epilayers were consequently processed using the proposed fractal analysis method. The depth histograms associated with Figs. 6.1 a-c of the AlN layers on sapphire substrates obtained at three different substrate temperatures (1000 K, 1300 K and 1500 K), are shown in the corresponding Figs. 6.2 a-c. It enables to observe the density of the distribution of the data points on the surface. The vertical axis of the histograms is graduated in depths: the horizontal axis is graduated in % of the whole population. For fractal analyses we used Mountains Map® 7 Software (Digital Surf, Besançon, France) [166]. We insert our data in this software and after processing the data we obtained the corresponding results. The Abbott-Firestone curve presents the bearing ratio curve, i.e. for a given depth, the percentage of the material traversed in relation to the area covered. This function is the cumulating function of the amplitude distribution function. The lower horizontal axis represents the bearing ratio (in %), and the vertical axis represents the depths (in the measurement unit).

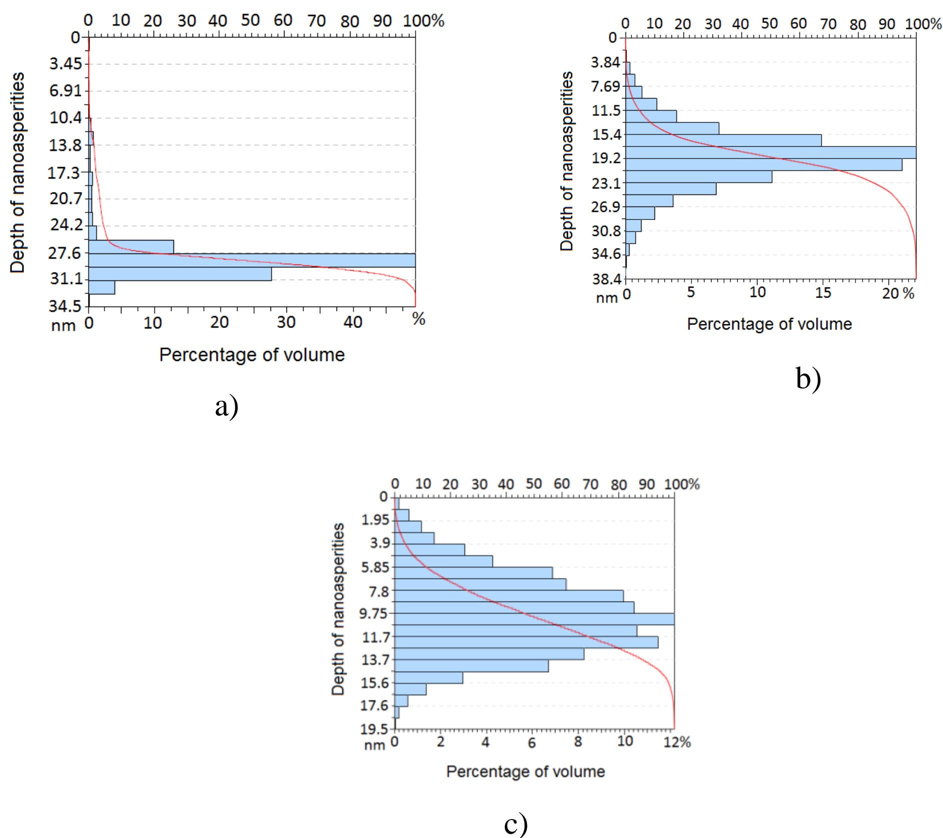

Figure 6.2. The depth histogram for theAlN epilayers on sapphire substrates obtained at: a) 1000K, b) 1300K and c) 1500K. The Abbott-Firestone curve (red).

The graph of the calculated volume for surfaces ($V\varepsilon$) drawn as a function of the scale (ε) (size of the structuring elements) associated with Figs. 6.2, a-c of the AlN layer on the sapphire substrate obtained at 1000K, 1300K and 1500K, are shown in Figs. 6.3 a-c.

The fractal dimension is calculated from the slope of one of the two regression lines that corresponds best (i.e. the one out of the two regression lines whose correlation coefficient is nearer to 1 for a profile and nearer to 2 for a surface). Table 6.1 presents a summary of the fractal dimensions D_f, for scanning square areas of (5×5)µm^2, for AlN epilayers on sapphire substrates obtained at: a) 1000K, b) 1300K and c) 1500K.

Table 6.1. The fractal dimensions D_f, for scanning square areas of (5×5)µm^2 of AlN epilayers on sapphire substrates deposited at: a) 1000K, b) 1300K and c) 1500K.

No.	Samples at temperature	D_f
1	1000 K	2.29 ± 0.0001
2	1300 K	2.42 ± 0.0001
3	1500 K	2.66 ± 0.0001

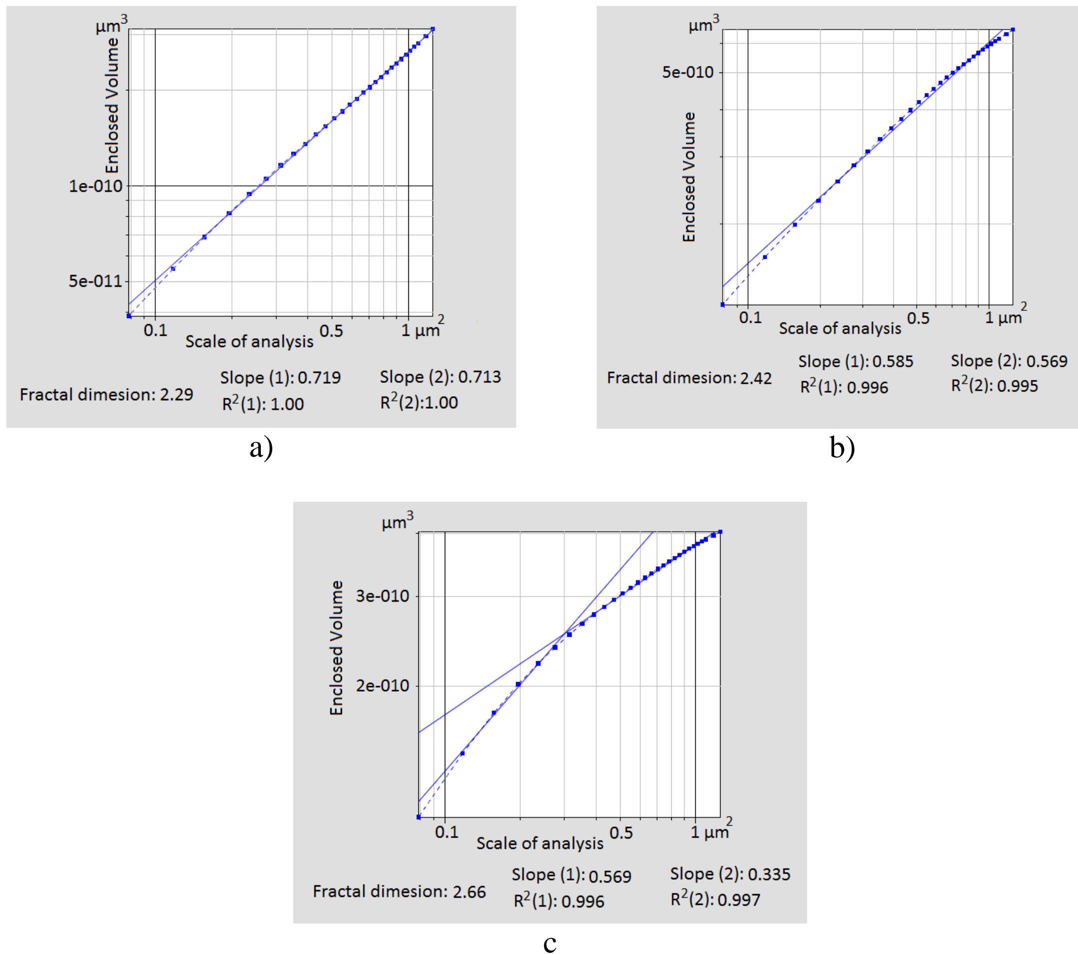

Fig. 6.3. Enclosed volume for AlN epilayers on sapphire substrates deposited at: a) 1000K, b) 1300K and c) 1500K. The fractal dimension is obtained from the slope(s) of the graphs.

The 3D surfaces of all the AlN samples (Fig. 6.1) are covered by nanoasperities (nano scaled protrusions and cavities which have irregular shapes, different sizes and

separations) and a specific distribution due to the preparation processes, which is evident for the entire magnification range. This structural pattern is an indirect indication of the fractal nature of the microstructure. A statistically significant difference ($P < 0.05$) was found for all fractal dimensions D_f. A comparison of the fractal dimensions D_f for the three films studied are summarized in Table 1. The applied method retrieves values of the fractal dimensions D_f (all with average ± standard deviation) commensurate with the surface roughness of the thin films.

6.1.5 Statistical analysis of morphological features

Stach et al [A3] reported the statistical characterization of the described above topography structures. The graphical study of volume parameters (surface): *Vmp*, *Vvc*, *Vmc* & *Vvv* parameters based upon the Abbott curve calculated on the basis of AFM data of the surface associated with Figs. 6.1 (a-c), are shown in Fig. 6.4.

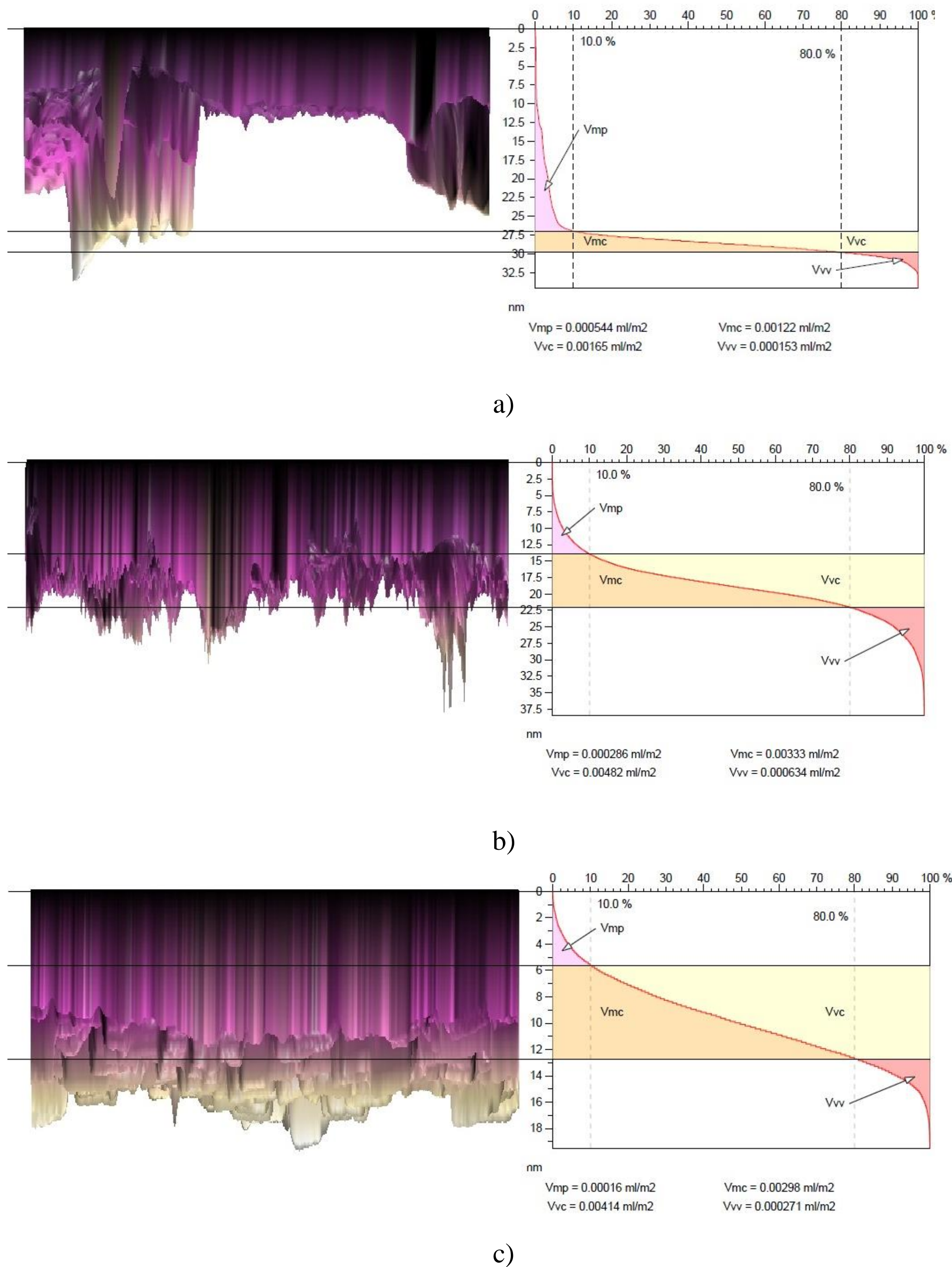

Figure 6.4. Face of AFM 3D images (left side) and graphical study of volume parameters (right side): *Vmp*, *Vvc*, *Vmc* & *Vvv* parameters based upon the Abbott curve calculated on the surface. Two bearing ratio thresholds are defined (using the vertical bars that are drawn with dotted lines). By default, these thresholds are set at bearing ratios of 10 % and 80 %. The first threshold, *p1* (default: 10 %), is used to define the cut level *c1* (and *p2* defines *c2*, respectively). AlN epilayer on the sapphire substrate obtained at: a) 1000K, b) 1300K and c) 1500K. [A3]

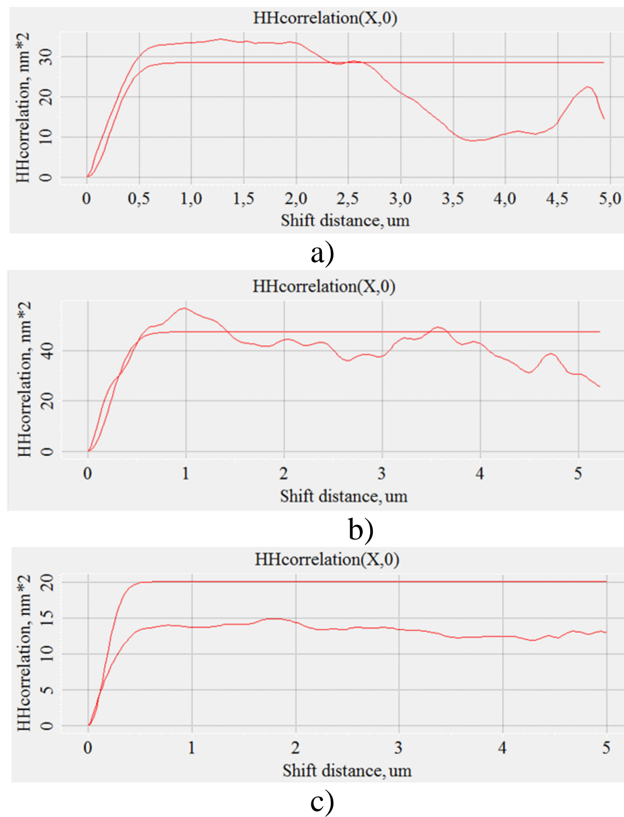

Figure 6.5. The height-height correlation function. AlN epilayer on the sapphire substrate obtained at: a) 1000K, (Correlation lengths: Lx = 319nm, Ly = 356nm); b) 1300K, (Correlation lengths: Lx = 317nm, Ly = 212nm); c) 1500K, (Correlation lengths: Lx = 224nm, Ly = 81.5nm). [A3]

The Abbote curve characterizes the quality and cleanliness of the surface. It shows the dependence of the features‘ area in dependence on its height (depth). Thus this curve is a well suited way to estimate the dependence of nano-geometry on the conditions of the surface preparation.

The correlation length, being the measure of irregularity, decreases with increasing of the substrate temperature during the deposition.

6.1.6 Discussion

In this study we have used sapphire substrates for deposition since Al_2O_3 has electro-physical, mechanical, and thermal properties which are suitable for extreme conditions devices. Dry etching and nitridization of a sapphire substrate were carried out before the sputtering of an Al target. Nitridization of the near-surface sapphire layer provides a good condition for subsequent growth of AlN epilayers in the (0001) plane. The morphology and structural investigations were executed on each step of the film

formation. Effectiveness of dry etching is proved by examining themorphology of the Al_2O_3 substrates after etching. X-ray fluorescence analysis revealed the successful nitridization of the substrate near the surface of the films. The AlN epilayers on the sapphire substrate surface of all samples appeared relatively smooth, with very fine nanoasperities spread on the surface due to the preparation processes.

The data of Fig. 6.1 shows the distribution of nanoasperities, but fractal analysis gives information about self-similarity of the films surface. If many samples are examined, the fractal dimension will be more robust compared to simply looking at the statistical roughness parameters, since it is more intelligence and comprehensive in comparison to statistical parameters in case of fractal nature of the surface.

The fractal analysis in correlation with the AFM data information opens a new avenue for both characterization and direct prediction of surface properties of AlN thin films. To our knowledge, this is the first fractal analytical study of surface roughness of AlN epilayers on sapphire substrates prepared by magnetron sputtering in current literature. The fractal analysis reveals the existence of self-similar and fractal characteristics in the surface morphologies which are reliable metrics of surface roughness and possibly other physical properties of AlNepilayers.

The result of this study is an experimental method for better fabrication of AlN thin films. Their surface morphologies obtained from AFM images were subjected to fractal analysis to quantitatively investigate their structural properties. In addition, the fractal nature of the AlN thin films real surface was investigated and the fractal dimensions *Df* can be used as a quantitative factor to estimate the of degree of fractality and to understand their 3D roughness. The presented results show that fractal dimensions include important surface topography information and can be used to investigate the AlN thin film surfaces. Our results suggest that AlN thin film surface morphology gets textured with an increase in temperature of the Al_2O_3 substrate, and can be tailored to feature particular morphologies. The obtained values are in agreement with the ones obtained in [A1], confirming the overall quality of the data reduction procedure. We have also demonstrated that the AlN thin films are fractal in nature.

6.2 Characterization of surface failure of solar cells by AFM data processing

Fractal techniques and statistical analysis are useful tools for fracture-surface characterization. The geometry of solar cells could be quantitively described by these methods. For qualitative description, scanning electron microscopy (Fig. 6.6) and atomic force microscopy (Fig.6.7) could be used. In case of optoelectronics devices the topography influences the wave length, intensity and direction of light.

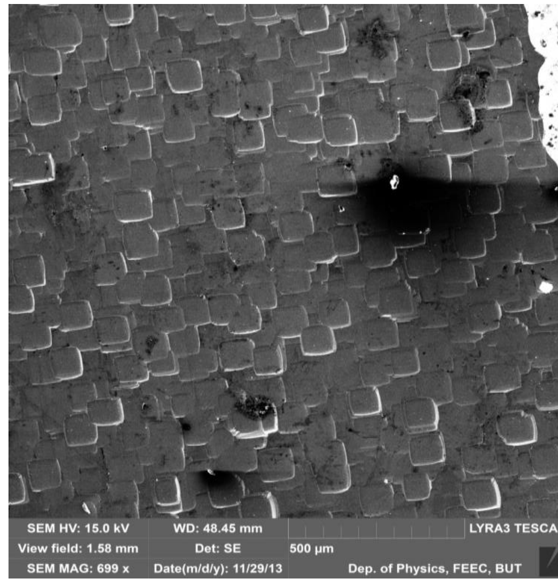

Figure 6.6. SEM of monocrystalline silicon solar cell.

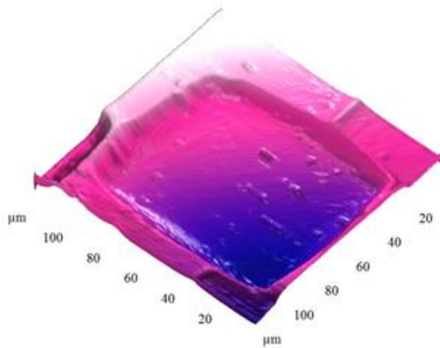

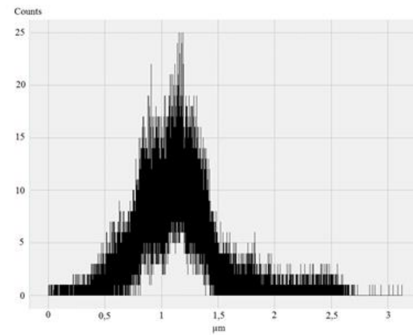

a) b)

Figure 6.7. a) AFM image of the solar cell area without surface defects, b) histogram of heights distribution.

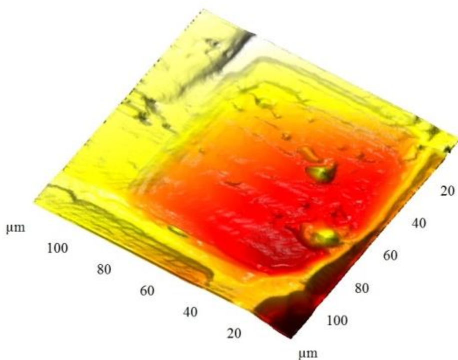

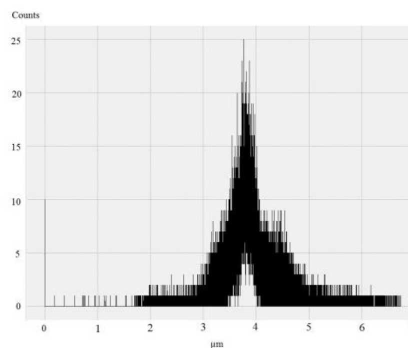

a) b)

Figure 6.8. a) AFM image of the solar cell area without surface defects, b) histogram of heights distribution.

The fractal analysis carried out by Gwyddion program [74] showed that the dimension of the defected area (2.21) is higher than the fractal dimension of the area without defect (2.13). The uncertainty could be caused by measurement conditions. Figures 6.7. b and 6.8 b give the maximum highs 25 nm for both areas. But fractal dimension (Fig. 6.7 a and 6.8 a) differs. This approaching explains the surface behavior dependence on its cosmetic appearance. Use of electron and force microscopy allows obtaining precise data about the samples‘ topography. The statistical analysis shows the distribution of micro and nanoasperities (valleys, peaks) and the fractal analysis gives information about the topography.

CONCLUSION

Current optoelectronic technologies demand a detailed analysis at the nanoscale level. In spite of a long history of research, surface investigations are still one of the most important fields to study. This is explained by the continuously decreasing size and scale of devices.

It is possible to note the following fields of this thesis contribution:

1. Measurements in micro- and nano-scale (survey and argumentation of SEM and AFM application in optoelecronics).
2. Solar cells study (review and description of the morphology impact to improving the quality and efficiency of solar cells).
3. Materials for optoelectronics (study and choice of process parameters for heterostructures preparation).

The text of thesis is organized into three parts. The first part contains investigation of surface morphology of solar cells. The most powerful existing methods for surface investigation are described. The second part is dedicated to heterostructure preparation, including processing of substrate material. In the third part, the mathematical processing of results are presented, kindly provided by Prof. Talu and his group.

My own contribution in every chapter is following.

The chapter 1 substantiates the necessity of coating, buffer and active layers using wide band gap semiconductors especially in space conditions. It transmits the wide range of the solar spectrum (above UV) and can be used as active layer for UV radiation. It explains the remaining AlN solar cell development in significant focus. My contribution in this part is the analysis of the studies concerned the topic of dissertation, definition of problems and subjections of its solution.

Currently, microscopes find an application in almost every field of study. The applications of AFM and SEM for precision metrology are reviewed in chapter 2. The personal contribution is AFM and SEM measurements of the samples, processing of images and preparation of papers.

The chapter 3 presents the comparison of SEM and AFM imaging of commercially available solar cell morphology and possibilities to provide not only average, but precise local data processing. I asked some companies to provide me with samples of the commercial solar cells. Some of them kindly helped me and sent the samples. I performed the microscopic measurements and analysis of results to show the importance of the such kinds of complete device investigation.

The chapters 4 and 5 concern technological processes of heterostructures preparation. The main attention is given to the topography of substrates and prepared films since it is closely connected to optical reflection, transmission, scattering. All experiments were

carried out by myself (measurements) or with my direct participation (samples preparation).

The chapter 6 describes processing of the topography data and reveals further information about the topography imperfections. My aim was to provide explanation of the fractal and statistical analysis made in collaboration with Prof. Talu and explain the connection between parameters.

The scientists which took part in this work are presented as co-authors of the articles. The results were published in articles listed in Appendix 1, also they were presented and discussed in national and international conferences. There are three citations of author in IF journals.

A large amount of references were used to prove and substitute the choice of methods and interpretation of results. The count of the studies in this field confirms the interest of scientists in the characterization and design methods for optoelectronics. In spite of the modern character of this work it has already made a lot of successful attempts in the field of preparation of prospective materials for optoelectronics, as well as in diagnostic of the optoelectronics devices.

RECOMMENDATIONS FOR FUTURE WORK

There are several fields to work for improvement of photovoltaic device performance. It includes researches from fundamental studies up to applications. Combination of optical and electrical measurements will provide an explanation of defect nature, so the optical and electron features measured by noise spectroscopy, local photo- and electro-luminescence and near-field techniques, as well as a correlation of results in far- and near-field brightness vs. applied voltage and frequency with noise spectral density will be useful to estimate the quality and reliability of optoelectronic devices.

It is possible to note the following perspectives:

1. The design of methods for manufacturing of operational optoelectronic and photonic structure samples with superior parameters.

2. Established choice of the materials and the parameters for the structures formation.

3. Evaluating of the prepared structures quality by scanning probe microscopy and scanning electron microscopy.

4. Further theoretical study of the interaction probe-sample – near-field distribution of electromagnetic field and measurement of the refractive index local contrast in materials with nanostructured features.

5. SPM probes etching and structures defects passivation by focused ion beam with consequent control of mechanical, electrical and optical properties of probes and proceeded structures.

6. STM, AFM and SNOM analysis of thin film layer structure before and after aging. Optoelectronic and photonic devices aging and lifetime estimation.

The measurement systems play an important role to right estimation of the device component quality. With the use of a novel SPM and SEM microscopes, the more advanced study of different aspects of nanostructured optoelectronic and photonic materials and devices will be possible.

Interfacial problems and solutions, application of wide-band-gap semiconductors and nanostructures in optoelectronic and photonic devices, aging, degradation mechanisms and reliability of devices are still of special interest.

REFERENCES

1. WOOD, Elisa. Solar Outlook 2015: Still Growing, But No Longer Energy's Young Kid [online]. 28th of January 2015 [cit. 2015-5-25]. Available from: http://www. renewableenergyworld. com/rea/news/article/2015/01/solar-outlook-2015-still-growing-but-no-longer-energys-young-kid
2. CHANDRA, A., ANDERSON, G., MELKOTE, S., WEI GAO, HAITJEMA, H., WEGENER. K. Role of surfaces and interfaces in solar cell manufacturing, *CIRP Annals - Manufacturing Technology,* 2014, vol. 63, pp. 797–819.
3. RAZYKOV, T.M., FEREKIDES, C.S., MOREL, D., STEFANAKOS, E., ULLAL, H.S., UPADHYAYA, H.M. Solar photovoltaic electricity: Current status and future prospects, *Solar Energy*, 2011, vol. 85, pp. 1580–1608.
4. BRODERICK, L.Z., ALBERT, B.R., PEARSON, B.S., KIMERLING, L.C., MICHEL, J. Design for energy: Modeling of spectrum, temperature and device structure dependences of solar cell energy production. *Solar Energy Materials & Solar Cells*, 2015, vol. 136 pp. 48–63.
5. VALLETI, K., KRISHNA, D. M., JOSHI, S.V. Functional multi-layer nitride coatings for high temperature solar selective applications. *Solar Energy Materials & Solar Cells*, 2014, vol. 121 pp.14–21.
6. GRANEK, F., REICHEL, C. Back-contact back-junction silicon solar cells under UV illumination. *Solar Energy Materials & Solar Cells*, 2010, vol. 94, pp. 1734–1740.
7. JIAN, W.H., LI, Zh., QIXUN, W., TAY, A. A.O., HEUKEN, M., SOO-JIN, Ch. Structural and morphological qualities of InGaN grown via elevated pressures in MOCVD on AlN/Si(111) substrates. *Journal of Crystal Growth*, 2013, vol. 383, pp.1–8.
8. FREEMAN, C. L., CLAEYSSENS, F., ALLAN, N. L., HARDING, J. H. Thin films of wurtzite materials—AlN vs. AlP. *Journal of Crystal Growth,* 2006, vol. 294, pp. 111–117.
9. LI, B., LI, J., WU, L., LIU, W., SUN, Y., ZHANG, Y. Barrier effect of AlN film in flexible Cu(In,Ga)Se2 solar cells on stainless steel foil and solar cell. *Journal of Alloys and Compounds*, 2015, vol. 627, pp. 1–6.
10. WU, Y., ZHENG, W., LIN, L., QU, Y., LAI, F. Colored solar selective absorbing coatings with metal Ti and dielectric AlN multilayer structure. *Solar Energy Materials & Solar Cells*, 2013, vol. 115, pp.145–150.
11. HUANG, K.C., CHEN, P-Y., VITTAL, R., HO, K.C. Enhanced performance of a quasi-solid-state dye-sensitized solar cell with aluminum nitride in its gel polymer electrolyte. *Solar Energy Materials & Solar Cells*, 2011, vol. 95, pp. 1990–1995.
12. REICHERTZ, L.A., GHERASOIU, I., KIN MAN YU, KAO, V. M., WALUKIEWICZ, W., AGER, J. W. Demonstration of a III–Nitride/Silicon tandem solar cell, *Applied Physics Express*, 2009, vol. 2, paper ID 122202 (3 pages).
13. KRUGEL, G., JENKNER, F., MOLDOVAN, A., WOLKE, W., RENTSCH, J., PREU, R. Investigations on the passivation mechanism of AlN:H and AlN:H-SiN:H stacks. *Energy Procedia*, 2014, vol. 55, pp. 797 – 804.
14. FEDLER, F., HAUENSTEIN, R.J., KLAUSING, H., MISTELE, D., SEMCHINOVA, O., ADERHOLD, J., GRAUL, J. Strain, morphological, and growth-mode changes in AlGaN single layers at high AlN mole fraction, *Journal of Crystal Growth*, 2002, vol. 241, pp. 535–542.
15. ZHANG, Q. C., SHEN, Y.G. High performance W–AlN cermet solar coatings designed by modelling calculations and deposited by DC magnetron sputtering. *Solar Energy Materials & Solar Cells*, 2004, vol. 81, pp. 25–37.

16. HU, P., ZHAO, P-P., JIN, Y., CHEN, Z.S. Experimental study on solid–solid phase change properties of pentaerythritol (PE)/nano-AlN composite for thermal storage. *Solar Energy*, 2014, vol. 102, pp. 91–97.
17. KEXIN, CH., HAIBO, J., HEPING, ZH. FERREIRA, J. Combustion synthesis of AlN-SiC solid solution particles. *Journal of European Ceramic Society*, 2000, vol. 20, pp. 2601-2606.
18. MEI, L., LI, J.-T. Synthesis of AlN–SiC solid solution through nitriding combustion of Al–C–Si3N4 in air. *Acta Materialia*, 2008, vol. 56, pp. 3543–3549.
19. DAVIS, R.F. Nitrides for electronic and optoelectronic applications, *Proceedings of the IEEE*, 1991, vol.79, no. 5, pp. 702-712.
20. ISHIKAWA, R., LUPINI, A. R., OBA, F., FINDLAY, S. D., SHIBATA, N., TANIGUCHI, T., WATANABE, K., HAYASHI, H., SAKAI, T., TANAKA, I., IKUHARA Y. PENNYCOOK, S. J. Atomic structure of luminescent centers in high-efficiency Ce-doped w-AlN single crystal. *Scientific reports*, 2013, vol. 3778, pp. 1-4.
21. AlN Technology Overview [online], [2015-7-6]. Available from: http://www.hexatechinc.com/aln-technology-overview.html
22. DALLAEVA, D., RAMAZANOV, S., RAMAZANOV, G., AKHMEDOV, R., TOMÁNEK, P., Characterizing SiC- AlN semiconductor solid solutions with indirect and direct bandgaps. *Proceedings of SPIE,* 2015, vol. 9450, paper ID 94501R (6 pages).
23. RAMAZANOV, Sh. M., KURBANOV, M. K., SAFARALIEV, G. K., BILALOV, B. A., KARGIN, N. I., GUSEV A. S. Structural properties of the epitaxial $(SiC)_{1-x}(AlN)_x$ solid solution films fabricated by magnetron sputtering of SiC-Al composite targets. *Technical Physics Letters*, 2013, vol. 40, no. 4, pp 300-302
24. SHEN, Y., SHI, Y., WANG, F. High-temperature optical properties and stability ofAlxOy–AlNx–Al solar selective absorbing surface prepared by DC magnetron reactive sputtering. *Solar Energy Materials & Solar Cells*, 2003, vol. 77, pp. 393–403.
25. YAFEI, X., CONG, W., WENWEN, W., YU, L., YONGXIN, W., YUPING, N., YING, S. Spectral properties and thermal stability of solar selective absorbing AlNi–Al2O3 cermet coating. *Solar Energy*, 2013, vol. 96, pp.113–118.
26. KAMINSKI, P. M., BASS, K., CLAUDIO, G. High bandgap dielectrics for antireflective coating in silicon solar cells by reactive ion sputtering. *Physica Status Solidi*, 2011, vol. 8, no. 4, pp. 1311–1314.
27. STAFINIAK, A., MUSZYŃSKA, D., SZYSZKA, A., PASZKIEWICZ, B., PTASIŃSKI, K., PATELA, S., PASZKIEWICZ, R., TŁACZAŁA. M. Properties of AlN thin films prepared by DC reactive magnetron sputtering. *OpticaApplicata*, 2009, vol. 39, no. 4, pp. 717 – 722.
28. JIAN-PING, M., ZHI-QIANG F., XIAO-PENG L., WEN, Y., CHENG-BIAO, W. Influence of ion/atom arrival ratio on structure and optical propertiesofAlN films by ion beam assisted deposition. *Applied Surface Science*, 2014, vol. 317, pp. 760–764.
29. ZHAO, Sh., WACKELGARD, E. The optical properties of sputtered composite of Al–AlN. *Solar Energy Materials & Solar Cells,* 2006, vol. 90, pp.1861–1874.
30. TANIYASU, Y., KASU, M., MAKIMOTO, T. Analuminium nitride light-emitting diode with a wavelength of 210 nanometres. *Nature,* 2006, vol. 441, pp. 325-328.
31. SYVÄJÄRVI, M., YAZDI, R., YAKIMOVA, R. SiC foundations assist AlN growth. Technology Materials Update, June 2009. [cit. 2015-6-7] Available from: http://www.liu.se/senmat/tumb/AlN_Compound_Semiconductor.pdf
32. DANZEBRINK, H.-U., KOENDERS, L., WILKENING, G., YACOOT, A., KUNZMANN, H. Advances in Scanning Force Microscopy for Dimensional Metrology. United Kingdom *Annals of the CIRP,* 2006, vol. 55, pp. 841-878.
33. RUSSELL, P., BATCHELOR, D., THORNTON, J. SEM and AFM: Complementary Techniques for High Resolution Surface Investigations. *Microscopy and Analysis*, 2001, pp. 9-12.

34. ABOU-RAS, D., DIETRICH, J., KAVALAKKATT, J., NICHTERWITZ, M., SCHMIDT, S.S., KOCH, C.T., CABALLERO, R., KLAER, J., RISSOM T. Analysis ofCu(In,Ga)(S,Se)2 thin-film solar cells by means of electron microscopy. *Solar Energy Materials & Solar Cells*, 2011, vol. 95, pp. 1452–1462.
35. SHELDEN, R. A., MEIER, L. P., CASERI, W. R., SUTER, U. W., HERMANN, R., MIJLLER, M., HEGNER, M., WAGNER, P. Nanophase molecular droplets: individual polystyrene molecules on mica imaged with scanning electron and atomic-force microscopy. *Polymer*, 1994, vol. 35, no. 8, pp.1571-1575.
36. IACOB, E., BERSANI, M., LUI, A., GIUBERTONI, D., BAROZZI, M., ANDERLE, M. Topography induced by sputtering in a magnetic sector instrument: an AFM and SEM study. *Applied Surface Science,* 2004, vol. 238, pp. 24–28.
37. SELVIN, P. Th., SABU, Th., Sri, B. Mechanical, atomic force microscopy and focussed ion beam studies of isotactic polystyrene/titanium dioxide composites. *Composites: Part A*. 2009, vol. 40, pp. 36–44
38. KWON, J., KIM, Y.-S., YOON, KW., LEE, S.-M, PARK, S. Advanced nanoscale metrology of pole-tip recession with AFM. *Ultramicroscopy,* 2005, vol. 105, pp. 51–56.
39. JENKINS, C., WESTWOOD, D.I., ELLIOTT, M., MACDONALD, J.E., MEATON, C., BLAND, S. Metrology of semiconductor device structures by cross-sectional AFM. *Materials Science and Engineering B,* 2001, vol. 80, pp. 138–141.
40. HSU, J.W.P. Near-field scanning optical microscopy studies of electronic and photonic materials and devices. *Materials Science and Engineering*, 2001, vol. 33, pp. 1-50.
41. BURATTO, St. K. Near-field scanning optical microscopy. *Current Opinion in Solid State & Materials Science,* 1996, vol. 1, pp. 405-492.
42. SAVIO, C. D., WOLFF, H., DZIOMBA, T., FU H.-A., DANZEBRINK, H.-U. A compact sensor head for simultaneous scanning force. and near-field optical microscopy. *Journal of the International Societies for Precision Engineering and Nanotechnology,* 2002, vol. 26, pp. 199–203.
43. CRAMER, R.M., SCHADE, W.R., HEIDERHOFF, R., BALK, L.J., CHIN, R. Scanning near-field optical microscopy analysesof electronic devices. *Microelectronics Reliability*, 1998, vol. 38, pp. 963-968.
44. SEEBACHER, S., OSTEN, W., VEIKO, V.P., VOZNESSENSKI, N.B. Inspection of nano-sized SNOM-tips by optical far-field evaluation. *Optics and Lasers in Engineering*, 2001, vol. 36, pp. 451–473.
45. YiN, Y., ZHU, X., FEI, T., XU, Sh., ZHOU, H., GAN, Z., SONG, F. A cryogenic near-field microscope working at LN temperature. *Proceedings of SPIE,* 1999, vol. 3791, paper doi:10.1117/12.363856.
46. FOSTER, A.S., HOFER, W.A. Scanning probe microscopy: atomic scale engineering by forces and currents. Liverpool: Springer, 2006.
47. PAREDES, J.I., ALONSO, A. M., TASCON, J.M.D. Application of scanning tunneling and atomic force microscopies to the characterization of microporous and mesoporous materials. *Microporous and Mesoporous Materials*, 2003, vol. 65, pp. 93–126.
48. Official web-page of NT-MDT company http://www.ntmdt.ru
49. MIRONOV, V.L. Fundamentals of scanning probe microscope, Nizhni Novgorod, 2004.
50. DALLAEVA, D.; TOMÁNEK, P.; RAMAZANOV, S. Scanning tunneling microscopy of high-resistance SiC- AlN solid solutions. In *New trends in physics 2012*. Brno: Vysoke uceni technicke v Brne, Fakulta elektrotechniky a komunikacnich technologii, Ustav fyziky, 2012. p. 149-152.
51. BILALOV, B., DALLAEVA, D.; MAGAMEDOVA, E.; Panoramic analysis of surface of high- resistance materials by scanning probe microscopy. In *Education in nanotechnology field - modern decision and pespectives*. Mocsow: 2010. p. 113-114.

52. KŘEČEK, Tomaš. Součastky na bazi SiC. [online] [cit 2015-6-7] Available from: http://www.roznovskastredni.cz/dwnl/pel2007/03/Krecek.pdf
53. PYO, S., OH, Y., YI, M. Organic thin-film transistors with submicrometer channel length fabricated by atomic force microscopy lithography. *Chemical Physics Letters*, 2006, vol. 419, pp. 115–119.
54. KIMA, Y.S., NAB, K.H., CHOIB, S.O., YANGA, S.H. Atomic force microscopy-based nano-lithography for nano-patterning: a molecular dynamic study. *Journal of Materials Processing Technology*, 2004, vol. 155–156, pp. 1847–1854.
55. XIE, X.N., CHUNG, H.J., SOW, C.H., WEE, A.T.S. Nanoscale materials patterning and engineering by atomic force microscopy nanolithography. *Materials Science and Engineering,* 2006, vol. 54, pp. 1–48.
56. JANG, E., KWUN, G., CHOI, W., LEE, H. Atomic force microscope anodization lithography using a triarylsulfonium salt photoinitiator. *Colloids and Surfaces A: Physicochemical and Engineering Aspects,* 2008, vol. 313–314, pp. 383–386.
57. KOPYCINSKA-MÜLLER, M., GEISS, R. H., HURLEY, D. C. Contact mechanics and tip shape in AFM-based nanomechanical measurements. *Ultramicroscopy*, 2006, vol. 106, no. 6, pp. 466–474
58. McCARTY, R., MAHMOODI, S. N. Dinamic mulitmode analysis of non-linear piezoelectric microcantilever probe in bistable region of tapping mode atomic force microscopy. *International Journal of Non-Linear Mechanics*, 2015, vol. 74, pp. 25–37.
59. ATABAK, M., ÜNVEDI, Ö., ÖZER, H. Ö., ORAL, A. Sub-Angstrom oscillation amplitude non-contact atomic force microscopy for lateral force gradient measurement. *Applied Surface Scienc*e, 2009, vol. 256, no. 5, pp. 1299–1303.
60. Pishkenari, H.N., Jalili, N,. Meghdari, A. Acquisition of high-precision images for non-contact atomic force microscopy. *Mechatronics,* 2006, vol. 16, no.10, pp. 655–664.
61. CAPPELLA, B., DIETLER, G. Force-distance curves by atomic force microscopy. *Surface Science Reports,* 1999, vol. 34, pp. 1-104.
62. LIN, Sh.-M., LIAUH, Ch.-Ts., WANG, W.-R., HO, Sh.-H. Analytical solutions of the frequency shifts of several modes in AFM scanning an inclined surface, subjected to the Lennard-Jones force. *International Journal of Solids and Structures,* 2007, vol. 44, pp. 799–810.
63. SCHRGDER, K.-P., MIRANDC, W., GEUTHER, H., HERRMANN, C. In quest of ylm accuracy: supporting optical metrology by rigorous diffraction theory and AFM topography. *Optics Communications,* 1995, vol. 115, pp. 568-575.
64. USHIKI, T., NAKAJIMA, M., CHOI, M., CHO, S.-J., IWATA, F. Scanning ion conductance microscopy for imaging biological samples in liquid: A comparative study with atomic force microscopy and scanning electron microscopy. *Micron*, 2012, vol. 43, pp. 1390–1398.
65. LUO, X.-P., SILIKAS, N., ALLAF, M., WILSON, N.H.F., WATTS, D.C. AFM and SEM study of the effects of etching on IPS-Empress 2TM dental ceramic. *Surface Science,* 2001, vol. 491, pp. 388-394.
66. KEHOE, T., REBOUD, V., TORRES, C. S. Inline metrology configuration for sub-wavelength diffraction using microscope optics. *Microelectronic Engineering,* 2009, vol. 86, pp. 1036–1039.
67. NanoScope 8.15 Software: User Guide http://www.nanophys.kth.se/nanophys/facilities/nfl/afm/icon/bruker-help/Content/SoftwareGuide/Offline/AnalysisFunct/TipQual.htm
68. YONG, Y. K., LIU, K., MOHEIMANI, S.O.R. Reducing cross-coupling in a compliant XY nanopositioner for fast and accurate raster scanning. *IEEE transactions on control systems technology*, 2010, vol. 18, no. 5, pp. 1172–1179.

69. MAZZEO, A.D., STEIN, A.J., TRUMPER, D.L., HOCKEN, R.J. Atomic force microscope for accurate dimensional metrology. *Precision Engineering*, 2009, vol. 33, pp. 135–149.
70. KUIPER, S., SCHITTER, G. Active damping of a piezoelectric tube scanner using self-sensing piezo actuation. *Mechatronics*, 2010, vol. 20, pp. 656–665.
71. DIRSCHERL, K., GARNAES, J., NIELSEN, L., JOGENSEN, J. F., SORENSEN, M. P. Modeling the hysteresis of a scanning probe microscope. *Journal of Vacuum Science and Technology B*, 2000, vol. 18.2., pp. 621-625.
72. KIM, W., VERMA, SH., SHAKIR, H. Design and precision construction of novel magnetic-levitation-based multi-axis nanoscale positioning systems. *Precision Engineering,* 2007, vol. 31, pp. 337–350.
73. CHEN, C. J. Introduction to Scanning Tunneling Microscopy.Second Edition. Oxford. University press, 2008.
74. Gwyddion software web page http://gwyddion.net/
75. ImageJ software web page http://imagej.nih.gov/ij/
76. KAMINSKYJ, S.G.W., DAHMS, T.E.S. High spatial resolution surface imaging and analysis of fungal cells using SEM and AFM. *Micron*, 2008, vol. 39, pp. 349–361.
77. B.G. Mendis, K.Durose. Prospects for electron microscopy characterization of solar cells: Opportunities and challenges. Ultramicroscopy 119 (2012) 82–96
78. L. Meng, D.Nagalingam, C.S.Bhatia, A.G.Street, J.C.H.Phang.Distinguishing morphological and electrical defects in polycrystalline silicon solar cells using scanning electron acoustic microscopy and electron beam induced current. Solar Energy Materials & Solar Cells 95 (2011) 2632–2637
79. B. Galiana, I.Rey-Stolle, I.Beinik, C.Algora, C.Teichert, J.M.Molina-Aldareguia, P.Tejedor. Characterization of antiphase domains on GaAs grown on Ge substrates by conductive atomic force microscopy for photovoltaic applications. Solar Energy Materials & Solar Cells 95 (2011) 1949–1954
80. Chiara Musumeci, Andrea Liscio, Vincenzo Palermo, Paolo Samori, Electronic characterization of supramolecular materials at the nanoscale by Conductive Atomic Force and Kelvin Probe Force microscopies. MaterialsToday, Volume 17, Number 10, December 2014, 504-517
81. ALEXEEV, A., LOOS, J. Conductive atomic force microscopy (C-AFM) analysisof photoactive layers in inert atmosphere. *Organic Electronics*, 2008, vol. 9, pp.149–154.
82. SADEWASSER, S., GLATZEL, Th., SCHULER, S., NISHIWAKI, S., KAIGAWA, R., LUX-STEINER, M.Ch. Kelvin probe force microscopy for the nano scale characterization of chalcopyrite solar cell materials and devices. *Thin Solid Films*, 2003, vol. 431 –432, pp. 257–261.
83. JIANG, C.-S., PTAK, A., YAN, B., MOUTINHO, H.R.. LI, J.V., AL-JASSIM, M.M. Microelectrical characterizations of junctions in solar cell devices by scanning Kelvin probe force microscopy. *Ultramicroscopy*, 2009, vol.109, pp. 952–957.
84. MOCZAŁA, M., SOSA, N., TOPOL, A., GOTSZALK, T. Investigation of multi-junction solar cells using electrostatic force microscopy methods. *Ultramicroscopy*, 2014, vol.141, pp.1–8.
85. DRIJKONINGEN, J., KESTERS, J., VANGERVEN, T., BOURGEOIS, E., LUTSEN, L., VANDERZANDE, D., MAES, W., D'HAEN, J., MANCA, J. Investigating the role of efficiency enhancing interlayers for bulk heterojunction solar cells by scanning probe microscopy. *Organic Electronics*, 2014, vol. 15, pp. 1282–1289.
86. GAO, H.L., ZHANG, X.W., MENG, J.H., YIN, Z.G., ZHANG, L.Q., WU, J.L., LIU, X. Quantitative characterization of phase separation in the photoactive layer of polymer solar cells by the phase image of atomic force microscopy. *Thin Solid Films*, 2015, vol. 576, pp. 81–87.

87. ZHU, F., CHEN, X., ZHOU, L., ZHOU, J., YANG, J., HUANG, S., SUN, Z. Dependence of the performance of inverted polymer solar cells on thickness of an electron selective ZnO layer deposited by magnetron sputtering. Thin Solid Films, 2014, vol. 551, pp. 131–135
88. POCHUHNEVA, E.L. System of energy supply of small space ships. *Space instrument-making: proceedings of forum of pupils and studens with international participatin. Tomsk*, 2013, pp. 107-110.
89. GREW, B., BOWERS, J. W., LISCO, F., ARNOU, N., WALLS, J. M., UPADHYAYA, H. M. High mobility titanium-doped indium oxide for use in tandem solar cells deposited via pulsed DC magnetron sputtering. *Energy Procedia,* 2014, vol. 60, pp. 148–155.
90. SEVER, M., KRČ, J., TOPIČ, M. Prediction of defective regions in optimisation of surface textures in thin-film silicon solar cells using combined model of layer growth. *Thin Solid Films,* 2014, vol. 573, pp. 176–184.
91. MAGNIN, V., HARARI, J., HALBWAX, M., BASTIDE, S., CHERFI, D., VILCOT, J.-P. Angle-dependent ray tracing simulations of reflectionson pyramidal textures for silicon solar cells. *Solar Energy,* 2014, vol. 110, pp. 378–385.
92. BRUZZONE, A.A.G., COSTA, H.L., LONARDO, P.M., LUCCA D.A. Advances in engineered surfaces for functional performance. *CIRP Annals - Manufacturing Technology*, 2008, vol. 57, pp. 750–769.
93. VINEIS, C., LEVY-FINKLSHTEIN, M., CAREY, J., KNIGHT, G., WEFRINGHAUS, E., HARNEY, R. Ultrafast laser texturing for enhanced solar cell performance and lower cost [cit. 2015-5-7] Available from: http://sionyx.com/pdf/solarcellperformancewhitepaper.pdf
94. DMITRUK, N.L., BORKOVSKAYA, O.YU., DMITRUK, I.N., MAMONTOVA, I.B. Analysis of thin film surface barrier solar cells with a microrelief interface. *Solar Energy Materials & Solar Cells,* 2003, vol. 76, pp. 625–635.
95. KHANNA, A., BASU, P.K., FILIPOVIC, A., SHANMUGAM, V., SCHMIGA, Ch., ABERLE, A.G. MUELLER Th. Influence of random pyramid surface texture on silver screen-printed contact formation for monocrystalline silicon wafer solar cells. *Solar Energy Materials & Solar Cells*, 2015, vol. 132, pp. 589–596.
96. JIANG, Q., LU, J., ZHANG, J., YUAN, Y., CAI , H., WU, Ch., SUN, R., LU, B., PAN, X., YE, ZH. Texture surfaces and etching mechanism of ZnO:Al films by a neutral agent for solar cells. *Solar Energy Materials &Solar Cells,* 2014, vol. 130, pp.264–271.
97. YANG, G., vanSWAAIJ, R.A.C.M.M., TAN, H., ISABELLA, O., ZEMAN, M. Modulated surface textured glass as substrate for high efficiency microcrystalline silicon solar cells. *Solar Energy Materials & Solar Cells*, 2015, vol. 133, pp. 156–162.
98. DOU, B., JIA, R., LI, H., CHEN, C., SUN, Y., ZHANG, Y., DING, W., MENG, Y., LIU, X., YE, T. Fabrication of ultra-small texture arrays on multicrystalline silicon surface for solar cell application. *Solar Energy*, 2013, vol. 91, pp. 145–151.
99. REN, X., ZI, W., MA, Q., XIAO, F., GAO, F., HU, Sh., ZHOU, Y., (FRANK) LIU, Sh. Topology and texture controlled ZnO thin film electro deposition for superior solar cell efficiency. *Solar Energy Materials&Solar Cells*, 2015, vol. 134, pp. 54–59.
100. DING, L., FANNI, L., MESSERSCHMIDT, D., ZABIHZADEH, S., MORALESMASIS, M., NICOLAY, S., BALLIF, C. Tailoring the surface morphology of zinc oxide films for high-performance micromorph solar cells. *Solar Energy Materials & Solar Cells,* 2014, vol. 128, pp. 378–385.
101. ERAYERKAN, M., CHAWLA, V., REPINS, I., SCARPULLA, M.A. Interplay between surface preparation and device performance in CZTSSe solar cells: Effects of KCN and NH4OH etching. *Solar Energy Materials & Solar Cells,* 2015, vol. 136, pp. 78–85.
102. LI, H.B.T., FRANKEN, R.H., RATH, J.K., SCHROPP, R.E.I. Structural defects caused by a rough substrate and their influence on the performance of

hydrogenated nano-crystalline silicon n–i–p solar cells. *Solar Energy Materials & Solar Cells*, 2009, vol. 93, pp. 338–349.

103. ZEMAN, M., ISABELLA, O., SOLNTSEV, S., JÄGER, K. Modelling of thin-film silicon solar cells. *Solar Energy Materials & Solar Cells*, 2013, vol.119, pp. 94–111.

104. SEVER, M., KRČ, J., TOPIČ, M. Optimisation of periodic surface textures in thin-film silicon solar cells using rigorous optical modelling by considering realistic layer growth. *Energy Procedia,* 2014, vol. 44, pp.138 – 144.

105. YANG, Y., GREEN, M.A., HO-BAILLIE, A., KAMPWERTH, H., PILLAI, S., MEHRVARZ, H. Characterization of 2-Dreflection pattern from textured front surfaces of silicon solar cells. *Solar Energy Materials & Solar Cells*, 2013, vol. 115, pp. 42–51.

106. SEVER, M., KRČ, J., TOPIČ, M. Prediction of defective regions in optimisation of surface textures in thin-film silicon solar cells using combined model of layer growth. *Thin Solid Films*, 2014, vol. 573, pp. 176–184.

107. SPRINGER, J., RECH, B., REETZ, W., MULLER, J., VANECEK, M. Light trapping and optical losses in microcrystalline silicon pin solar cells deposited on surface-textured glass/ZnO substrates. *Solar Energy Materials & Solar Cells*, 2005, vol. 85, pp. 1–11.

108. ČAMPA, A., MEIER, M., BOCCARD, M., MERCALDO, L.V., GHOSH, M., ZHANG, C., MERDZHANOVA, T., KRČ, J., HAUG, F.-J., TOPIČ, M. Micromorph silicon solar cell optical performance: Influence of intermediate reflector and front electrode surface texture. *Solar Energy Materials&Solar Cells,* 2014, vol. 130, pp. 401–409.

109. DZHAFAROV, T. Silicon Solar Cells with Nanoporous Silicon Layer, Solar Cells - Research and Application Perspectives, Prof. Arturo Morales-Acevedo (Ed.). 2013. [cit. 2015-8-7]. Available from: http://www.intechopen.com/books/solar-cells-research-and-application-perspectives/silicon-solar-cells-with-nanoporous-silicon-layer .

110. BORODINA, N.M., LETIN., V.A. Modelling of volt-ampere characteristids of the solar cells and solar panels. *Electrochemical industry*, 1986, vol. 1, no. 7, pp. 1—64.

111. SILVESTRE, S., CHOUDER, A. Effects of Shadowing on Photovoltaic Module Performance. *Progress in Photovoltaics: Research and applications*, 2007, vol. 16, no. 2, pp. 141-149.

112. TOPIČ, M., SEVER, M., LIPOVŠEK, B., ČAMPA, A., KRČ, J. Approaches and challenges in optical modelling and simulation of thin-film solar cells. *Solar Energy Materials & Solar Cells*, 2015, vol. 135, pp. 57-66.

113. AL KARIM, M.A. *Structural and optical properties of the solar cells on the basis of ZnO and AlN*. Sumy: Sumy State University, 2012. Ph.D. Thesis. 154 p.

114. RAY, B., NAIR, P. R., ALAM, M.A. Morphology Dependent Short Circuit Current in Bulk Heterojunction Solar cell. *35th IEEE Photovoltaic Specialist Conference*, 2010. Available from: http://docs.lib.purdue.edu/nanopub/522

115. MÚGICA-VIDAL, R., ALBA-ELÍAS, F., SAINZ-GARCÍA, E., ORDIERES-MERÉ, J. Atmospheric plasma-polymerization of hydrophobic and wear-resistant coatings on glass substrates. *Surface & Coatings Technology,* 2014, vol. 259, pp. 374–385.

116. ROPPOLOB, I., SHAHZAD, N., SACCO, A., TRESSO, E., SANGERMANO, M. Multifunctional NIR-reflective and self-cleaning UV-cured coating forsolar cell applications based on cycloaliphatic epoxy resin. *Progress in Organic Coatings*, 2014, vol. 77, pp. 458– 462.

117. LEEM, J.W., CHUNG, K.S., YU, J.S. Antireflective properties of disordered Si SWSs with hydrophobic surface by thermally dewetted Pt nanomask patterns for Si-based solar cells. *Current Applied Physics*, 2012, vol. 12, pp. 291-298.

118. XU, Y.J., LIAO, J.X., CAI, Q.W., YANG, X.X. Preparation ofahighly-reflectiveTiO2/SiO2/Ag thin film with self-cleaning properties by magnetron sputtering for solar front reflectors. *Solar Energy Materials & Solar Cells,* 2013, vol. 113, pp. 7–12.

119. ZHANG, W., ZHANG, D., FAN, T., GU, J., DING, J., WANG, H., GUO, Q., OGAWA, H. Novel Photoanode Structure Templated from Butterfly Wing Scales. *Chemistry of Materials,* 2009, vol. 21, pp. 33–40.

120. ZHANG, D., GU, J., LIU, Q., SU, H., ZHU, S., ZHANG. W. Study on Morph-genetic Materials Derived from Natural Materials. *Journal of Analytical Science & Technology,* 2011 vol. 2, pp. A140-A145.

121. JIN, L., ZHAI, J., HENG, L., WEI, T., WEN, L., JIANG, L., ZHAO, X., ZHANG, X. Bio-inspired multi-scale structures in dye-sensitized solar cell. *Journal of Photochemistry and Photobiology C: Photochemistry Reviews,* 2009, vol. 10, no. 4, pp. 149–158.

122. RAGAEI, M., SABRY, AL-K. H. Insect wings as a solar cell system. *International Journal of Open Scientific Research,* 2013, vol. 1, no. 3, pp. 10-26.

123. DUPARRÉ, A., FLEMMING, M., STEINERT, J., REIHS, K. Optical coatings with enhanced roughness for ultrahydrophobic, low-scatter applications, *Applied Optics*, 2002, vol. 41, pp. 3294-3298.

124. . KUISMA, R., PESONEN-LEINONEN, E., REDSVEN, I., KYMALAINEN, H-R., SAARIKOSKI, I., SJOBERG, A.-M., HAUTALA, M. Utilization of profilometry, SEM, AFM and contact angle measurements in describing surfaces of plastic floor coverings and explaining their clean ability. *Surface Science*, 2005, vol. 584, pp. 119–125.

125. SALVADOR, A. Nanostructured Solar Energy Devices. [cit. 2015-8-7] Available from: http://www.pcieerd.dost.gov.ph/images/downloads/ presentation_materials/pcieerd4thanniversary/session_b/2_Nanostructured_Solar_Energ y_Devices-Juana_Invest_with_video.pdf

126. ZANUCCOLI, M., MAGNONE, P., SANGIORGI, E., FIEGNA, C. Analysis of the impact of geometrical and technological parameters on recombination losses in interdigitated back-contact solar cells. *Solar Energy*, 2015, vol. 116, pp. 37–44.

127. WALTER, D., FELL, A., FRANKLIN, E., WANG, D., FONG, K., KHO, T., WEBER, K., BLAKERS, A.W. Damage-free ultraviolet nanosecond laser ablation for high efficiency back contact solar cell fabrication. *Solar Energy Materials & Solar Cells*, 2015, vol. 136, pp. 1–10.

128. SCHULTE-HUXEL, H., ROMER, U., BLANKEMEYER, S., MERKLE, A., LARIONOVA, Y., STECKENREITER, V., PEIBST, R., KAJARI-SCHROEDER, S., BRENDEL, R. Two-level metallization and module integration of point-contacted solar cells. *Energy Procedia*, 2014, vol. 55, pp. 361 – 368.

129. BALUCANI, M., SERENELLI, L., KHOLOSTOV, K., NENZI, P., MILICIANI, M., MURA, F., IZZI, M., TUCCI, M. Aluminum-Silicon interdiffusion in screen printed metal contacts for silicon based solar cells applications. Energy Procedia, 2013, vol. 43, pp.100 – 110.

130. KAMP, M., MAYWALD, A., BARTSCH, J., EFINGER, R., KEDING, R., GLATTHAAR, M., GLUNZ, S.W., KROSSING, I. Electrochemical Contact Separation for PVD Aluminum Back Contact Solar Cells. Energy Procedia, 2015, vol. 67, pp. 70 – 75.

131. TZENG, Y. LINn, T.H., Dry etching of silicon materials in SF6 based plasmas, Journal of Electrochemical Society, 1987, vol. 134, No. 9, p. 2304-2309.

132. SCHNEIDER, A., T. PERNAU, K. PETER, P. FATH, Mechanical wafer stability enhancements and texturing effects of remote downstream plasma etching. *Proceedings of 3rd World Conference on Photovoltaic Energy Conversion*, 2003, vol. 2, pp. 1419 – 1422.

133. LIU, J., NEMCHUK, N.I., AST D.G., COUILLARD, J.G. Etch rate and surface morphology of plasma etched glass and glass-ceramic substrates, *Journal of* Non-*Crystalline Solids*, 2004, vol. 324, pp. 110-115.
134. LIAO, F., PARK, S., LARSON, J.M., ZACHARIAH, M.R., GIRSHICK, S.L. High-rate chemical vapor deposition of nanocrystalline silicon carbide films by radio frequency thermal plasma, *Materials Letters*, 2003, vol. 57, pp. 1982–1986.
135. ANDRIEVSKI, R.A., Synthesis, structure and properties of nanosized silicon carbide, *Reviews on advanced materials science,* 2009*,* vol. 2, pp. 21-20.
136. BUNOIU, O., NICOARA, I. AND DUFFAR, T. Solute distribution in shaped sapphire crystals obtained by EFG method, *Journal of Optoelectronics and Advanced Materials*, 2005, vol. 7, no. 2, pp. 615 – 618.
137. KANG, D.-W., KWON, J.-Y., SHIM, J., LEE, H.-M., HAN, M.-K. Al_2O_3 antireflection layer between glass and transparent conducting oxide for enhanced light trapping in microcrystalline silicon thin film solar cells. *Solar Energy Materials & Solar Cells*, 2012, vol. 101, pp. 22-25.
138. SOUM-GLAUDE, A., BOUSQUET, I., BICHOTTE, M., QUOIZOLA, S., THOMAS, L., FLAMANT, G. Optical characterization and modeling of coatings intended as high temperature solar selective absorbers. *Energy Procedia,* 2014, vol. 49, pp. 530 – 537.
139. Ion Beam Etching. [cit. 2015-8-7] Available from: http://www.azom.com/article.aspx?ArticleID=7533
140. HAN, K.-M., CHO, J.-S., YOO, J. Monocrystalline-like silicon solar cells fabricated by wet and dry texturing processes for improving light-trapping effect. *Vacuum*, 2015, vol. 115, pp. 85-88.
141. KAZMI, S.N.R., SALM, C., SCHMITZ, J. Deep reactive ion etching of in situ boron doped LPCVD Ge0.7Si0.3 using SF6 and O2 plasma. *Microelectronic Engineering*, 2013, vol. 110, pp. 311–314.
142. Lee, D.Y., Chung, C.W. Etch characteristics of indium zinc oxide thin films using inductively coupled plasma of a Cl2/Ar gas. *Thin Solid Films*, 2009, vol. 517, pp. 4047–4051.
143. LEEM, J.W., YU, J. S., JUN, D.-H., HEO, J., PARK, W.-K. Efficiency improvement of III–V GaAs solar cells using biomimetic TiO2 subwavelength structure swith wide-angle and broad band antireflection properties. *Solar Energy Materials & Solar Cells,* 2014, vol. 127, pp. 43–49.
144. SUNG, Y.-M., KIM, H.-J. Sputter deposition and surface treatment of TiO2 films for dye-sensitized solar cells using reactive RF plasma. *Thin Solid Films*, 2007, vol. 515, pp. 4996–4999.
145. LEE, D. Y., CHUNG, C. W. Etch characteristics of indium zinc oxide thin films in a C2F6/Ar plasma. *Thin Solid Films*, 2009, vol. 518, pp. 372–377.
146. TAMULEVIČIUS, T., TAMULEVICIENE, A., VIRGANAVICIUS, D., VASILIAUSKAS, A., KOPUSTINSKAS, V., MEŠKINIS, Š., TAMULEVIČIUS, S. Structuring of DLC:Ag nanocomposite thin films employing plasma chemical etching and ion sputtering. *Nuclear Instruments and Methods in Physics Research B,* 2014, vol. 341, pp. 1–6.
147. MICHALCIK, Z., HORAKOVA, M., SPATENKA, P., KLEMENTOVA, S., ZLAMAL, M., MARTIN, N. Photocatalytic Activity of Nanostructured Titanium Dioxide Thin Films. *International Journal of Photoenergy,* 2012, vol. 2012, pp. 689154-1 – 689154-8.
148. HUANG, Y., SAHRAEI, N., WIDENBORG, P., PETERS, I. M., DALAPATI, G. K., ISKANDER, A., ABERLE, A. G. Enhanced light trapping in polycrystalline silicon thin-film solar cells using plasma-etched submicron textures. *Solar Energy Materials & Solar Cells*, 2014, vol. 122, pp. 146–151.

149. XU, Y.J., CAI, Q.W., YANG, X.X., ZUO, Y.Z., SONG, H., LIU, Z.M., HANG, Y.P. Preparation of novel SiO2 protected Ag thin films with high reflectivity by magnetron sputtering for solar front reflectors. *Solar Energy Materials & Solar Cells*, 2012, vol. 107, pp. 316–321.

150. KIM, K., KIM, S., AN, S., LEE, G.-H., KIM, D., HAN, S. Anti-reflection porousSiO2 thin film deposited using reactive high-power impulse magnetron sputtering at high working pressure for use in a-Si:H solar cells. *Solar Energy Materials & Solar Cells,* 2014, vol. 130, pp. 582–586.

151. SCHULTE, J., HARBAUER, K., ELLMER, K. Reactive magnetron co-sputtering of Cu(In,Ga)Se2 absorber layers by a 2-stage process: Role of substrate type and Na-doping. *Thin Solid Films*, 2015, vol. 582, pp. 95-99.

152. LI, L., CHEN, R., JING, G., ZHANG, G., WU, F., CHEN, S. Improved performance of TiO2 electrodes coated with NiO by magnetron sputtering for dye-sensitized solar cells. *Applied Surface Science*, 2010, vol. 256, pp. 4533–4537.

153. WU, S., HAN, H., TAI, Q., ZHANG, J., XU, S., ZHOU, C., YANG, Y., HU, H., CHEN, B., ZHAO, X. Improvement in dye-sensitized solar cells employing TiO2 electrodes coated with Al2O3 by reactive direct current magnetron sputtering. *Journal of Power Sources,* 2008, vol.182, pp. 119–123.

154. CHEN, X., WANG, F., GENG, X., ZHANG, D., WEI, C., ZHANG, X., ZHAO, Y. Natively textured surface Al-doped ZnO-TCO layers with gradual oxygen growth for thin film solar cells via magnetron sputtering. *Applied Surface Science,* 2012, vol. 258, pp. 4092– 4096.

155. CHEN, X., LI, L., WANG, F., NI, J., GENG, X., ZHANG, X., ZHAO, Y. Natively textured surface aluminum-doped zinc oxide transparent conductive layers for thin film solar cells via pulsed direct-current reactive magnetron sputtering. *Thin Solid Films*, 2012, vol. 520, pp. 5392–5399.

156. HSU, F.-H., WANG, N.-F., TSAI, Y.-Z., CHUANG, M.-C., CHENG, Y.-S., HOUNG, M.-P. Study of working pressure on the optoelectrical properties of Al–Y codoped ZnO thin-film deposited using DC magnetron sputtering for solar cell applications. *Applied Surface Science,* 2013, vol. 280, pp. 104– 108.

157. TIAN, C., CHEN, X., NI, J., LIU, J., ZHANG, D., HUANG, Q., ZHAO, Y., ZHANG, X. Transparent conductive Mg and Ga co-doped ZnO thin films for solar cells grown by magnetron sputtering: H2 induced changes. *Solar Energy Materials and Solar Cells*, 2014; vol. 125, pp. 59–65.

158. ZHAO, L., ZHOU, Z., PENG, H., CUI, R. Indium tin oxide thin films by bias magnetron rf sputtering for heterojunction solar cells application. *Applied Surface Science*, 2005, vol. 252, pp. 385–392.

159. ZHANG, C., CHEN, X., GENG, X., TIAN, C., HUANG, Q., ZHAO, Y., ZHANG, X. Temperature-dependent growth and properties of W-doped ZnO thin films deposited by reactive magnetron sputtering. *Applied Surface Science*, 2013, vol. 274, pp. 371– 377.

160. SCOTT, C., SMITH, R. Modelling the sputtering of Au surfaces using a multitime-scale technique. *Proceedings of the royal Society A,* 2013, vol. 469, pp. 20120480-1 – 20120480-14.

161. SCHULTE, J., BRUNKEN, S., ELLMER, K. Nucleation and phase formation during reactive magnetron co-sputtering of Cu(In,Ga)S2 films, investigated by in situ EDXRD. *Journal of Crystal Growth*, 2013, vol. 384, pp.114–121.

162. Atomic Force Microscopy. Nanoscience Instruments, Inc. [cit. 2013-09-05]. Available from: http://www.nanoscience.com/ education/afm.html.

163. MUNZ, M. Force calibration in lateral force microscopy – a review of the experimental methods. *Journal of Physics D: Applied Physics*, 2010, vol. 43, no. 6, pp. 063001-1 – 063001-34.

164. LOU, S., JIANG, X., SCOTT, P. J. Application of the morphological alpha shape method to the extraction of topographical features from engineering surfaces. *Measurement*, 2013, vol. 46, no. 2, pp. 1002-1008.
165. CHHABRA, A., JENSEN, R. V. Direct determination of the f (α) singularity spectrum, *Physical Review Letter*, 1989, vol. 62, no. 12, pp. 1327-1330.
166. Software. Available from: http://www.digitalsurf.fr (last accessed January 10, 2014).

APPENDIX 1. LIST OF PUBLICATION IN IMPACT JOURNALS

A1. DALLAEVA, D. S., BILALOV, B. A., GITIKCHIEV, M. A., KARDASHOVA, G. D., SAFARALIEV, G. K., TOMANEK, P., SKARVADA, P., SMITH, S., Structural properties of Al_2O_3/AlN thin film prepared by magnetron sputtering of Al in HF-activated nitrogen plasma. *Thin Solid Films*. 2012, vol. 526. p. 92-96. WOS:000313703200015. **IF 1.867**

A2. DALLAEVA, D., TALU, S., STACH, S., SKARVADA, P., TOMANEK, P., GRMELA, L. AFM imaging and fractal analysis of surface roughness of AIN epilayers on sapphire substrates. *Applied Surface Science*. 2014, vol. 312, p. 81-86, WOS: 000339998700014. **IF 2.538**

A3. STACH, S., DALLAEVA, D., TALU, S., KASPAR, P., TOMÁNEK, P., GIOVANZANA, S., GRMELA, L. Morphological features in aluminum nitride epilayers prepared by magnetron sputtering. *Materials Science-Poland*. 2015, vol. 33(1), p. 175-184. ISSN: 0137- 1339. **IF 0.327**

A4. ŠKARVADA, P., TOMÁNEK, P., KOKTAVY, P.; MACKU, R., SICNER, J., VONDRA, M., DALLAEVA, D., SMITH, S., GRMELA, L., A variety of microstructural defects in crystalline silicon solar cells. *Applied Surface Science*, 2014, vol. 312, p. 50-56, WOS: 000339998700009. **IF 2.538**

APPENDIX 2. LIST OF PUBLICATION CITED IN SCOPUS

B1. DALLAEVA, D., RAMAZANOV, S., PROKOPYEVA, E., TOMANEK, P., GRMELA, L. Local topography of optoelectronic substrates prepared by dry plasma etching process. *Proceedings of SPIE. Optics and measurement conference 2014*. V. 9442. Article Number: 9442082015.2015. WOS:000349403500007

B2. SAFARALIEV, G., BILALOV, B., DALLAEVA, D., RAMAZANOV, S.,GERAEV, K., TOMANEK, P. Investigation of optical properties of $SiC/(SiC)_{(1-x)}(AlN)_{(x)}$ heterostructures. *Proceedings of SPIE. Photonics, devices, and systems V*. Vol. 8306. Article Number: 83061K. AUG 24-26, 2011. WOS:000297582500056

B3. DALLAEVA, D., TOMANEK, P., PROKOPYEVA, E., KASPAR, P., GRMELA, L., SKARVADA, P., AFM imaging of natural optical structures. *Proceedings of SPIE. Optics and measurement conference 2014*. Vol. 9442. Article Number: 944209. WOS: 000349403500008

B4. DALLAEVA, D., RAMAZANOV, S., RAMAZANOV, G., AKHMEDOV, R., TOMANEK, P. Characterizing SiC-AlN semiconductor solid solutions with indirect and direct bandgaps. *Proceedings of SPIE*. Photonics, devices, and systems VI. Vol. 9450. Article Number: 94501R. 2015. WOS: 000349404500061

B5. DALLAEVA, D., TOMANEK, P., SKARVADA, P., GRMELA, L. Realization of microscale detection and localization of low light emitting spots in monocrystalline silicon solar cells. *Proceedings of SPIE*. Photonics, devices, and systems VI. Vol. 9450.Article Number: 94501O. 2015. WOS:000349404500058

B6. SKARVADA, P., MACKU, R., DALLAEVA, D., SEDLAK, P., GRMELA, L., TOMANEK, P., SEM and AFM imaging of solar cells defects. *Proceedings of SPIE*. Photonics, devices, and systems VI. V. 9450. Article Number: 94501M. 2015. WOS: 000349404500056

B7. DALLAEVA, D., KARDASHOVA, G., SAFARALIEV, G., TOMANEK, P., High-density ceramic materials on the basis of silicon carbide.7th International Conference on Materials Structure and Micromechanics of Fracture (MSMF 7). *Key Engineering Materials*.2014. V. 592-593. Pages: 397-400. WOS:000336694400087

B8. DALLAEVA, D., KOROSTYLEV, E., BILALOV, B., TOMANEK, P. Scanning proximal microscopy study of the thin layers of silicon carbide-aluminum nitride solid solution manufactured by fast sublimation epitaxy. *EPJ Web of Conferences*. OAM 2012 - Optics and measurement international conference. V. 48. Article Number: 00002. 2013.WOS: 000326985500001

B9. KLAMPAR, M., SPOHNER, M., SKARVADA, P., DALLAEVA, D., KOBRTEK, J., LIEDERMANN, K. Dielectric properties of epoxy resins with

oxide nanofillers and their accelerated ageing. IEEE.2013 *IEEE electrical insulation conference* 2013. Pages: 286-290. WOS: 000326735500055

B10. SKARVADA, P., TOMANEK, P., KOKTAVY, P., DALLAEVA, D. Microscopic optoelectronic defectoscopy of solar cells. *EPJ Web of Conferences*.OAM 2012 - Optics and measurement international conference.V. 48. Article Number: 00026. 2013. WOS: 000326985500025

B11. SKARVADA, P., MACKU, R., DALLAEVA, D., PROKOPYEVA, E., TOMANEK, P., GRMELA, L., SMITH, S., Optical and electrical detection and localization of solar cell defects on microscale. *Proceedings of SPIE. Reliability of photovoltaic cells, modules, components, and systems VI*. 2013, vol. 8825, Article Number: UNSP 882507. 2013. WOS: 000325973200006

Professional CV

Dinara Sultanovna DALLAEVA, M.Sc.
24.12.1988 Kaspyisk, Russian Federation

Languages: Native Russian, Fluent English, Middle level Czech

EDUCATION AND QUALIFICATION:
Dagestan State University, Machachkala, Russian Federation
- Bachelor "Electronics and microelectronics" (2004-2008),
Topic: Ohmic contact to silicon carbide.
- Master "Electronics and microelectronics" (2008-2010),
Topic: Study of morphology and structure of SiC and AlN layers by AFM and X-ray diffractometry.
Dagestan State University, Machachkala, Russian Federation
- Postgraduate study (2010-2014 unfinished)

Brno University of Technology, Brno, Czech Republic
- Doctoral study (2011-2015)
Field: Physical Electronics and Nanotechnology.
Topic: Local investigation of optoelectronic devices.

EMPLOYMENT HISTORY:
- Dagestan State University (www.dsu.ru) laboratory assistant (2009-2011)
- Dagestan State Technical University (www.dstu.ru) - Research center "Nanotechnology and microelectronics" (engineer, research assistant for 3 years). (2008-2011)
- Brno University of Technology, Brno, Czech Republic (from 2012 till now).
  - European Centre of Excellence CEITEC CZ.1.05/1.1.00/02.0068 (form 2014 till now)
  - Sensor, Information and Communication Systems SIX CZ.1.05/2.1.00/03.0072 (form 2013 till now)
  - Visegrad fund scholarship (2014-2015)
- FEI, Brno, Czech Republic (from 2014 till now) intern (application engineer).

PROFESSIONAL PRACTICE, INTERSHIPS, SOLVED SCIENTIFIC PROJECTS:
Skills: AFM, SNOM measurements, thin films preparation

Participation at Research grants of Federal task program in Russia:
1. Development of formation technology and study of nanostructured high-resistance layers of $(SiC)_{1-x}$-$(AlN)_x$ solid solutions by scanning probe microscopy (2009-2010).
2. Investigation of electro-physical properties of $(SiC)_{1-x}(AlN)_x$ thin high-resistance films by scanning probe microscopy (2009-2011).
3. Standardized method development of investigation of electro-physical properties of $(SiC)_{1-x}(AlN)_x$ thin high-resistance films by scanning tunnel spectroscopy (2010-2011).
4. Development of obtaining and investigation technology of structrures with surface barriers on the base of solid solutions of silicon carbide and aluminum nitride for high-voltage and high-temperature Schottky diodes (2009-2010).
5. Development of physical-technical bases of nanostructured ceramic materials obtaining on the basis of silicon carbide and its solid solutions with aluminum nitride for extreme conditions of using (2009-2011).

In Czech Republic
1. Centrum senzorických, informačních a komunikačních systémů - Sensor, Information and Communication Systems SIX **CZ.1.05/2.1.00/03.0072**
2. MŠMT ČR – KONTAKT LH11060 – Studium lokálních elektronických a optických charakteristik solárních článků (2011-2014).

Intership
1. Moscow Institute of Physics and Technology - Short-term training of professional skills (2010). Program: Scanning probe microscopy.
2. Kurz základů vědecké práce v Akademii věd ČR, Brno, 16-20. 05. 2013.
3. International PhD school on Application of scanning probe microscopy in life sciences, soft matter and nanofabrication. Aalborg University (Denmark), 26-30. 08. 2013.
4. Podzimní škola základů elektronové mikroskopie, Ústav přístrojové techniky AV ČR, v. v. i., Brno, 14-18. 10. 2013.